Digital Cognitive Companions for Marine Vessels

On the Path Towards Autonomous Ships

Lager, Mårten

2021

Document Version:
Publisher's PDF, also known as Version of record

Digital Cognitive Companions for Marine Vessels

On the Path Towards Autonomous Ships

Digital Cognitive Companions for Marine Vessels

On the Path Towards Autonomous Ships

Mårten Lager

LUND
UNIVERSITY

Thesis for the degree of PhD
Thesis advisors: Prof. Jacek Malec, Dr. Elin A. Topp
Faculty opponent: Prof. Henrik I. Christensen

To be presented, with the permission of the Faculty of Engineering of Lund University, for public criticism in the E:B lecture hall in E-huset at the Department of Computer Science on Friday, the 12th of February 2021 at 14:15.

Organization	Document name
LUND UNIVERSITY Department of Computer Science Box 118 SE-221 00, Lund Sweden	DOCTORAL DISSERTATION
	Date of issue 12 February 2021
	Sponsoring organization Wallenberg AI, Autonomous Systems and Software Program (WASP) funded by Knut and Alice Wallenberg Foundation
Author(s) Mårten Lager	

Title and subtitle

Digital Cognitive Companions for Marine Vessels - On the Path Towards Autonomous Ships

Abstract

As for the automotive industry, industry and academia are making extensive efforts to create autonomous ships. The solutions for this are very technology-intense. Many building blocks, often relying on AI technology, need to work together to create a complete system that is safe and reliable to use. Even when the ships are fully unmanned, humans are still foreseen to guide the ships when unknown situations arise. This will be done through teleoperation systems.

In this thesis, methods are presented to enhance the capability of two building blocks that are important for autonomous ships; a positioning system, and a system for teleoperation.

The positioning system has been constructed to not rely on the Global Positioning System (GPS), as this system can be jammed or spoofed. Instead, it uses Bayesian calculations to compare the bottom depth and magnetic field measurements with known sea charts and magnetic field maps, in order to estimate the position. State-of-the-art techniques for this method typically use high-resolution maps. The problem is that there are hardly any high-resolution terrain maps available in the world. Hence we present a method using standard sea-charts. We compensate for the lower accuracy by using other domains, such as magnetic field intensity and bearings to landmarks. For one of the tests, we also used high-accuracy navigation sensors, which resulted in a mean position error of 10.2m during a 20h long test run. Using data from a field trial, we showed the fusion method using multiple domains was more robust than using only one domain.

In the second building block, we first investigated how 3D and VR approaches could support the remote operation of unmanned ships with a data connection with low throughput, by comparing respective graphical user interfaces (GUI) with a Baseline GUI following the currently applied interfaces in such contexts. Our findings show that both the 3D and VR approaches outperform the traditional approach significantly. We found the 3D GUI and VR GUI users to be better at reacting to potentially dangerous situations than the Baseline GUI users, and they could keep track of the surroundings more accurately. Building from this, we conducted a teleoperation user study using real-world data from a field-trial in the archipelago, where the users should assist the positioning system with bearings to landmarks. The users experienced the tool to give a good overview, and despite the connection with the low throughput, they managed through the GUI to significantly improve the positioning accuracy.

Key words: Teleoperation; Terrain-Aided Navigation, Particle Filter, Navigation, Safe Navigation, Virtual Reality, Localization, ASV, USV, Autonomous System, User Interaction

Classification system and/or index termes (if any):

Supplementary bibliographical information:	Language
	English
ISSN and key title: 1404-1219	ISBN 978-91-7895-608-1 (print) 978-91-7895-609-8 (pdf)

Recipient's notes	Number of pages 249	Price
	Security classification	

Digital Cognitive Companions for Marine Vessels

On the Path Towards Autonomous Ships

Mårten Lager

LUND
UNIVERSITY

Faculty Opponent

Prof. Henrik I. Christensen
University of California, San Diego
San Diego, USA

Evaluation Committee

Prof. Thomas Porathe
Norwegian University of Science and Technology
Trondheim, Norway

Prof. Amy Loutfi
University of Örebro
Örebro, Sweden

Dr. Fahimeh Farahnakian
University of Turku
Turku, Finland

Cover Illustration: Photography by Mårten Lager.

This work was partially supported by the Wallenberg AI, Autonomous Systems and Software Program (WASP) funded by Knut and Alice Wallenberg Foundation.

ISSN: 1404-1219
Dissertation 65, 2021
LU-CS-DISS: 2021-01

ISBN: 978-91-7895-608-1 (print)
ISBN: 978-91-7895-609-8 (pdf)

Department of Computer Science
Lund University
Box 118
SE-221 00 Lund
Sweden

E-mail: marten.lager@cs.lth.e
Webpage: http://cs.lth.se/marten-lager/

Typeset using LaTeX
Printed in Sweden by Tryckeriet i E-huset, Lund 2021

Dedicated to my children
Tove, Vera, and Axel
and my beautiful wife Sara

Abstract

As for the automotive industry, industry and academia are making extensive efforts to create autonomous ships. The solutions for this are very technology-intense. Many building blocks, often relying on AI technology, need to work together to create a complete system that is safe and reliable to use. Even when the ships are fully unmanned, humans are still foreseen to guide the ships when unknown situations arise. This will be done through teleoperation systems.

In this thesis, methods are presented to enhance the capability of two building blocks that are important for autonomous ships; a positioning system, and a system for teleoperation.

The positioning system has been constructed to not rely on the Global Positioning System (GPS), as this system can be jammed or spoofed. Instead, it uses Bayesian calculations to compare the bottom depth and magnetic field measurements with known sea charts and magnetic field maps, in order to estimate the position. State-of-the-art techniques for this method typically use high-resolution maps. The problem is that there are hardly any high-resolution terrain maps available in the world. Hence we present a method using standard sea-charts. We compensate for the lower accuracy by using other domains, such as magnetic field intensity and bearings to landmarks. Using data from a field trial, we showed that the fusion method using multiple domains was more robust than using only one domain.

In the second building block, we first investigated how 3D and VR approaches could support the remote operation of unmanned ships with a data connection with low throughput, by comparing respective graphical user interfaces (GUI) with a *Baseline GUI* following the currently applied interfaces in such contexts. Our findings show that both the 3D and VR approaches outperform the traditional approach significantly. We found the *3D GUI* and *VR GUI* users to be better at reacting to potentially dangerous situations than the *Baseline GUI* users, and they could keep track of the surroundings more accurately. Building from this, we conducted a teleoperation user study using real-world data from a field-trial in the archipelago, where the users should assist the positioning system with bearings to landmarks. The users experienced the tool to give a good overview, and despite the connection with the low throughput, they managed through the GUI to significantly improve the positioning accuracy.

Acknowledgements

First of all, I would like to thank my supervisor Elin A. Topp, and my co-supervisor Jacek Malec, who have been supporting me and keeping me on track. Thank you, Elin, for all discussions regarding my research, for teaching me how to write and structure my papers, how to conduct user studies, and for taking the time to guide me in the research jungle. Thank you, Jacek, for your well thought through reflections about my research and for teaching me how to think about research.

Furthermore, I would like to thank all the supporting colleagues at Saab Kockums. My industrial supervisor Roger Berg has supported me with valuable knowledge about how my research fits into the bigger picture. He has connected me to the right persons within Saab, and has shown interest in my research. I would also like to thank Jens-Olof Lindh for all valuable discussions about user interfaces and autonomous ships, Jonas Rosquist for help with the autonomous vessels and data collections, and Tobias Almén for all support regarding the simulation kernel.

Thank you also to all colleagues, friends, and teachers of WASP, who have given me so much valuable knowledge and insights of the future world that is upon us!

I also want to thank my lovely wife and my children for all support and time you have provided, also when sharing the home as a workplace during the Covid-19 pandemic. Thank you also to my extended family, and friends for help and support.

This work was partially supported by the Wallenberg AI, Autonomous Systems and Software Program (WASP) [1] funded by Knut and Alice Wallenberg Foundation. The funding is gratefully acknowledged.

Popular Summary

As for the car industry, large efforts are being made to create unmanned ships. The main advantages are increased safety, cost savings, and better sustainability. Fully autonomous cargo vessels are expected to cross the Atlantic ocean before the year 2030. Until then, technology will gradually increase safety and replace work tasks that are nowadays conducted by humans. Even for unmanned ships, humans are expected to conduct essential work tasks, but then by teleoperating various systems.

In this thesis, methods are presented to enhance two building blocks that are vital for autonomous ships; one positioning system that is not GPS-dependent, and one tool for teleoperation of unmanned ships with a communication link with limited throughput.

The positioning system uses a technique called *Particle filter*. The particle filter compares measured depth and magnetism with known maps, and can with likelihood calculations estimate where the ship is located. It uses thousands of position estimations (particles) that are spread on the map, building a particle cloud. Suppose the ship, e.g., measures a depth of 10m, but the map shows a bottom depth of 20m where the particle is located. In that case, it is unlikely that the particle is placed in the correct location, which leads to this particle being discarded to the benefit of other particles having a better depth match. After each iteration, the particle cloud will re-shape to follow the correct position of the ship.

The system for teleoperation of unmanned ships receives the position from the supervised ship, as well as information about detected objects in the surroundings. This information, along with maps, is used to create a user interface within a 3D world, from which the ship can be teleoperated. By creating a virtual world from maps, less data about the surroundings need to be sent from the ship, minimizing the throughput need. A user study in a simulated world showed the user-interface in 3D led to fewer accidents and a better overall understanding of the situation than a traditional interface.

In the last step of the research, we combined the two sub-projects about positioning and teleoperation, using data recordings from a field-trial. The users of the teleoperation system used a 360° image of the real world to measure bearings to surrounding landmarks. These bearings were used by the positioning system. Despite the low-quality of the images due to the communication link with low throughput, they contributed to enhanced positioning accuracy.

Populärvetenskaplig Sammanfattning

Precis som för bilindustrin investeras stora belopp i att skapa obemannade fartyg. De huvudsakliga fördelarna är att säkerheten förväntas förbättras, vinsterna kommer att öka, samt att utsläppen kommer att minska. Helt autonoma fraktfartyg förväntas kunna korsa Atlanten helt obemannat innan år 2030, och fram tills dess förväntas tekniken gradvis förbättra säkerheten och ersätta arbetsuppgifter som idag utförs av människor. Även för obemannade fartyg förväntas människor utföra viktiga arbetsuppgifter, men då genom att fjärrstyra olika system.

I denna avhandling presenteras metoder för att förbättra två olika byggblock som är viktiga för autonoma fartyg; ett positioneringssystem som inte är GPS-beroende, och ett verktyg för fjärrövervakning av obemannade fartyg med begränsad dataöverföringskapacitet.

Positioneringssystemet använder sig av en teknik som kallas *Partikelfilter*. Partikelfiltret jämför uppmätt djup och magnetism med kända kartor, och kan med hjälp av sannolikhetsberäkning estimera var fartyget befinner sig. Till sin hjälp används tusentals positionsuppskattningar (partiklar) som sprids på kartan, vilket bildar ett partikelmoln. Om fartyget t.ex. mäter ett djup på 10 m, men kartan visar att det ska vara 20 m djupt där partikeln är placerad, är det osannolikt att partikeln är korrekt placerad, vilket leder till att partikeln tas bort, till förmån för partiklar som är bättre placerade. Efter varje iteration kommer partikelmolnet att uppdateras och omformas, och därmed följa fartygets korrekta position.

Systemet för fjärrövervakning av ett obemannat fartyg tar från fartyget emot position och information om detekterade omgivande objekt. Denna information, tillsammans med känd kartinformation, används för att skapa en 3D-värld och ett användargränssnitt, där man kan övervaka fartyget i den virtuella världen. Genom att skapa en virtuell värld utifrån kartor, så behöver mindre data som beskriver omgivningen sändas från skeppet, vilket minskar dataöverföringsbehovet. En användarstudie i en simulerad värld visade att användargränssnittet i 3D ger mindre olyckor och bättre överblick jämfört med ett traditionellt användargränssnitt.

I den sista delen av forskningsprojektet kombinerade vi de två delprojekten genom att använda inspelningar från en datainsamling i Västervik. Användarna använde sig av 3D-världen och en 360°-bild, presenterad i VR, till att mäta bäringar till landmärken i den verkliga omgivningen. Dessa bäringar användes sedan av positioneringssystemet. Trots att bilderna hade låg kvalité på grund av den låga dataöverföringskapaciteten, så ökade de positionsnoggrannheten.

Contents

Part I

Background

1 Introduction

There have been significant breakthroughs specifically within the last decade when it comes to autonomous vessels. Both industry and academia have made tremendous efforts to enhance the autonomous capability of cars, trucks, airplanes, helicopters, and now also of ships. There are many different advancements in technologies that boost this evolution. Sensors such as camera, radar, and *light detection and ranging* (Lidar) have become better and cheaper as larger volumes have been produced. Artificial intelligence (AI), and more specifically machine learning (ML) have evolved, and so have the graphical processing units (GPU) and neural processing units (NPU) that process the ML calculations. AI methods are often used to interpret sensor data such as visual information, but also for solving high-level tasks such as finding the most efficient route between two waypoints. While deploying unmanned vessels but still having humans in the loop, another essential ability is to have reliable communication between a human operator and the unmanned vessel. New satellite communication systems play an essential role for ships, as they can provide communication links almost anywhere in the world [2].

In this thesis, we focus on two research areas to enhance ships' autonomy capability. The thesis first introduces the naval domain and explains how autonomous ships can be beneficial, and then focuses on the specific research areas within positioning and teleoperation. In the positioning domain, we have investigated how to estimate a vessel's position without using the Global Positioning System (GPS). In the teleoperation domain, we have developed and investigated various types of GUI designs for teleoperation of an *unmanned surface vessel* (USV).

Throughout the years, the acronyms *unmanned surface vehicle* (USV), *autonomous surface craft* (ASC), and *autonomous surface vehicle* (ASV) have also been used to symbolize the same type of vessel as *unmanned surface vessel*. For larger ships, the terms *autonomous cargo ship*, *autonomous container ship* or *maritime autonomous surface ship* (MASS) are often used. Strictly speaking, there is a difference between *autonomous*, *autonomy*, *automation* and *unmanned*. Automation refers to the ability of a system to control a vehicle, like cruise control. For autonomy, the vehicle also needs the ability to respond to unexpected hazards. Autonomy and automation are used for creating autonomous vehicles, which are normally unmanned.

An autonomous vehicle by definition cannot be controlled by humans. In this thesis, we do not use this strict definition, but instead use a more relaxed definition, which is more in line with the literature about autonomous ships. We define an *autonomous vehicle* or *autonomous vessel* to be a surface vehicle or ship that, to a varying degree, can operate independently of human interaction. The definition does not restrict a human from, e.g., giving high-level goals via teleoperation technique to an *autonomous vessel*. We also use the term *unmanned vehicle*, as a reference to an unmanned, often autonomous, vehicle.

1.1 Thesis Outline

The thesis is divided into two parts; this part, named *Background*, and the second part *Research Papers*. The *Background* first contains an introduction to the areas *naval domain*, *unmanned surface vessels* (USV), and *navigation at sea*, followed by the *Research Questions* and the used *Research Methodology*. Then related work about *USVs*, *navigation at sea*, and *teleoperation* is presented. A brief description of the two sub-projects' investigations, implementations, and evaluations follows and is summarized by a discussion and conclusions. The second part consists of five peer-reviewed publications, named Paper I, II, III, IV, and V. Paper I and II present a method for estimating the own position at sea by comparing own bottom depth measurements and magnetic field measurements with known sea charts and magnetic field maps. Paper III describes the design of a graphical user interface (GUI) intended for teleoperation, which is evaluated in a user study described in Paper IV. Paper V combines the two sub-projects into a system where the user via teleoperation supports the positioning system.

1.2 Background Knowledge about the Naval Domain

As in all technology domains, the naval domain has its own eco-system with its nomenclature, regulations, and equipment. To set the research field, this section provides an overall summary of present ship technology, which is followed by the foreseen future of autonomous shipping with USVs.

1.2.1 Regulations for Safety at Sea

In order to enhance safety at sea, the International Maritime Organization (IMO) has introduced several conventions, recommendations, and other instruments [3].

Because of these, navigation and shipping work in the same way, almost independently of the location in the world. Larger ships have stricter requirements than smaller ones, and, e.g., small pleasure crafts have no technical regulations at all. Military ships typically fulfill the civilian regulations but are often equipped with more sensors and complement the technology with additional functions for higher precision.

The most important regulations are *Safety of Life at Sea* (SOLAS), which regulates safety at sea, *Convention on the International Regulations for Preventing Collisions at Sea* (COLREG), which regulates how to prevent collisions, and *The Standards for Training, Certification, and Watch-keeping* (STCW), which is a convention for training and watch-keeping regulating commercial ships. SOLAS covers various topics, e.g., ship safety, fire protection, radio communication, and navigation safety. In contrast to COLREG, the regulations from SOLAS only apply to vessels engaged on international voyages. Nations set the regulations themselves for domestic waters, which means that various nations can allow unmanned vessels locally even if international voyages are not allowed according to SOLAS yet. The regulations have been developed over many years and have slowly evolved to match available technology. A current problem with the implementation of COLREG for autonomous ships is that the regulation often is vague and is open for interpretation. Rule number 2 in COLREG basically says that the COLREG rules must always be followed, but they should not be followed when necessary to avoid an accident. Formulations like *the ordinary practice of seamen*, *good seamanship*, *early* and *substantial* are part of the regulation. Porathe [4] argues that these types of formulations should be quantified into nautical miles (NM), degrees of arc, and clock minutes to make it easier to integrate them into the autonomous systems.

A problem with changing the IMO regulations is that it takes a long time. Henrik Tunfors at the Swedish Transport Agency [5] estimates the IMO regulations will not be changed to allow autonomous ocean-going ships until after 2030, probably late 2030's, although there is a need to do so already.

1.2.2 Main Equipment for Navigation

There are many navigation sensors onboard a ship. The primary tool for positioning a ship is a Global Navigation Satellite System (GNSS) system. A GNSS receiver receives time signals from multiple satellites, and uses the variation of the delays, caused by the distances to the satellites, to calculate the ship's position. The most common GNSS system is GPS. Differentiell GPS (DGPS) is a GPS with enhanced accuracy, which also receives offset errors from calibrated coastal stations.

Even though the GPS can estimate the global position with great precision, it is *not* very accurate when estimating the current heading and speed. To compensate for this, ships are equipped with a magnetic compass or a gyrocompass. Some ships are also equipped with an inertial navigation system (INS), which works like a high precision inertial measuring unit (IMU). It can dead reckon the position even if the GPS signal is not currently available. The INS position is accurate after proper initialization, but if it loses connection to GPS, it gradually degrades in position accuracy as time increases. Some costly INS systems guarantee to have a smaller position error than 1.0NM (1,852m) after 72h of continuous operation time without GPS support [6].

Many regulations are related to the volume of a ship measured in gross tonnage (GT). As a size example, a trawler with 468GT is presented in Figure 1.1. A ship with 300GT shall be equipped with a speed log, as well as an echo sounder system [7], which measures the bottom depth so that it can alert when there is a risk for groundings.

Figure 1.1: GT is a measurement unit of volume, and 260GTs is equal to about $1{,}000m^3$ [8]. As an example, the trawler ORKA, seen in the image, has the volume 468GT.

A ship with a size greater size than 300GT shall have an X-band radar (frequency of 9GHz), and a ship with a size greater than 3,000GT shall also have a secondary S-band radar (frequency of 3GHz) [7]. SOLAS regulates, e.g., the functionality of the radar equipment and some aspects of how the GUI should be designed. The radar GUI is required to plot detected *tracks*, i.e., symbols tracking

detected targets. The system for presenting digital sea charts is called *electronic chart display and information system* (ECDIS), and can typically present tracks detected by radar and AIS. In Figure 1.2, an ECDIS GUI and a radar GUI are presented onboard a Combat Boat 90E. The radar is in stand-by mode.

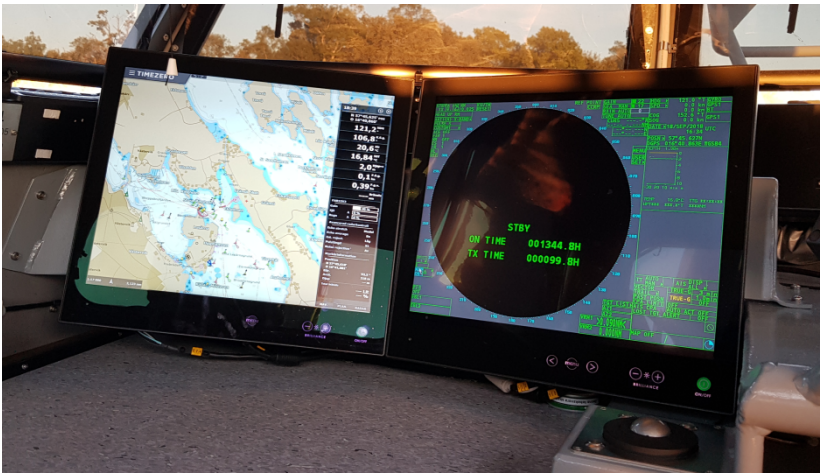

Figure 1.2: The ECDIS GUI and radar GUI onboard a Combat Boat 90H.

The ECDIS system presents the sea chart for the operator. It is highly regulated what information to present, how to present the information, and how the ECDIS system shall connect to all the navigation sensors. In many situations, it is beneficial for the operator to have a sea chart underlay below the radar plots, which is a function that is available in many radar systems.

A system called *Automatic Identification System* (AIS) is used to share knowledge about the own ship, such as id, position, heading, and speed. IMO requires AIS for all vessels above 500GT, for any vessels larger than 300GT on an international voyage, and for all passenger vessels regardless of size [9]. The AIS is connected to the navigation sensors and transmits and receives information to and from surrounding vessels. The ECDIS system typically presents the gathered information on the sea chart.

1.2.3 Main Equipment for Communication

Reliable radio communication is vital at sea. Mobile communication technologies such as 3G, 4G, and 5G are usable technologies in highly populated areas, as they can provide affordable communication with high throughput in the vicinity of

each base station antenna. Ships are often beyond these antennas' coverage area; hence, mobile communication standards are not used for regulated ship communication. For the same reason, Wi-Fi is not used either.

For safety at sea, SOLAS regulates what equipment needs to be carried to send and receive distress signals and safety information as well as for normal communication at sea. The regulation is called *Global Maritime Distress and Safety System* (GMDSS), and is mandatory for all passenger and cargo ships larger than 300GT on international voyages. All these ships need to have terrestrial radio communication equipment, and the ships that are going in specified areas far away from land also need to have equipment for satellite communication [3].

For autonomous vessels, communication will be vital. A mix of different communication techniques is foreseen to be used. In harbors, where a large amount of data are required to be sent to guide the remote officer in the complicated environment, 3G, 4G, 5G, or Wi-Fi can be used. Near the coasts, radio communication techniques with lower frequency, such as Very High Frequency (VHF), might be used to some extent. When near-shore communication is not available, satellite communication must be used, which costs much more. Smaller antennas with Fleet Broadband can provide data rates of between 150kbps to 432kbps. Larger, more costly antennas can provide more massive throughput. Inmarsat has, e.g., a solution for providing up to 50Mbps, but only 5Mbps for upload [10]. The downside is that both the equipment and every MB are expensive. SpaceX will perhaps provide more affordable Internet coverage for ships in the future, compared to current technologies. They are currently deploying thousands of satellites in their Starlink program, providing worldwide Internet coverage. It is assumed that they also will provide Internet connections for ships, as they are testing it on ten different ships (near-shore), including two unmanned ships used for rocket recoveries [11]. Compared to other satellite connections, a benefit with Starlink is the low latency, as the satellites are much closer to Earth. They are also foreseen to be cheaper to operate. Whether Starlink will provide communication links for ships with affordable connections and gyro-stabilized antennas remains to be seen.

1.3 Reasons for using Unmanned Surface Vessels

There are many reasons for developing large and small unmanned surface vessels (USV). Some of the most important reasons are *safety*, *cost*, *sustainability*, and *work environment* [2, 12], described in more detail below:

1.3.1 Safety

In the year 2018, 3,174 marine casualties and incidents were reported internationally. During 2011–2018, 230 ships were lost, 23,073 casualties and incidents were reported, 7,694 persons were injured, and there were 696 fatalities [13]. In the range of 89−96% of all collision accidents at sea since 1999 are caused by human errors. Human errors are causing 84−88% of tanker accidents, 79% of towing vessel groundings, and 75% of fires and explosions [14]. 54.2% of the casualties with ships are of navigational nature, such as contacts, grounding, stranding, and collisions [13]. With all these accidents caused by human errors, there is a considerable potential to increase safety by autonomy.

There are many sub-tasks at sea that could be replaced by machines. IMO regulations demand lookouts on the bridge to constantly look for potential surrounding threats. This is an important task, but can in the long term be very tiresome. By instead having cameras and radars with autonomous capability scanning the surrounding area, the safety is foreseen to increase [15]. Another critical issue is fatigue. Humans sometimes get tired and exhausted and can have other things on their minds. Alcohol, among other things, can also influence a human's judgment. In contrast, a machine can perform a repetitive task without degradation, and AI systems can even learn from the experience of the total fleet.

Piracy has also become a considerable problem for maritime traffic. Armed pirates board large ships and hold the crew hostage until a ransom is paid. An unmanned ship would be a much less attractive target for piracy, as there is no crew to hold hostage. It is also possible to make the ships more difficult to board and control for human intruders. Furthermore, it would be much easier to recapture the ship without any hostage.

Even if autonomy can decrease accidents, some aspects need to be addressed regarding this solution. Manned ships have evolved to minimize risks caused by human errors and failure of systems. These risks are still substantial when remotely controlling a vessel. Still, the global quality assurance and risk management company DNV GL believes the main risk factors for unmanned vessels are likely related to errors on sensors, software, and communication [16], which are errors that usually a crew can compensate for on a manned vessel.

1.3.2 Cost

It has already been concluded many times that autonomous ships will lead to significant cost savings compared to manned ships [2, 17, 18]. The MUNIN research

project has compared the highest costs for manned cargo ships, with cost estimations for unmanned cargo ships [19]. The results show that the crew salaries are the highest cost for manned ships, making it possible to save money when using autonomous ships. However, they estimate it will be slightly more expensive with land-based services for autonomous ships. They also estimate the more complex ship design of autonomous ships will increase cost more than the cost reduces by removing deckhouse and other units that come with a human workforce. In total, mostly because of the salary savings, the MUNIN project concludes there will be room for significant cost savings when going autonomous. Furthermore, as the technology used for autonomous ships gets more mainstream, the cost savings are foreseen to increase even further.

1.3.3 Sustainability

IMO has decided on a strategy in 2018 for reducing greenhouse gas (GHG) emissions, where they have set a vision to reduce emissions by at least 50% by the year 2050 compared to 2008 [20]. The vision is also to totally phase out GHG emissions as early as possible in this century. Most of the reduction will come from replacing fossil fuels with alternative fuels and/or energy sources.

Autonomous vessels will also contribute to the reduction of GHG emissions [19, 21–24]. The reduction will be made in various ways:

- By removing units such as the deckhouse, the ships can be constructed lighter or make room for more cargo. The removal of the deckhouse also makes it possible to apply a more streamlined design with less wind resistance, reducing fuel consumption. The hotel load, i.e., the power consumption needed for humans, will also be reduced. For large bulk carriers, the hotel load is typically around 5% of the total consumption, but for some other smaller ships, like offshore supply vessels, the hotel load can be as much as 50% of the total fuel consumption [16]. Rolls Royce Commercial Maritime estimates all these changes in total will reduce an average vessel's fuel consumption by 10−15% [25].

- When not having an expensive crew on board that want to come home to their families within a reasonable time, it will be easier to reduce the speed, leading to fuel savings, and thereby a reduction of GHG emissions. When reducing speed, more ships will be needed though to transport the same goods. The DNV GL ReVolt project found that two vessels with a

speed of 6 knots pollute 30−50% less GHG than one vessel operating at 12 knots [16, 26].

- If goods can be transported closer to their destinations with clean ship transportation, road transports and thereby GHG emissions can be reduced. Autonomy makes these transports easier and more efficient [24]. YARA Birkeland is one example of an autonomous vessel like this, which replaces a diesel engine with batteries. YARA Birkeland is a project in Norway, where a battery-powered ship will replace about 40,000 diesel-powered truck transports per year, with all their NO_x and CO_2 emissions [22].

Figure 1.3: The wind-powered sailing ship developed by Wallenius Marine. Image from Wallenius Marine [27]. Used with permission.

- Solar and wind power can also be used to reduce fuel consumption significantly. Łebkowski [23] elaborates on various types of autonomous ships that use these techniques. If speed is less important, it is actually possible to use wind as the main propulsor. Dhomé et al. [28] present a small autonomous sailing boat that is fully powered by wind, which they have tested for 19 days in Stockholm's archipelago. In Sweden, Wallenius Marine, KTH, and SSPA have jointly developed a wind-powered sailing ship,

which is currently tested in a 7m model of a scale of 1:30. It is initially designed as a car carrier with a capacity of 6000 vehicles, see Figure 1.3, scheduled to set sail in 2024. A crossing of the Atlantic ocean is expected to take 12 days, compared with the eight days it takes today's cargo ships to complete the voyage [27, 29]. The rigs will operate mostly autonomously, but at least initially, the ship itself will not navigate or operate autonomously [30].

1.3.4 Work Environment

The crew members will need new and more complicated skills as the mechanical and electronic complexity increases on ships. At the same time, fewer people, especially from developed countries, are willing to spend weeks or months away from home and family [2]. This has led to a large shortage of seafarers [31], and most parties agree that this will be a problem in the long run [18]. By using autonomous or remotely controlled ships, where ships are controlled from shore control centers (SCC) by specialists, the problem is foreseen to be contained.

1.3.5 Reasons for using Small Unmanned Surface Vessels

Even though most of the benefits are the same for large and small USVs, some benefits are valid in particular for small USVs. When removing the crew from small USVs, they will be very cheap to operate, making it possible to use a larger fleet of vessels. It will also be possible to cost-effectively operate vessels with very slow or no speed, as there are no humans on board that costs. It will be possible to use them in areas or weather conditions where it would be dangerous for humans to operate. Typical missions can be:

- Search and rescue (SAR) missions.
- Research Missions.
- Military reconnaissance missions.
- Coast Guard reconnaissance missions.
- Taxi services.
- Delivery of goods to customers in the archipelago.
- Sea level measurement.

1.4 Levels of Automation

To achieve the benefits of USVs, it is often easier to gradually improve the automation capability in an iterative approach, instead of going from no automation to full automation in one step. The same is true for the automotive industry, where the Society of Automotive Engineers [32] (SAE) has decided on six levels on automation, see Table 1.1. The automotive industry has widely adopted these levels and uses them to describe how much autonomy a car has.

Table 1.1: Levels of automation in the automotive industry [32].

Automation Level	Meaning
0	No Automation
1	Driver Assistance
2	Partial Automation
3	Conditional Automation
4	High Automation
5	Full Automation

On level 1, the systems are working to assist the driver in increasing safety. Driving-assistance features are already available at sea, but could be further developed. Sensor capability can be increased both for ships and cars with, e.g., ML approaches to interpret camera images. Furthermore, as the system can digitally interpret an increasing portion of the sensor data, better situational awareness can be created. This better situational awareness is difficult to visualize for a car driver, as the driver should look at the road. The car can provide the driver with warnings or break, however. On the other hand, for ships, it is possible to gradually enhance the GUI capabilities to guide the navigation officer more efficiently. By creating better GUIs for ships, which present the right knowledge to the operator at the right time, it is possible to reduce the cognitive load while giving the operator the best possible knowledge about the surrounding world.

When a car goes from SAE-level 1 to SAE-level 2, some autonomous driving features are enabled, but the driver needs to take immediate action when a dangerous situation arises. On level 3, the driver can safely read a book or watch a movie but must be ready to intervene when the car alerts the driver. On level 4, the driver can go to sleep, as the car is fully autonomous as long as it is in some defined areas

or situations. On level 5, the car does not need a steering wheel anymore, as the car can manage all situations by itself [33]. When the car has level 4 or 5, it is foreseen that accidents are reduced significantly. On the other hand, when the car is driving on level 2 or 3, it will be in command most of the time. However, when there is a challenging situation where the car cannot guarantee safety, such as when there is snow or fog, the human will need to drive. Hence, the human will not get as much driving experience as before, but will still need to master the most difficult situations. This might lead to accidents.

When the cars have almost full automation, level 4 or 5, there will still be situations that are hard to solve for the car. One example can be if a tree has fallen over a road, blocking it, far away from the city. The car will then slow down and stop but will perhaps not understand that it can go straight through the thin tree limbs. If the car is not equipped with a steering wheel, one possibility is to teleoperate the car from a control center. Then a human can remotely slowly guide the car past the tree. Even if the automotive industry does not speak much about this technology, most car companies that are developing autonomous vehicles also develop teleoperation technology [34–37].

Table 1.2: Kongsberg - levels of autonomy [38].

Level	Description
1	The computer offers no assistance, human in charge of all decisions and actions.
2	The computer offers a complete set of decision alternatives.
3	Computer narrows alternatives down to a few.
4	Computer suggests single alternative.
5	The computer executes the suggested action if human approves.
6	The computer allows human a restricted time to veto before automatic execution.
7	The computer executes automatically, when necessary informing human.
8	The computer informs human only if asked.
9	The computer informs human only if it (the computer) decides so.
10	The computer does everything autonomously, ignores human.

In the domain of autonomous ships, many different scales are defining the automation levels. Kongsberg has ten different levels ranging from when the human is in charge of everything, to full automation where the computer ignores human input, see Table 1.2 [38].

Table 1.3: SARUMS - levels of autonomy [39].

Level	Description
0	Human on board
1	Operated
2	Directed
3	Delegated
4	Monitored
5	Autonomous

The European Defence Agency's Safety and Regulations for European Unmanned Maritime Systems (SARUMS) group defines six levels, see Table 1.3 [39]. *0: Human on board* means that the vessel is manned and controlled by operators onboard. From level 1 to level 5, the vessel is unmanned. *1: Operated* means that the unmanned vessel is operated remotely by a human. In level *2: Directed*, the vessel has some intelligence and can support the operator and suggest actions. The remote operator is still in control. In level *3: Delegated*, the vessel is authorized to perform some tasks autonomously. It reports back to the human, which can abort or change the actions if needed. In level *4: Monitored*, the operator receives information from the vessel but can not change any actions. The vessel runs autonomously. In *5: Autonomous*, the vessel runs fully autonomously as in *4: Monitored*, but does not report to the human operator.

The class societies DNV GL and Lloyd's Register also have their definition of *levels of autonomy*. DNV GL have a scale with five steps, see Table 1.4 [40]. The focus is on whether the human or computer is in control or not. The human can be either remotely or onboard the ship. Lloyds Register has seven levels, see Table 1.5 [41] with definitions much resembling the scale from SARUMS.

IMO has defined the automation level in a short scale with four steps, see Table 1.6 [42]. It starts with level 1, which is the level of a current typical ship. Level 2 and 3 are defining a remotely controlled ship, where level 2 have seafarers on board. In level 4, the ship is fully autonomous.

Table 1.4: DNV GL - levels of autonomy [40].

Level	Description
M	Manual operated functions.
DS	System decision supported functions.
DSE	System decision supported function with conditional system execution capabilities.
SC	Self controlled function - the human is able to override the action.
A	Autonomous function - normally without the possibility for a human to intervene.

Table 1.5: Lloyd's Register - levels of autonomy [41].

Level	Description
1	Manual - No autonomous function.
2	On-board Decision Support - All actions and decision-making performed manually.
3	On & Off-board Decision Support - All actions taken by human operator, but the decision support tool can present options.
4	*Active* Human in the loop - Decisions and actions are performed with human supervision.
5	Human on the loop - Decisions and actions are performed autonomously with human supervision.
6	Fully autonomous - Rarely supervised operation.
7	Fully autonomous - Unsupervised operation.

Table 1.6: IMO - levels of autonomy [42].

Level	Description
1	Ships with automated processes and decision support.
2	Remotely controlled ships with seafarers on board.
3	Remotely controlled ships without seafarers on board.
4	Fully autonomous ships.

There are many similarities between the different scales. Some scales are quite coarse, and others quite fine-grained. It seems like the different organizations have tried to capture the important aspects of a multi-dimensional question into a single-dimensional scale. When they interpret these questions, they also focus on various aspects. For instance, IMO is probably focusing on legislation, and Kongsberg more on developing the system. Examples of the underlying questions seem to be:

- Are there seafarers on board?
- Which is the level of decision support?
- Is the vessel remotely operated?
- How many of the actions are decided by the computer compared to by a human?
- How many of the actions can the human override?

Even though many automotive manufacturers also develop tools for teleoperation [35–37], the SAE scale does not show it is important for car automation. In contrast to this, the scales for autonomous vessels clearly show that teleoperation technology is essential. It is foreseen that the vessels will move between automation levels. The vessel can, e.g., use full automation without teleoperation for long transits, and when arriving at the destination, the human can take control over the situation via teleoperation technique. This use-case can, e.g., be used during SAR missions to minimize human workload. Rolls Royce Commercial Maritime (now acquired by Kongsberg) sees teleoperation as a key technology in the transferring

process towards autonomous ships [2]. The functionalities to increase safety, situational awareness, and reducing the cognitive load are applicable for teleoperation applications in the same way as the functionalities apply to manned ships.

1.5 Building Blocks for Autonomous Ships

As for the automotive industry, autonomous ships comprise many building blocks. The vessel needs to have appropriate sensors, where the most important ones are:

- Navigation sensors
- Visual camera
- Infra-red (IR) camera
- Radar
- AIS
- Lidar

The system needs to interpret the sensor data, and most often, ML algorithms can be helpful in this step. To use ML, a large amount of training data needs to be collected. The system fusions the sensor data into tracks tracking targets, so that it does not present surrounding objects multiple times. These tracks are compiled into a situational picture, giving the machine a good situational awareness (overall picture) of the surrounding world. The machine then needs to decide what to do next and make up an effective plan to perform the actions. Autonomous vessels can learn from other vessels' experiences, and can together create a collective knowledge base on how to act in various situations.

1.6 The Path Towards Fully Autonomous Ships

Ships will not become fully autonomous instantly. It is instead foreseen that the capabilities will gradually improve. Rolls Royce Commercial Maritime foresaw the following steps [2]:

1. Year 2018 - Remote Support, operation of certain functions.
2. Year 2020 - Remote and Autonomous Local Vessel.

3. Year 2025 - Remote and Autonomous Short Sea Vessel.
4. Year 202X - Remote and Autonomous Ocean Going Vessel. (The time depends on regulatory constraints.)

To meet the timeline, the ships need to evolve in various fields. The overall tasks the autonomous ships need to master are:

1. Be able to estimate its position.
2. Know what is around the ship - Situational Awareness.
3. Predict what is going to happen next.
4. Make decisions autonomously or present the overall picture to a remote human who makes a decision.
5. Act according to the decision, e.g., make a turn.

As can be seen, there are many essential tasks for autonomous ships, which all need their sub-tasks and subsystems. We have chosen to develop two subsystems; a positioning system that does not use input from a GNSS system and a teleoperation subsystem to be used when communicating with limited throughput.

1.6.1 Positioning System without using GNSS System

To be able to determine the position at sea at all times is vital. The position can be determined in many ways. A GNSS system is commonly used for this, where GPS is the most common. The significant disadvantage with GNSS systems is that the navigation capability is dependent on the signals from the satellites both being received and being correct. The problem is that the threats of denial of GNSS services are increasing [43]. The transmission can be jammed unintentionally by commercial high power transmitters, ultra-wide-band radar, television, very-high frequency (VHF) radio transmission, mobile satellite services, and personal electronic devices. They can also be jammed or even spoofed intentionally by equipment, which is rapidly becoming more available. A crew on board a manned ship is constantly cross-checking the position by comparing clues, such as surrounding landmarks, with the sea-chart. An unmanned vessel is more vulnerable to a loss of the position estimation from the GNSS receiver. DNV GL believes the autonomous vessels may need an alternative positioning system as redundancy to GNSS [16].

In these cases, when the GNSS position is lost, it is vital to be able to estimate the position in another way. One way of doing this is presented in Papers I, II, and V.

1.6.2 Teleoperation with a Data Connection with Limited Throughput

At least in the next 20 years, it is foreseen that teleoperation of ships will be used to enhance the capabilities of unmanned ships. As the ships get smarter, the decisions can gradually be moved from the human operators to the machines. For huge ships far away from the coastline, satellite communication provides the communication channel for this. On small USVs, large satellite antennas would often be too bulky. The satellite communication equipment is also expensive to both buy and to use.

An alternative approach is to rely on VHF radio equipment when either situated near the coastline or when controlling the ship from a mothership. VHF transceivers are standard equipment at sea. The technique is affordable, small, and has a long range. The drawback is that the throughput is very limited, with the same capacity (9.6kbps) as a data modem provided before the year 2000. With this constraint in mind, we have developed a teleoperating interface presented in Papers III and IV.

A solution in-between large satellite antennas and VHF radio equipment is to use small satellite antennas. They are more expensive to use than VHF, but provide larger throughput (150kbps to 432kbps) and can be used far away from the coastline. The teleoperating interface presented in Paper V uses 48kbps, leaving more room for other teleoperation features.

Even though the interface is developed with teleoperation in mind, the design is also applicable for manned vehicles, where an augmented reality (AR) head-mounted display (HMD) would be used instead of a virtual reality (VR) HMD. In this scenario, I believe the same benefits with better safety, better situational awareness, and lower cognitive load would boost manned vehicles' performance. This provides scope for further studies.

1.7 Research Questions

The previous sections have described several challenges at sea that are likely to be reduced using USVs instead of manned ships. To actualize USVs, teleoperation is often seen as a critical technology to bridge the gap between *no automation* and *full*

automation. It is also vital to be able to determine the position at all times, both for manned and unmanned ships. All this leads us to our key research question:

How can smart techniques assist humans in operating unmanned ships?

This question entails the following more detailed questions:

1. How can a human operator teleoperate a USV through a low throughput connection, giving the user a good and safe overview of the situation while maintaining a low cognitive load?
2. How can a human operator gain trust in the USV's ability to navigate when using a low throughput connection? How does the operator know the position is correct?
3. When not using a GNSS system, is it possible to estimate the position accurately enough for navigation purposes by using a high accuracy INS, and measuring the bottom depth and the magnetic field?
4. When not using a GNSS system, is it possible to estimate the position accurately enough for navigation purposes by using a compass and speed log, and measuring the bottom depth and the magnetic field?
5. Can the human operator help the positioning system via a teleoperation system using a low throughput connection? Is the image quality sufficient for this?

1.8 Methodology

I have carried out my research according to design science research methodology (DSRM). Hevner et al. [44] define it as: *Design science research is a research paradigm in which a designer answers questions relevant to human problems via the creation of innovative artifacts, thereby contributing new knowledge to the body of scientific evidence. The designed artifacts are both useful and fundamental in understanding that problem*.

Much science starts with a hypothesis, and after tests with data, the researcher can prove or disprove the hypothesis, potentially leading to a theory. In DSRM, the researcher instead uses problem-solving to produce or enhance an artifact, much resembling normal engineering work in the industry. An evaluation follows the development of the artifact. The research produced provides information about how to improve artifacts so they become better than existing solutions. DSRM is common for architects, engineers and computer scientists [44].

Peffers et al. [45] have summarized multiple papers that have suggested elements for creating a process for the methodology. From this, they have created a comprehensive framework for the methodology. The framework suggests using six steps, visualized in Figure 1.4. The six steps are: *problem identification and motivation*, the *definition of the objectives for a solution*, *design and development*, *demonstration*, *evaluation*, and *communication*.

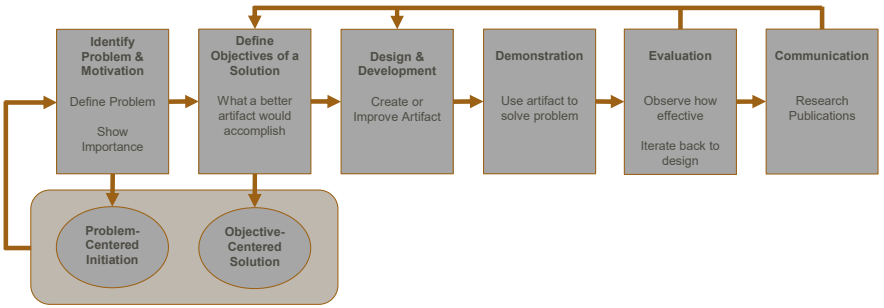

Figure 1.4: The process of using DSRM.

As USVs are not fully developed yet, there are still many problems to solve in this domain. I have focused on two problems: USVs will need a robust and thereby redundant positioning system that can be used in most places; hence only relying on GPS is not enough, and normal maps should be possible to use. USVs also need a teleoperation method. Smaller affordable vessels will more specifically need teleoperation that meets the limitation with a small satellite antenna that only can provide low throughput. These problems and objectives have been used as research entry points, seen in the circles in Figure 1.4. The research has resulted in two primary artifacts: a positioning system and a teleoperation system, which have been implemented in multiple iterations and versions for various purposes. The artifacts have been evaluated multiple times by myself with guidance from my supervisors, resulting in further iterations and enhancements. Our artifacts have been the positioning system in Papers I, II, and V, and the teleoperating GUI in Papers III, IV, and V.

After several iterations, the design was completed for a more extensive evaluation (with new findings). It was conducted, in Papers I, II and V, by comparing the performance of the particle filter using various settings and input data. In Papers IV and V, the evaluations have been conducted in user studies. Figure 1.5 shows to which sub-project each paper belongs to.

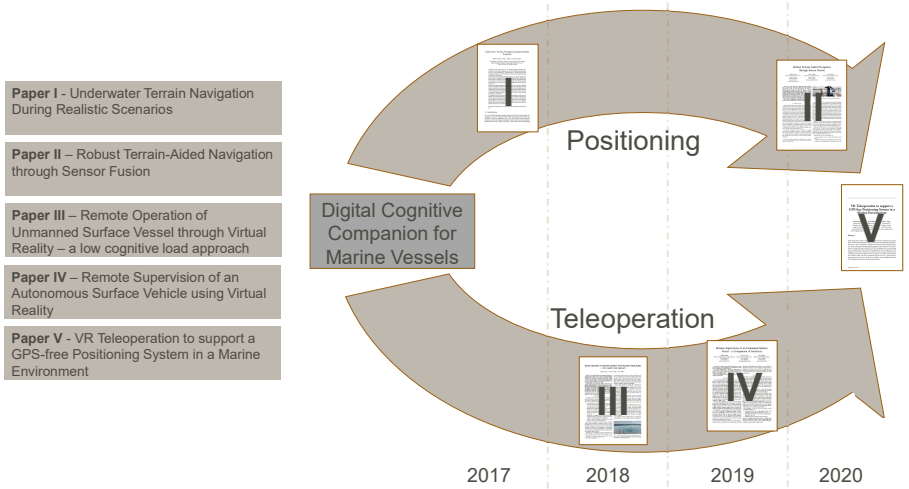

Figure 1.5: An overview of all five included papers, and which sub-project they belong to.

1.9 Contributions

This section describes the contributions of this thesis. Papers I, II, and V describe the positioning method, and Papers III–V describe the teleoperation tool. The main contributions are the following:

1. **Insights about using sea-charts for a positioning method for GNSS-denied environments.** For terrain navigation, the current state-of-the-art approaches use low-accuracy navigation sensors and a particle filter to compare bottom depth measurements with high accuracy terrain maps to estimate the position. The problem is that there are hardly any areas in the world where that kind of maps are available. Because of this, our particle filter algorithm does the opposite, namely relying on normal sea charts and using high-accuracy navigation sensors to compensate for the lower performance. While previous research on this topic has applied to nearly all vessels in areas where uncommon 3D terrain maps are available, our research applies to vehicles with expensive navigation sensors, but in nearly all areas. We show that the method provides accurate position estimation, complementing GNSS equipment (Paper I).

2. **A comparison of fusion methods for the positioning method for GNSS-denied environments.** Not only bottom depth measurements have been used for the positioning method, but also the magnetic field value. The input data for the Correction Step of the particle filter can be fused in various ways, and a comparison between methods is evaluated and presented (Paper I).

3. **A validation of the positioning method by testing it with data from a field-trial in real-world terrain.** We conducted a field-trial in Västervik to collect navigation sensor data, bottom depth measurements, magnetic intensity measurements, and 360° video files. Low-cost navigation sensors were used (compass and speed log). We then used these data to test the performance and robustness of the system, comparing different fusion methods. We found that using multiple domains instead of relying on a single source makes the system more robust (Paper II).

4. **Insights about a GUI for teleoperation of a small USV.** Teleoperation is vital in the path towards autonomous ships. State-of-the-art systems normally rely on a high throughput connection, through Wi-Fi, 3G/4G, or satellite, to transfer video streams. Instead, our developed teleoperation system relies on a low throughput connection to provide the user with surrounding objects in a 3D world. The GUI design in the 3D world is inspired by relevant research about navigation for manned ships. Our focus has been to provide valuable information for the operator to maintain a safe operation of the vehicle. By augmenting objects in the surrounding, and by rotating, e.g., the sea chart, the cognitive load have been reduced. The developed GUI can be presented in 3D on a computer screen as well as in VR. We conducted a user study to evaluate the performance, which showed the VR GUI and the 3D GUI outperformed a traditional GUI (Papers III and IV).

5. **A validation of the teleoperation system using field-trial data. Validation of the positioning system when guided by the teleoperation system.** The teleoperation system was evolved to comprehend support for using real-world data from the field-trial in Västervik. The user experiences the surrounding world from a virtual 3D world, using VR. The virtual world is complemented with an augmented real-world 360° image, with low quality, as the poor communication link limits the quality. A user study was conducted, where the users guided the positioning tool by taking bearings to surrounding landmarks. We found that the users experienced the tool, with

guidance from the 360° images, to provide a good navigational overview. Despite the low-quality images, they managed through the GUI to significantly improve the positioning accuracy (Paper V).

2 Related Work

The ultimate goal is to reach full autonomy for at least larger ships, where the ships can leave the harbor, cross the ocean, and then dock in a foreign port, all done safely and reliably without human intervention.

However, the ultimate goal lies several years ahead. To reach the goal, some technologies must evolve to make the ships smarter than today. Moreover, when having smarter techniques while the human is in control, it is important to enhance the interaction between the human and the machine. By this, the command can gradually be transferred to the machine. In this thesis, I am therefore investigating how unmanned ships are evolving, how ships can position themselves, how safety during navigation can be enhanced while reducing human workload, how situational awareness is created and transferred to the humans, and how USVs can be teleoperated.

2.1 Current Ship Projects with High Automation

Many civilian and military companies and academia are putting a great effort into developing USVs. To provide an overview of the field of USVs, example projects are presented below. These can also be seen as sample platforms that could use the research outcome from this thesis.

2.1.1 Small Unmanned Surface Vessels

The first small USV was named *ARTEMIS* and was developed in 1993 by MIT Sea Grant College Program [46]. Since then, many more small USVs have been developed by universities with increasingly complex capabilities. In general, universities need affordable sea platforms that can collect valuable research data at sea, and in this field, USVs plays an important role. The need for USVs has often been combined with research about how to develop functions for an efficient USV. The ALANIS project developed by CNR-ISSIA Genova is an example of this [47], as well as the Delfim project [48].

In Amsterdam, USVs called *Roboat* are used in a large-scale research project to explore the possibilities of using small unmanned vessels for transportation of goods and people [49].

Small USVs are also foreseen to be useful during security patrols and environmental monitoring. These missions are often costly because of the long-running missions. Camilli describes their USV, and how the robust design of a wave adaptive modular-vessel (WAM-V) is a suitable type of vessel for these missions [50].

Mayflower

Figure 2.1: The Mayflower Autonomous Ship. Image from IBM/ProMare [51]. Used with permission.

IBM UK and Promare have developed a trimaran ASV with a futuristic look, see Figure 2.1, which is planned to cross the Atlantic Ocean in April 2021 [52]. It is called Mayflower Autonomous Ship and is equipped with 30 sensors, including six cameras with image recognition capability. It has been trained with millions of nautical images collected from the Plymouth Sound in the UK and open-source databases [51]. The satellite communication link will not provide a connection with high throughput, and even if it is equipped with satellite communication and GPS, it is designed to not rely on it, using software for autonomous actions [53]. It operates according to the *Sense – Decide – Act* approach [51], where it first uses

its *sensors* to find obstacles and objects in the environment. It then *decides* what to do and finally uses its actuators to *act*, such as changing course and speed. It then repeats this approach iteratively, to constantly re-evaluate the situation.

2.1.2 Large Unmanned Surface Vessels

As already described in the Introduction on page 1, the industry sees considerable benefits when it comes to large USVs. In the car industry, environmentally friendly technologies such as battery-powered vehicles often go hand in hand with the automation level. The same is true for USVs. Here are a couple of examples of recent projects with large USVs, some also with sustainability focus:

ReVolt

The ReVolt project was launched in 2013 and is a battery-powered USV developed by DNV GL [26]. A 1:20 scale model was produced as a test-bench for sensor fusion and collision avoidance development by the Norwegian University of Science and Technology (NTNU). They designed it to move slowly at a speed of 6 knots, making it possible to reduce power consumption significantly.

Kongsberg

Figure 2.2: A battery container ship named Yara Birkeland, constructed to be fully autonomous. Image from Kongsberg Maritime [54]. Used with permission.

Another Norwegian company named *Kongsberg* is also developing techniques regarding USVs. The battery-powered USV YARA Birkeland, see Figure 2.2, has

already been built and will be fitted with the internal equipment before starting the initial testing [55]. This ship will initially be manned, remotely operated for some time, and then run autonomously after approximately two years. Kongsberg initially planned for it to be fully autonomous by 2022 but has currently stalled the project due to the Covid-19-related lockdown, which has influenced the needed infrastructure [5, 56].

Figure 2.3: A ferry with autonomous capability from Kongsberg. Image from Kongsberg Maritime [54]. Used with permission.

Kongsberg has also equipped a passenger ferry that crosses the Oslofjord between Horten and Moss with autonomous capability [57], see Figure 2.3. It still has a complete crew on board for safety but can perform all tasks, including docking, autonomously. The autonomous functions have also led to the ferry holding the time-table within 2 seconds during the initial test month.

In 2020, Kongsberg started a large project funded by the EU to develop and build two autonomous vessels to demonstrate autonomous capability for short sea coastal shipping and going between large cities in Europe's inland canal waterways [58].

Rolls Royce Commercial Maritime

Rolls Royce Commercial Maritime in Finland has also focused on autonomous ships and have developed an eco-system with various ship types. They believe the transit towards large USVs will become a disruptive change for the shipping industry. As already stated on page 16, they believe USVs will be used to fully

autonomously cross the Atlantic ocean before 2030 if regulations are changed to support the new technology in time [2]. They also believe human operators and expert technicians will be essential to cope with the fact that the machine still needs help in complicated scenarios.

Figure 2.4 shows their future concept with large autonomous ocean-going container ships, as well as their concept for teleoperation.

(a)

(b)

Figure 2.4: (a) Five large autonomous container ships, designed by Rolls Royce Commercial Maritime. (b) A human operator is supervising the USV when crossing the ocean, and is ready to guide the ship when necessary. Images from Kongsberg Maritime [54]. Used with permission.

In late 2018 a ferry, developed by Finferries and Rolls Royce Commercial Maritime, went between the cities Parainen and Nauvo in Finland, first navigating autonomously and then remotely operated when returning [59, 60]. In 2019, Kongsberg acquired Rolls Royce Commercial Maritime.

2.1.3 Military Unmanned Surface Vessels

In the military industry, USVs are foreseen to play an important role, complementing the manned vessels. The vessels are much cheaper to operate; hence, a larger number of vessels can be used. The USVs can be out at missions for a much longer time and can operate in more dangerous operations than manned vessels. Many military projects are evolving in the military industry, where mainly the USA and China are leading the way:

DARPA's Sea Hunter

The Sea Hunter, developed by *Defense Advanced Research Projects Agency* (DARPA) in the USA, is a prototype USV produced to support the development of a USV

that can chase submarines. They claim it will be about 40 times cheaper to operate compared to a destroyer. The US Navy estimates some ships will be operable before the year 2023, and they claim the USVs will always be under some sort of human control [61].

Saab Kockums

Figure 2.5: The Piraya from Saab Kockums.

Saab Kockums has some smaller speedboats that they have rebuilt into USVs called Piraya. They are equipped with sensors like cameras, echo sounder, communication equipment, gyros, etc. [62]. The Piraya can be seen in Figure 2.5. Saab Kockums also has a larger patrol boat, which has been rebuilt from a Combat Boat 90H, see Figure 2.6. It is equipped with systems for autonomous driving with safety personnel onboard. The plan is to develop a research system in which one autonomous patrol boat can work with several autonomous Pirayas [62]. These boats have been used in collaboration with the Wallenberg AI, Autonomous Systems, and Software Program (WASP), and have been used in both research subprojects in this thesis.

Unmanned Surface Vessels in China

China is also developing many military USVs. One example of this is the SeaFly-01, which has a maximum speed of 45 knots and can be used, e.g., for coastal

Figure 2.6: The patrol boat, rebuilt from a Combat Boat 90H.

patrols, armed confrontations, submarine detection, and water-quality monitoring [63].

2.1.4 Areas for Improvement

Even though many research projects exist with USVs, there are still many areas to improve. It is essential to develop systems for safe shipping. To do this, it is vital to determine the position at all times and conditions. It is also crucial to generate an accurate situational awareness and take the right action decisions at all times. While a human is in the loop, the human must have a reliable connection to the vessel. In the next two sections, related work for the two sub-projects of this thesis is presented, namely navigation and teleoperation.

2.2 Navigation at Sea

To accurately navigate at sea, many sub-tasks need to be mastered. The most fundamental thing is to know the ship's position. Knowing this makes it possible to find all fixed objects around the ship in the sea chart. The rest of the objects need to be discovered by sensors or humans. The ship's route then needs to be planned so that no groundings or collisions occur and to efficiently reach the destination.

2.2.1 Finding out the Ship's Location

There are many ways to find the correct location of a ship. A couple of decades ago, the most used method was to know the original position when leaving the harbor, and then update the position in the sea chart as the ship was moving a known distance in a direction according to the compass. This method is called *dead reckoning* (DR). In this technique, it is also possible to compensate for the vessel's estimated drift and sea current. However, as it is not possible to estimate the drift and sea current completely accurately, the position error starts increasing, as each position estimation is relative to the previous one, which means that the position error is accumulated over time.

It is possible to overcome this deficiency in various ways. By regularly determining the position compared to surrounding known landmarks, the accumulation of error is reset. But if landmarks cannot be found because the ship is on open water, there are two solutions. Either there is a need for increasing the accuracy of the dead reckoning by using better equipment (e.g., compass, speed logs, gyro, accelerometers, inertial sensors), or there is a need to use information about the environment that can be seen out on open waters. During the 18th century, celestial navigation was invented, which uses angle measurements to the sun, moon, and stars to greatly improve the long-term accuracy of navigation. Nowadays, celestial navigation has almost completely been abandoned because GNSS systems can accurately and efficiently determine the position. The most common and oldest GNSS system is GPS, but there are also other systems, e.g., Galileo and Glonass [64].

The GNSS systems have made it very simple to determine a vessel's position with excellent accuracy, but there are still some disadvantages. One substantial disadvantage is that the ship needs to rely on external information from the GNSS satellites, sent to the GNSS receiver onboard. It is quite simple to jam the radio reception from the GNSS satellites either unintentionally or intentionally, which results in that it is not possible to determine the position anymore. Even worse, it is possible to spoof the GNSS transmission information with advanced equipment, resulting in an incorrect position being provided [65]. In summary, GNSS systems estimate the position accurately most of the time. However, if a robust positioning system is needed, it is essential to complement it with some alternative positioning technique. The global quality assurance and risk management company *DNV GL* believes unmanned ships may need alternative positioning methods to convince authorities that their safety is satisfactory [16].

Terrain-Aided Navigation for Position Estimations

If a dependency on the GNSS system is not desired, other methods can replace or complement it. One method is to estimate the position using terrain-aided navigation (TAN) to compare known terrain, such as bottom depth and magnetic intensity, with known maps. Because it uses distributions that are highly nonlinear, non-Gaussian, and multimodal, classical methods with low computer power needs, such as Kalman Filter (KF), perform poorly [66]. By this, KF implementations, which were more common before the year 2000, have nowadays mainly been replaced by implementations of particle filters (PF) and point mass filters (PMF) [67]. We apply the multi-hypothesis filtering method PF, with the ability to tackle the mentioned difficulties [68, 69].

Some airplanes have used the technique for decades, where, e.g., Gustafsson et al. [70] describe how the systems on an airplane measure the altitude and compare it to a known terrain map with a PF algorithm, thereby estimating the position.

Many papers describe how ships can use the same technique, where the position is estimated by comparing the bottom depth with a known high-resolution 3D terrain map [68, 69, 71–76]. Many of these references focus on a use-case for autonomous underwater vehicles (AUV) [69, 71–76], where it is of particular importance to be able to navigate without a GNSS system. An AUV is typically equipped with a multibeam sonar to map the seabed, and as the equipment is already available, it has also been used for the PF [69, 71–74]. This increases the PF performance, as it is possible to evaluate if the bottom readings match the map with better precision [73]. Another way to improve the performance is to use the bottom's sediment layers, where the lower layers' depth most often varies more than the sea floor [77]. The problem with this technique is the poor availability of maps. We use a single-beam echosounder instead, which makes the use-case relevant for a substantial portion of ships.

The current research in this field has mainly focused on achieving good performance of the positioning systems when having a limited performance of the sensor suite, but nearly unlimited accuracy of the map. In these conditions, there is much research that shows that a PF can be used for position estimation [68, 69, 71–76]. The problem is that there are not that many areas where high-resolution maps have been created. Because of this, AUV deployments are typically preceded by a ship-based multibeam *bathymetry survey*[1] of the operating area, followed by processing of the data (outliers are removed), and the construction of the gridded bathymet-

[1]In a *bathymetry survey*, a 3D map of the sea bed is created by measuring the bottom depths in the area.

ric reference map [78]. This puts a considerable limitation on the usage of TAN technology. A solution to these two problems would be to use normal bottom sea charts and to complement the depth measurements with other measurements to increase the performance. We have done this in Papers I, II, and V by also comparing measurements from a magnetometer with a magnetic anomaly map. In Papers II and V, a digital compass and speed log was used for estimating the ship's velocity, resulting in quite a good positioning accuracy. To further increase the performance, we used a high-accuracy INS in Paper I, which is available mainly on some larger, often military, ships.

The PF performance also increases with varied terrain, but in some areas, the terrain is relatively flat, resulting in poor accuracy [77, 79, 80]. There can also be a problem with sample impoverishment in symmetric terrain, which can occur when the particle cloud is divided to follow paths that give similar measurement values. Teixeira et al. reduce this problem by using three different types of PFs to different terrain types [75]. Another difficulty that generally is not mitigated is that a PF is vulnerable to outliers in the maps or depth measurements. Peng et al. point out that these outliers can occur in many ways, and they describe how to alleviate the effect by using the Huber function when setting the importance weights for the PF [69].

By relying on multiple domains instead of only relying on depth measurements, we in our work mitigate the problems with sample impoverishment and problems with outliers.

The other domain that we work with is the magnetic field, which surrounds Earth, where each ferromagnetic element disturbs this field. These disturbances can be even more significant for indoor environments than the natural magnetic field of Earth [81]. For indoor environments, numerous ferromagnetic elements create a complex magnetic field where the magnetic vector varies greatly depending on the location. The magnetic field is also relatively stable if no major furniture or iron walls are moved. This information can be compared to a magnetic map using a PF. In conjunction with some sort of odometry, such as wheel encoders or inertial sensors, it has been possible to localize a human or robot [82]. Le Grand et al. [81] only use cheap smartphone sensors, and the magnetic field and acceleration are used for determining the position of the human user.

Although Le Grand et al. [81] and Frassl et al. [82] have explored indoor environments, the same technique applies to outdoor environments. The magnetic field does not fluctuate as fast as in indoor environments, but on the other hand, it is more stable because no furniture or building parts are moved around as in

the indoor environments. There are satellite maps available covering the entire magnetic field of Earth, and in some areas of the world, higher resolution maps have been created, e.g., by low flying airplanes. Hence, the magnetic field has been used in the PF algorithm in Papers I, II, and V to estimate the ship's position. Our implementation shows that the magnetic field intensity serves as a good complement to bottom depth measurements when it comes to improving the accuracy and robustness of the position estimation.

The bottom depth and the magnetic field are good candidates for the PF algorithm when estimating the position, but there are other alternatives. In addition to the bottom depth, Karlsson et al. [68] also used range measurements to land to support a PF algorithm. They measured the range to land by radar, and compared it to a sea-chart database. This idea was further enhanced in 2020, by comparing a digital elevation map of the surrounding area with either a 360° image around the USV [83], or with radar data [84].

It is also possible to compare the current gravity with a gravity anomaly map, which Musso et al. show can be beneficial for navigation [85]. Karlsson et al. also propose to use celestial navigation in combination with PFs, where, e.g., a star in a specific direction is present or not [68].

We have used bearings to landmarks in Papers II and V as a third data source to increase the robustness and the performance of the system.

2.2.2 Navigation at Sea and Cognitive Load

The traditional way to navigate at sea is to use a paper sea chart, showing an abstracted map of, e.g., islands, groundings, depths measurements, and sea marks. The paper sea chart is constructed with north facing up. During the last two decades, there has been a transition on bigger ships to use electronic chart systems, where the sea chart is instead visualized digitally on a computer screen. The main benefit is that the own ship's position, generally received from the GPS, is visualized at the correct location in the sea chart. The chart system can present the sea chart with either north-up or head-up.

The human ability to mentally rotate a map or sea chart so that the map's symbols can be matched with surrounding real-world objects is somewhat limited. Shepard et al. [86] showed that the time to recognize that two perspective drawings show the same three-dimensional shape is linearly increasing with the angular difference of the perspectives. This means that a human can match the ship's surrounding quite well when steering in the north direction and reading a north-up oriented sea chart, but will need more time reading the same north-up

oriented sea chart when steering in the opposite direction. Operators often choose to present the sea chart with north-up and the radar with head-up rotation [87]; thus, mental rotations are needed both between those two systems and between the systems and the surrounding real world. Using north-up orientation for the chart system is especially common for large vessels and when out at sea, but the usage varies depending on personal preferences.

Another way of presenting a map is to view it from the driver's perspective. GPS navigators for car drivers usually use this perspective. The benefit is that the driver can quickly understand which roads and buildings on the map that match the roads and buildings in the real world surrounding. By letting the machine do the mental rotations instead of the human operator, valuable time is saved, and many accidents are thereby likely to be avoided.

Porathe [88] compares four map views in a simplified indoor environment where persons navigate on a floor trying to navigate fast but striving to avoid simulated groundings. The compared views are:

1. Traditional paper sea chart (north-up).
2. Electronic chart system (north-up).
3. Electronic chart system (head-up).
4. 3D map with an ego-centric view.

The test results show that (4) gives the fastest decision-making, least amount of groundings, and is perceived as the most user-friendly. The results also show that using an electronic chart system gives better results than using paper charts.

Some user groups are more skilled than others when it comes to interpretation and mental rotations of maps, but for all user groups, (4) gives the best results, followed by (3), (2), and (1) [89]. Interestingly, persons who have long experience using electronic chart systems still perform better when switching to 3D maps, despite not being used to it.

With the results in mind, Porathe [87] suggests using a 3D map with the ego-centric view as a navigation aid, viewed on a computer screen or tablet. Witt [90] has also proposed a similar solution with a tablet where the ego-centric view helps the operator reducing the cognitive load.

Our GUI, presented in Papers III, IV, and V, with the ability to teleoperate a USV, is influenced by these results. We place the operator directly into the 3D world, where the surrounding world can easily be matched with the sea chart.

2.3 Teleoperation of Ships

Teleoperation can be used for remote controlling, e.g., industrial robots [91], unmanned ground vehicles (UGV) [92–96], cars [34–37, 97–99], drones [100, 101] or ships [102]. The different fields have various delay requirements. Lu et al. [93] investigate how this delay time affects the teleoperating capability when teleoperating a UGV. The studied papers [93, 97, 99, 103] elaborate on how to perform teleoperation of cars, where it can be even more difficult in city traffic due to its high dynamics. Several research papers propose methods to compensate or predict the teleoperated vehicle's pose (position and orientation) to mitigate the latency problem [104–106]. In general, ships are not as vulnerable to latency as cars. Still, as we need to accurately measure bearings to surrounding objects in the subproject described by Paper V, we also need to compensate for the delay by using the course and speed to predict the position.

Figure 2.7: A GUI used for teleoperation of a tug in Copenhagen. Image from Kongsberg Maritime [54]. Used with permission.

Another constraint is the communication link's throughput capacity. Larger ships can use bulky and expensive satellite antennas, where every MB is expensive to use. Ships that are close to a base station can also use mobile connections or Wi-

Fi. Wi-Fi is also often used for demonstrating autonomous and remote capability. Kongsberg demonstrated teleoperation of a tug boat in the port of Copenhagen in 2017 [107], see Figure 2.7. In 2018, they remotely controlled a large car ferry, using a similar GUI design [60]. In our work, we can not rely on streamed video, as we want to create a GUI for small affordable vessels.

While teleoperating a machine/robot, it is also important to improve the human's perception of what the machine's sensors detect of the surrounding world. Williams et al. [108] elaborate on how VR, augmented reality (AR), and mixed reality can strengthen visualization, and thereby the total communication between a robot and a human, and how various viewpoints, e.g., the ego-centric view can be used. Hedayati et al. [100] have a more specific use-case, where they explore how they can use AR for augmenting a drone's field of view for a user collocated with the drone. When not collocated, VR is often a better presentation technique. Hosseini et al. [98] and Shen et al. [97] show how VR can enhance situational awareness when driving a car.

Some research has also been investigating how AR can reduce cognitive load when navigating. In these applications, head-mounted displays (HMD), generally with see-through technology, augment important information, such as sea lanes, conning information, and information about own and other nearby ships from, e.g., the AIS information [109–113]. In our application, AR is not applicable because we can not look at the surrounding real world as we are remote from it. Instead, we use the approach to augment the critical information in the virtual environment (VE).

3 Implementation and Evaluation

This thesis consists of two sub-projects; one positioning system and one teleoperation system. Each of the sub-projects has its own design and implementation and has resulted in several papers. An overall design description is given in this chapter, while the details are found in Papers I – V, included in this thesis.

3.1 Positioning System

The positioning system sub-project uses a particle filter (PF) to estimate the position of a vessel, which we developed in many iterations. The initial algorithm and application, as well as the first enhancement, are described in publications not included in this thesis [114, 115]. It was then further evolved into the versions in Papers I, II, and V.

The method presented in these papers uses a PF to compare the measured bottom depth and magnetic field measurements with known maps to estimate the ship's position. The PF algorithm has the following steps:

1. **Initialization** - Generate N particles and give them a random starting position around a manual estimation of the starting position.

2. **Prediction** - Move each particle according to the velocity vector predicted by the navigation sensors (INS in Paper I, and compass and speed log in Papers II and V). Then move each particle according to a random velocity vector to simulate the velocity vector error of the navigation sensors.

3. **Correction** - Calculate the weights for each particle given the maps and each particle's position, see Figure 3.1. The weights are calculated for the depth, magnetic intensity, and a combination of those two. Normalize the weights.

4. **Re-sampling** - The particles are re-sampled according to a predefined distribution from subsets, see Figure 3.2.

5. **Iteration** Go to step 2.

3.1.1 Correction Step

In the third step of the algorithm, *Correction*, the measured values are compared to known maps to estimate the position. The process of how this works in the developed algorithm is presented in Figure 3.1. It shows how the weights for the PF are calculated separately in the *Depth Workflow* and the *Magnetic Workflow*. The figure shows the workflow of Paper I explicitly. The difference is that in Papers II and V, the ground truth for bottom depth (a4) and magnetic field (b1) are not simulated, but measured from real-world terrain.

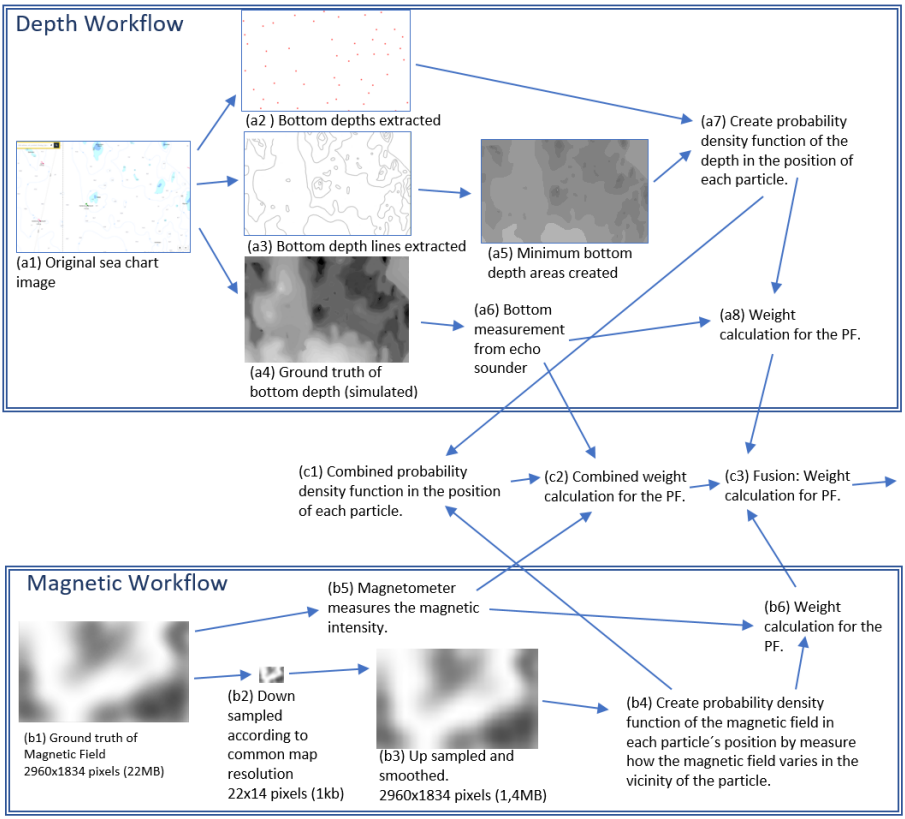

Figure 3.1: The process of how to go from a sea chart and a magnetic field map, to weights, used in the *Correction Step* in the PF.

Depth Workflow

The figure shows the original sea-chart in (a1). From the sea chart, all bottom depth points are extracted (a2), and so are all the bottom depth lines (a3). From the bottom depth lines, a *Minimum Bottom Depth Map* is created (a5), where the application can look up all minimum bottom depth at all positions. The application then creates a probability density function (PDF) (a7), for each location of the particles. For this, it uses either only data from (a2), or a combination of data from (a2) and (a5), depending on if the bottom lines should be used or not. A simulated map for *ground truth* has been drawn in a drawing tool, with smooth color gradients (a4). The purpose of this map is to resemble the real world terrain as much as possible. As the ship moves in the map, it measures the alpha-value from the grey-scale ground truth image, which is converted to a bottom depth measurement (a6). The bottom depth measurement (a6) is then used in combination with the PDF (a7) for each particle, to calculate the weights for each of the particles (a8). (a8) answers the question; **How likely is it that the specific particle is placed at the correct location, given my measured bottom depth?**

Magnetic Workflow

A ground truth map of the magnetic values is drawn in a drawing tool (b1), with the intention to as much as possible resemble a real-world variation of the magnetic field. As the ship moves, the application measures the magnetic field in the map's correct location (b5). High-resolution maps are seldom available, though; hence, a low-resolution map is created by downsampling the ground truth, where each pixel corresponds to a square with a size of 185m$\times$185m (b2). (This is the same resolution as the real-world map used in Papers II and V.) The downsampled map is used to estimate a high-resolution map by upsampling and smoothing it (b3). The application creates a PDF for each location of the particles (b4). It calculates weights for all particles (b6) by comparing the PDF (b4) with the measured magnetic field (b5). (b6) answers the question; **How likely is it that the particle is placed at the correct location, given my measured magnetic field?**

Fusion of Workflows

From (a7) and (b4), the application creates a combined PDF (c1). This PDF is used in (c2) to calculate weights for each particle. (c2) answers the question: **How likely is it that the particle is placed at the correct location, given my measured bottom depth and the measured magnetic field?** It then fuses the weights from

bottom depth (a8), the magnetic field (b6), and the combined weights (c2) into a combined weight (c3).

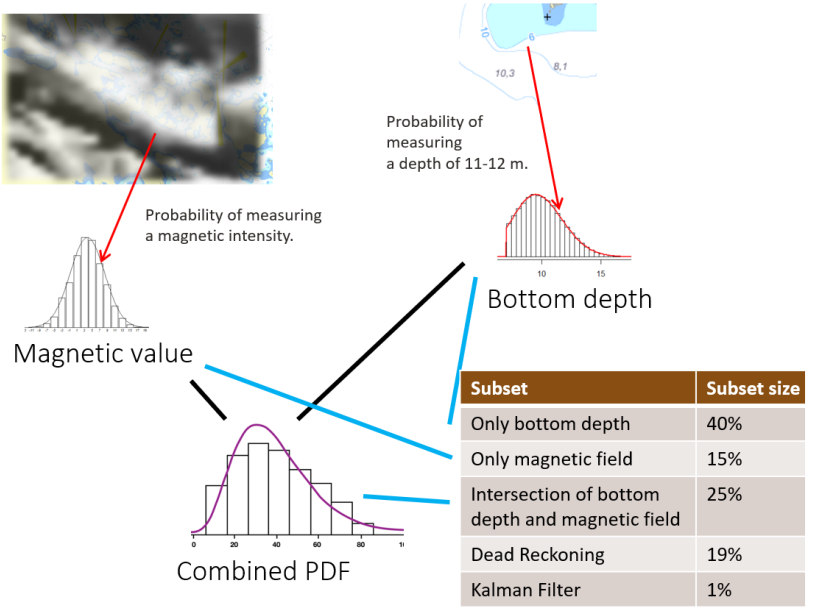

Subset	Subset size
Only bottom depth	40%
Only magnetic field	15%
Intersection of bottom depth and magnetic field	25%
Dead Reckoning	19%
Kalman Filter	1%

Figure 3.2: By comparing the sensor measurements with maps, PDFs are created for depth, magnetic field, and a combination of those. The table shows an example of subset sizes which are used to determine how large portions of the particles that should be re-sampled using each PDF.

In the last step (c3) in Figure 3.1, the application fuses the results from the different weights. It does this by evaluating a portion of the particles according to each of the methods. In Figure 3.2, it can be seen how the application creates PDFs for each particle's location. For the bottom depth, the PDF shows how likely every bottom depth is, given the sea chart. The PDF for the magnetic field shows how likely various magnetic field values are. When measuring a bottom depth or a magnetic field value, it then uses the PDFs to estimate how likely the bottom depth or magnetic field value is. The combined PDF is used to figure out how likely a particular bottom depth measurement and a magnetic field measurement are in combination. The subset table is used to determine how large a portion of the particles should be evaluated according to each method. In the example, 40%

of the particles are evaluated according to bottom depth (a8), 15% according to the magnetic field (b6), 25% according to Combined (c2), and 19% are just dead reckoned according to the navigation sensor movement. 1% of the particles are re-created in the location of a Kalman filtering of the particle cloud. In Papers I and II, we compare how the performance changes when using various sizes of these subsets.

3.1.2 Example Images from Running the Program

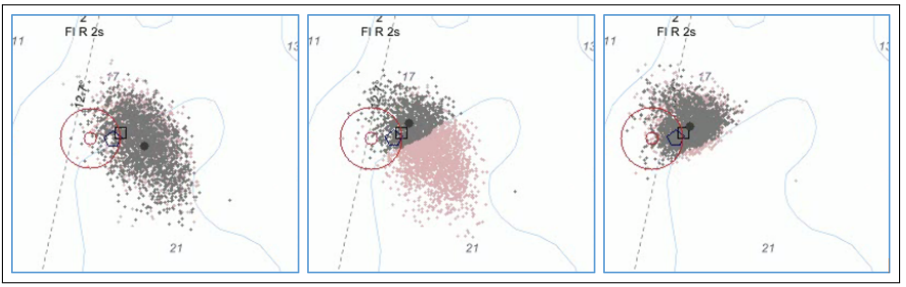

Figure 3.3: The figure shows a sequence of images when the ship is going in the west direction. For a symbol legend, see Table I.2 on page 94. In the left image, the particle cloud is spread to the east from the true position. The center image shows how the particles to the south-east of the 20m bottom depth line are discarded, when the echo sounder system onboard the ship measures a depth of below 20m. In the right image, the discarded particles are no longer shown.

The images in Figure 3.3 show how the ship moves west in the simulations from Paper I. After passing the 20m bottom depth line, the PF can discard many of the wrongly positioned particles (to the south-east) and is thereby able to estimate the position more accurately.

A comparable situation to Figure 3.3 is shown in Figure 3.4, from Paper II. A sequence of images from the GUI used in Paper II is shown. The boat, visualized with a boat icon, is moving west. In the first image to the left, the particle cloud is somewhat misplaced above the true position, but as the bottom depth measurement does not correlate with the sea chart, it moves closer to the correct location. In the last image, to the right, the particle cloud covers most of the ship, indicating the correct location.

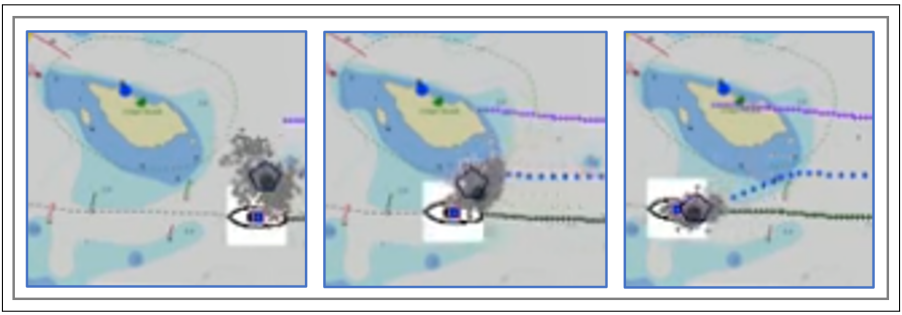

Figure 3.4: A sequence of images from the GUI used in Paper II, showing how the particle cloud corrects the position estimation by comparing the bottom depth and the sea chart.

3.1.3 Performance of the Algorithm

The algorithm was tested in various ways and has been updated between the different papers that describe it. In Paper I, an accurate INS was used as the navigation sensor. These are very accurate in the beginning but then exponentially degrade in performance. All the work related to Paper I was done in simulation. In Paper II, a compass and a speed log were instead used as navigation sensors. Compass and speed log do not degrade in performance with time, so the sensor performance was stable in these simulations. To test the robustness of the system, we added some drift speed to the test. The simulations made to evaluate the performance are based on real-world data recorded outside Västervik. In Paper II, we conducted some tests to evaluate how bearing measurements to known landmarks influence the positioning performance. In Paper V, test subjects, in a user study with a VR-interface, carried out these bearing measurements using recordings from the same field-trial in Västervik.

The results from Paper I show that when fusing the different PF methods in a 20h long test, the mean of the position errors for the high-end INS has been calculated to be 10.2m when using the bottom depth lines, and 30.5m when not using them. This accuracy is most often good enough to use for navigation at sea. After around 20h, the performance of the INS is so bad that the PF's position accuracy is significantly reduced. Table 3.1 shows a 24h test setup from Paper I. In, e.g., test (1), all the particles are evaluated according to the bottom depth in the Correction Step, giving a mean position error of 22.5m. In (2), all the particles are evaluated according to the magnetic field measurements, giving a worse

Table 3.1: Test setup and results for a 24h long test with a high-accuracy INS.

Evaluation method	**(1)**	**(2)**	**(3)**	**(4)**	**(5)**
Depth	100%	0%	0%	30%	25%
Magnetic Field	0%	100%	0%	15%	10%
Depth & Magnetism	0%	0%	100%	55%	65%
Skip PF (Only INS)	0%	0%	0%	0%	0%
KF Mean (m)	22.5	28.9	19.8	17.0	**16.8**
KF maximum error during 24h (m)	120.0	72.9	77.9	74.0	84.9

accuracy of 28.9m. In test (4) and (5), the particles are evaluated by combining various methods, giving better performance with a mean position error of 17.0m and 16.8m. The PF performance increases when using the more accurate source Depth, compared to the Magnetic Field. By also using multiple fused sources, the accuracy is increased even further.

In Figure 3.5, a graph shows two test runs of the program, where the PF uses a combination of evaluation methods for the Correction Step. The difference between the two graphs is that one of the test runs used the information from the bottom depth lines in the sea chart, and the other did not. Even though the performance decreases while not using the depth lines, the PF still manages to maintain a mean position error of only 34.0m. The graph also shows that the INS's performance, and thereby the performance of the PF, gradually decreases after 1200min (20h).

For Papers II and V, real-world data and maps were used by simulations to evaluate the algorithm. The data were collected in a field-trial outside Västervik in Sweden. Compass and speed log were used instead of the INS, making the technique affordable and suitable for smaller vessels. In the simulations from Paper II, we compared how the drift speed influences the algorithm's robustness when using various subset sizes of the PDFs. Figure 3.6 shows various drift speeds on the x-axis, which have been added to test the robustness. As shown in the graph, the best robustness throughout all drift speeds is gained when combining all the different PDFs (blue line) instead of using a single subset at the time. Especially when having a larger drift speed, the PFs relying on individual PDFs gave large position errors.

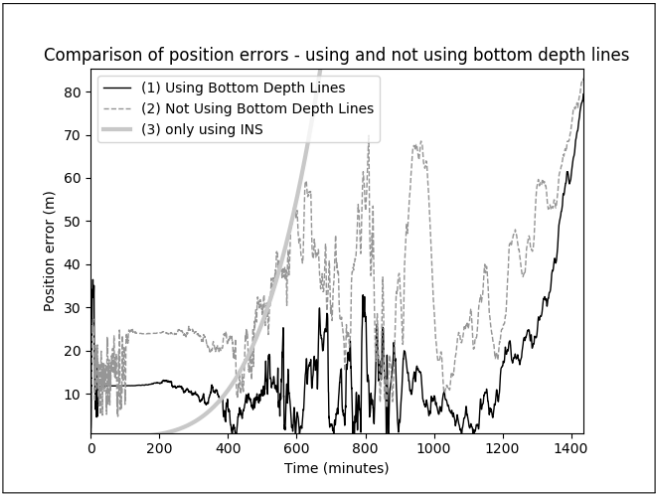

Figure 3.5: The PF uses the high-accuracy INS. The performance is influenced by using or not using the bottom depth lines in the sea chart. Even though the performance is lower when not using them, the PF still manages to track the correct position during the 24h test. A mean position error of 34.0m is maintained.

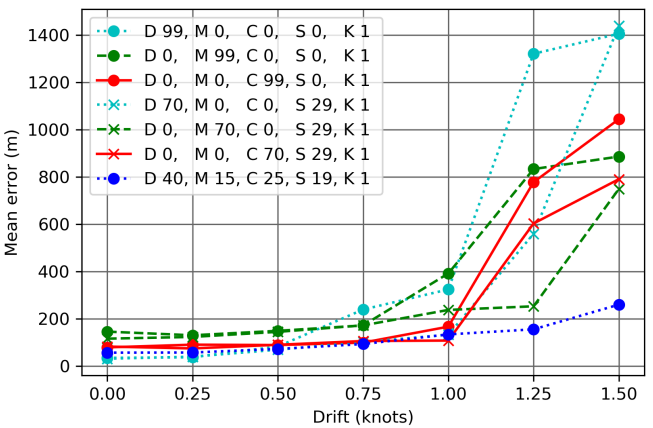

Figure 3.6: The diagram shows the results from 49 simulations when using various mixes during various drift speeds. The PF which re-samples from multiple subsets (blue line) has the best robustness, and performs well during all drift speeds. It has a good accuracy for all drift speeds.

In Paper V, the same algorithm was used as in Paper II, but always supported with bearings to landmarks. These bearings were manually detected by users using a VR setup to compare a surrounding virtual world with a recorded 360° image. A simulated drift speed of 0.5 knots was used. During a 20-minute long test for the 16 users conducting the user study, the mean position error was around 35m.

3.2 The Positioning System using Machine Learning

The fusion of different PF domains described in Paper I and II is made by properly setting the subset sizes. The subset sizes have been manually set after gaining experience and understanding of the algorithm. An interesting research topic is exploring if it is possible to automatically set these subset sizes, e.g., by letting a Machine Learning (ML) algorithm examine the current situation and trying to learn which proportions result in the best performance. An implementation and some initial tests have been conducted limited by insufficient training data availability; hence it has not resulted in any published papers. It is still described in this section, to give a complete picture of the work done.

3.2.1 The Approach

If the terrain is flat, a PF using the depth domain performs poorly [77]. In contrast to this, if passing an underwater rock, the PF using the depth domain performs well. However, to pass an area with lower underwater terrain than the surroundings does not automatically imply better performance. This is because deeper areas are not necessarily displayed in the sea chart, as they do not endanger any vessels. It is not easy to know which type of depth terrain and magnetic intensity terrain that positively influence the PF. By instead letting an ML algorithm evaluate the surroundings, we hypothesize it should be able to learn when either the depth or magnetic domain works well so that it could optimize the subset sizes for it. What can be available for the ML algorithm is:

- Own estimated position.
- The current particle cloud.
- The surrounding sea chart around the estimated position with bottom depth lines and individual bottom readings.
- The surrounding magnetic anomaly map around the estimated position.

- The current measured bottom depth.
- The current measured magnetic intensity.

The ML solution can be implemented in many ways. We initially tried to implement it as a regression problem, i.e., to get a float value describing how well depth or magnetic field would perform compared to just dead reckoning the position. As we do not have much training data, this design did not perform well after training. Instead, we re-implemented it as two separate classification problems. The first network classified depth images and either proposed using depth or dead reckoning of the particles, and the other network classified magnetic images and proposed using magnetic or dead reckoning. As convolutional neural networks (CNN) have proved to be efficient when classifying images [116–118], we use them for our classification problem.

It is important to guide the ML algorithm as much as possible by preparing the images. As the bottom depth varies much depending on where the ship is located, we suspect it is better to create images with a bottom depth relative to measured bottom depth. The images will then look similar independent of if it is, e.g., 20m deep or 70m deep. If, e.g., the echo sounder measures a bottom depth of 20m, and the sea chart around the estimated position shows depths of between 10m and 30m, 20m are subtracted so that a map with depths between -10m and 10m is created. Individual bottom readings are handled in the same way. Similarly, the current magnetic intensity is subtracted from the nearby magnetic anomaly map. We also believe it is important for the CNN to interpret the shape of the particle cloud; hence this is saved into the images as well. As digital images are coded with three layers (red, green, and blue), the data is coded into these layers. The layers of the depth images contain:

- Bottom depth lines relative to own bottom depth (blue).
- Bottom depth readings relative to own bottom depth (green).
- Particle cloud (red).

The magnetic images contain:

- Magnetic anomaly relative to own magnetic field (green)
- Particle cloud (red)

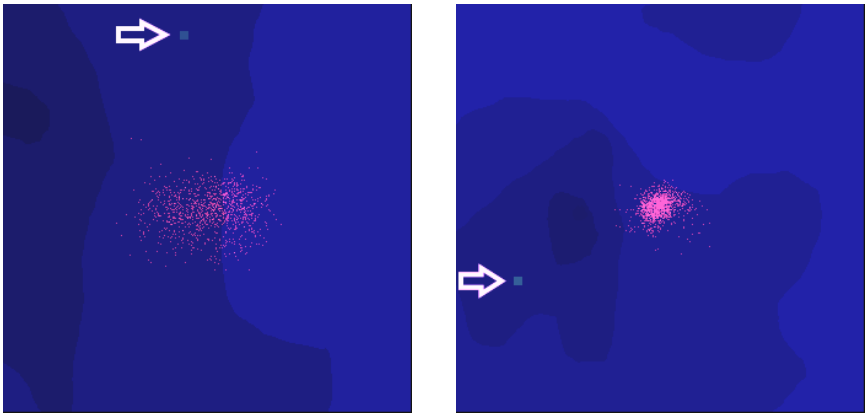

(a) (b)

Figure 3.7: (a) A depth image used for CNN interpretation. The particle cloud is quite spread. A depth reading can barely be seen as a large dot in the top, with a green color representing the bottom depth in this point. An arrow (which has been added for visualization purpose) point towards it. (b) Another depth image with a more compact particle cloud. An arrow points towards a depth reading.

Because the bottom depth lines determine minimum depth in each pixel, and the value is colored blue, each pixel will have a blue value. In contrast, the green and red data are only available in a few pixels, hence the depth images are mostly blue. For the same reason, the magnetic field images are mostly green. In Figure 3.7, two examples of depth images can be seen with the particle cloud in the middle. The various blue shades show the bottom depth lines, and the large dot at the top of the left image indicates a bottom depth reading in the sea chart.

Figure 3.8 shows two examples of magnetic images. The various shades of green indicate the magnetic field is varying on the map.

The simulated ship went around in the map to train the network, collecting images for depth and magnetic field together with data showing how the performance changed when comparing depth versus dead reckoning or magnetic field versus dead reckoning. Figure 3.9 shows the map where the application collected the data. For each image it saved, it drew two dots in the position. If depth was better to use than dead reckoning, it drew a blue dot, otherwise grey. If the magnetic field was better to use than dead reckoning, it drew a red dot, otherwise grey. The figure gives a good visualization of that there are some areas where it is better

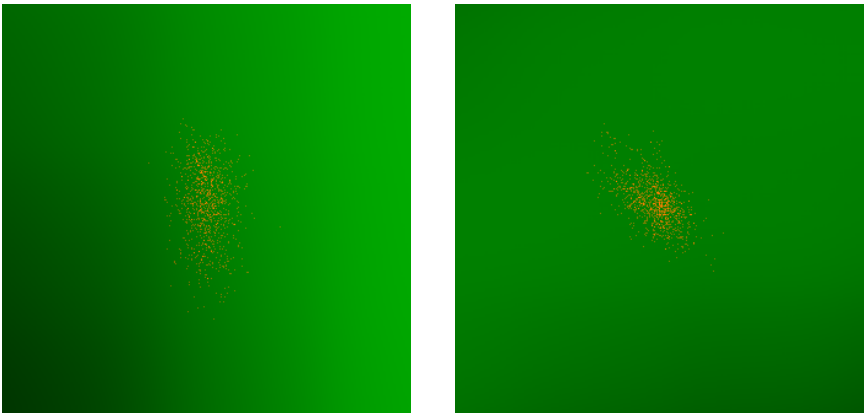

(a) (b)

Figure 3.8: (a) A magnetic image used for CNN interpretation. The various shades of green indicate the varying magnetic field in the map.(b) Another magnetic image.

to use various subset sizes. The application saved the results as float performance values, so they could be used for training of the CNN.

3.2.2 Implementation of the CNN

We implemented the CNN in Keras using Python. 40'000 images were collected with related performance measurements used for the loss function. Half of the images are showing depth and half magnetism. Half of the images showed situations where it would be better to dead reckoning the particles. The images had a size of 100×100 pixels. The classification networks were implemented identically. In the first four layers, CNN layers were used, which were then flattened in the last three layers, see Figure 3.10. In the output layer, one value (0.0–1.0) showed if the PF should trust in depth/magnetism or if the particles instead should be dead reckoned.

To prepare the images for training, we separated them into classes (e.g., depth and dead reckoning) depending on if the saved performance value gave a higher value than 0.5 or not. A value of 0.5001 should be classified as depth, and 0.4999 should be classified as dead reckoning, although the images could be almost identical. The initial tests using the PF, which relied on the CNN, performed poorly. As a comparison, an example of training cats and dogs is given. If having multi-

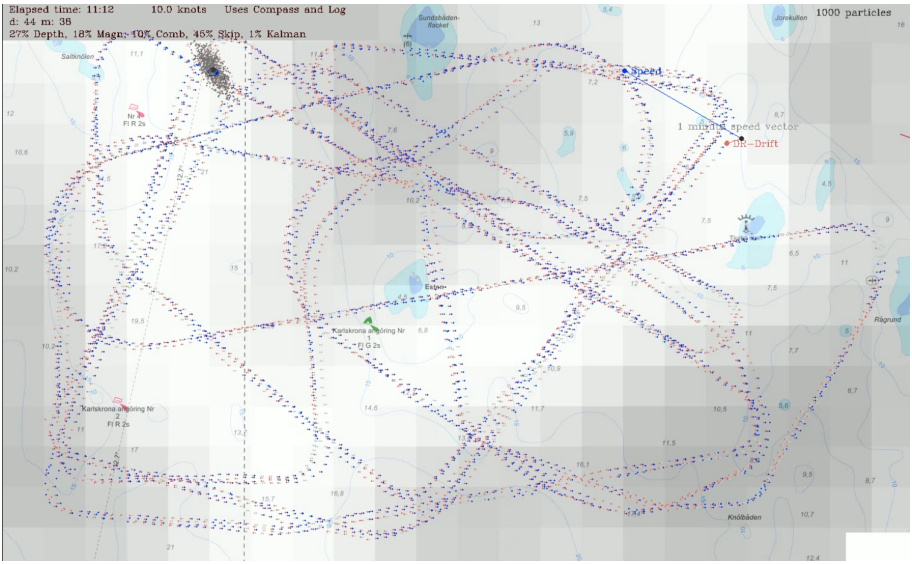

Figure 3.9: The GUI of the positioning system. The blue and red dots indicate that it is better to use depth and magnetic field, respectively, compared to just dead reckoning the particles.

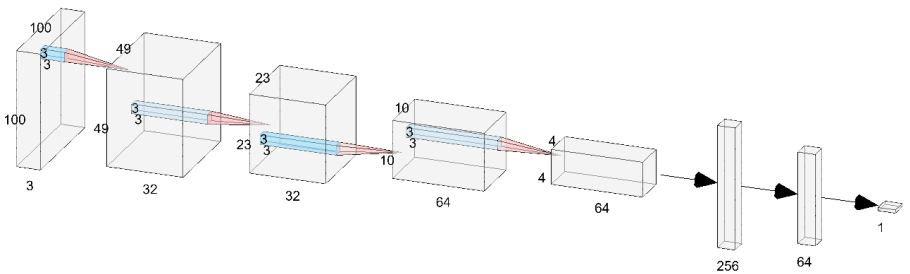

Figure 3.10: The CNN used for classifying the depth images and the magnetic intensity images.

ple training images of cats and dogs, a CNN can be trained to classify them with great accuracy. However, if adding images that are difficult to classify, where an expert just flips a coin when labeling the images, the CNN's will lose performance. By this, we decided to remove all training images with values 0.3–0.7, which improved performance significantly. Now the CNN could start learning what an image looks like where depth helps a PF perform well. The two CNNs result in two values (0.0–1.0) for depth and magnetism. We then used these values to create weights for *Depth*, *Magnetic* field, *Combination* or *Dead Reckoning*.

3.2.3 Evaluation

The algorithm was tested through simulations using the same map as it was trained in, but using another route. The ship used a compass and speed log for the prediction step, which gives poorer position accuracy than one of the INSes used in Paper I. To compensate for this, bearings to landmarks were used to strengthen the position estimation further. Bearings complement the depth and magnetic domains well. Bearing measurements to three defined landmarks were simulated. Every particle outside a corridor in the bearing direction is moved into the corridor, and then spread with a normal distribution. In half of the tests, one bearing was measured each minute. In the other half, two bearings were measured each minute, resulting in better position accuracy. For evaluation, the particles in the tests were divided into two portions, with portion sizes according to *Portion using CNN* in Table 3.2. When, e.g., *Portion using CNN* was 20%, 20% of the particles were dynamically divided into subset sizes set by the CNN algorithm, and 80% of the particles had their subset sizes set according to Table 3.3, As can be seen in Table 3.2, the algorithm has the best performance when having a better position accuracy from the 2 bearings per minute, and when using 50%, 80% or 100% CNN support.

Table 3.2: Performance using ML

Portion using CNN	**0%**	**20%**	**50%**	**80%**	**100%**
Position error - 1 bearings/min	23.3m	22.4m	23.6m	22.7m	23.2m
Position error - 2 bearings/min	18.2m	17.1m	**13.8m**	**14.3m**	**14.6m**

Figure 3.11 shows a comparison between two tests using 2 bearings per minute. The tests have a duration of 12h, but to make the graph readable, we only present

Table 3.3: Subset sizes for particles not using CNN

Evaluation method	
Depth	27%
Magnetic Field	18%
Depth & Magnetitic Field	10%
Skip PF (Only Compass and Speed Log)	45%
Kalman filter	1%

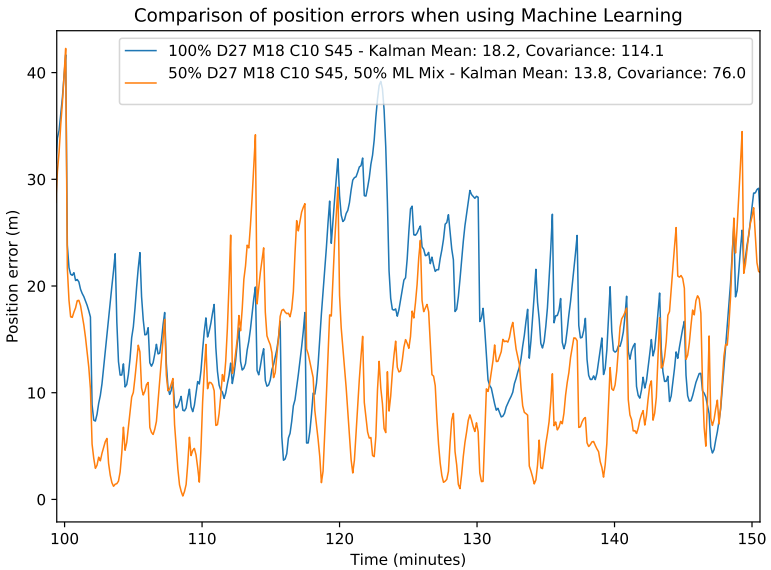

Figure 3.11: A graph that compares the algorithm using or not using ML for setting subset sizes. Fixed subset sizes are used for all the particles in the first test (blue). Fixed subset sizes are used for 50% of the particles of the second test, and 50% of the particles are set using ML. The graph shows 50min of the 720min (12h) long test.

50min. As can be seen, the test that sets half of the particle's subset sizes using CNN has better performance; a mean position error of 13,8m instead of 18.2m. A video of the full 12h test that only uses preset sizes can be found on YouTube[1]. The test where half of the particles use CNN can also be found on YouTube[2].

3.2.4 Discussion

The reason for the CNN supported PF to perform better when it already has quite an accurate position, is probably because it creates an image of the surrounding map based on the estimated position. The better estimation of the correct position it already has, the better its image will correspond to the correct map. If the position, e.g., differs by 50m, the CNN might optimize the subset sizes in a completely wrong way, making the position accuracy worse. By this, it seems like the CNN contributes to a better position accuracy if the ship already has a quite accurate position estimation.

The evaluation has been made using the same maps as the training. The CNN might have overfitted to the map, which in that case increases the performance in the evaluation. We believe it has not influenced the results much, but are not certain. It would be better to use a completely different map for evaluation. However, we suspect various areas have various terrain characteristics, hence much training data must be gathered to allow the algorithm to be used in all terrains with good results. We tried using the CNN in an area outside Västervik, but the characteristics were so different that the CNN did not improve the accuracy.

When collecting more sensor data from various types of terrains, it would be interesting to continue the work and see if it works in real-world terrain. Nevertheless, to use it, we believe the ship should not have a mean position error exceeding approximately 20m.

3.3 Teleoperation System

The second sub-project focuses on how a GUI can be implemented to remotely supervise a small USV, while the communication throughput between the USV and the operator is limited, which is a realistic scenario for small affordable vessels. The sub-project has resulted in three of the included papers (Papers III, IV, and V). Of particular interest is to see how the user's *situational awareness* and *cognitive load*

[1] https://youtu.be/a75di60_G5A
[2] https://youtu.be/pKsxOOhzhyQ

are affected when using such GUIs in comparison to using traditional ones. To answer these questions, we propose a 3D-visualisation of the ship's surroundings either on a computer screen or in a virtual reality (VR) setup. The perception of a 3D GUI in VR resembles how a human normally perceives the world, assumed to be beneficial for human-machine communication. The GUI design is based on ideas from the available research regarding manned ships to increase situational awareness while maintaining a low cognitive load.

We assume we can create an easy-to-use GUI which provides a good situational awareness, and thereby increase safety, by:

- creating the GUI in 3D, and preferably present it in VR;
- providing different views of the surrounding environment, optimized for various situations;
- augmenting objects and information directly in the 3D world; and
- providing a 360° image of the real-world environment, so that the operator can compare the 3D world with the real world, to increase situational awareness and to manually detect objects.

Our hypotheses are that a user operating a GUI built by these foundations will have a better overall understanding of the situation, and will observe potentially dangerous situations earlier.

Three different GUIs have been developed and tested for Papers III and IV; one *Baseline GUI*, representing traditional navigation tools, one 3D tool presented on a laptop, called *3D GUI*, and one 3D tool presented in VR, called *VR GUI*. All these GUI types are shown in Figure 3.12.

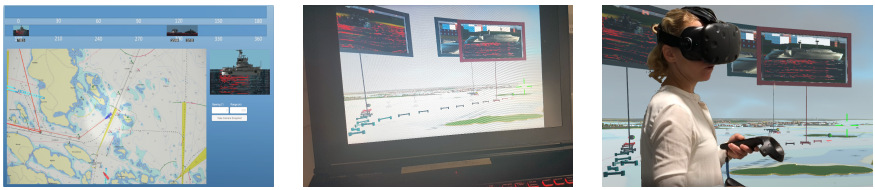

(a) Baseline 2D GUI (b) 3D GUI on a laptop (c) VR GUI

Figure 3.12: Three types of GUIs have been developed. (a) is a 2D GUI, that represents a traditional GUI. (b) and (c) are created in 3D, where (b) is presented on a laptop and (c) in VR.

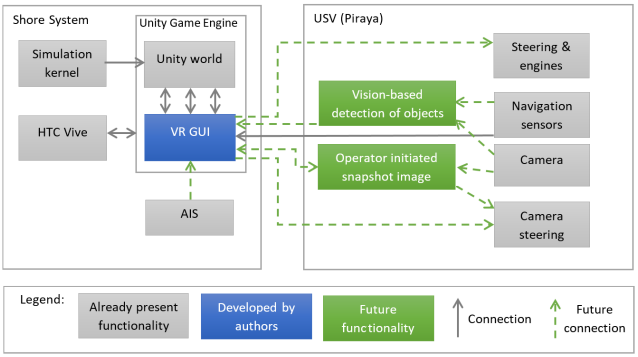

Figure 3.13: The VR GUI (or 3D GUI) is the main application where the interface is created for the operator. It presents the GUI in the Unity world, which is a 3D virtual environment (VE) with a virtual world positioned in the own ship's location with surrounding ships simulated by the simulation kernel. In the current implementation, the real world USV's position can be transferred to the VR GUI so that the virtual USV is presented at the correct location in the VE. Many functions or interfaces are not yet implemented in the real world but are instead simulated. These are marked with green boxes and dashed green lines. The steering interface is not implemented yet in the simulation tool.

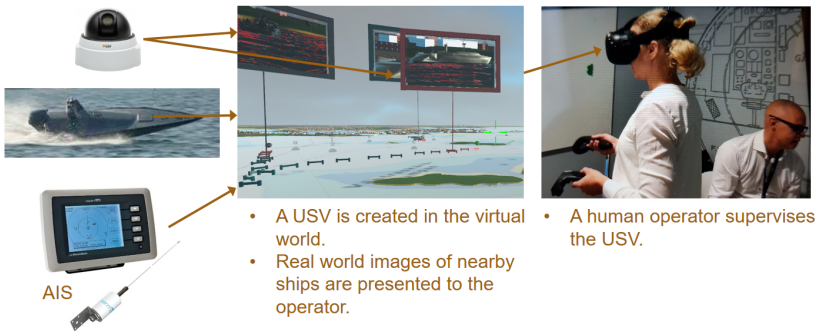

Figure 3.14: The location of the USV is used for creating a VE around this location. The sensor data from the camera and AIS detects ships, which are presented in the VE. The VE is then overlayed with the GUI, and presented for the human operator.

The application for teleoperation is implemented in Unity 3D [119], which is a development tool normally used for creating 2D and 3D games. A 3D world (called *Unity World*), developed by the shipyard Saab Kockums AB [120], is used as a foundation for the GUI, see Figure 3.13. A USV, also produced by Saab Kockums, has been used for initial testing. Some functionality, such as ship detection, is not implemented onboard the real world USV yet. By this, most of the implementation and testing for Papers III and IV have been conducted virtually instead. The Simulation Kernel is, in this case, simulating also the own ship, and the cameras are taking photos from the VE. Figure 3.14 shows how the VE receives the images and GPS position so that a 3D world can be created with a virtual ship in the middle of the world in the same location as the real-world USV. Also, AIS information is presented. The GUI is then presented for the operator, who supervises the own vessel's route. It is only possible to supervise the USV, as any steering is not yet implemented. To evaluate the design described in Papers III and IV, we conducted a user study with 16 participants.

The GUI evaluated in Paper IV was further developed to incorporate functions for supporting the Terrain-Aided Navigation (TAN) application with bearings to landmarks. This work is presented in Paper V. The GUI was also further developed, so it could use real-world data from the field-trial in Västervik, where navigation data and video from a 360° camera were recorded. We wanted to see if users could use the low quality 360° image from the 360° camera to detect landmarks so they could be used to support the TAN application. We also wanted to evaluate the user experience when having a 360° image of the real-world environment that corresponded with the simulated 3D world. Interesting topics to evaluate are how the users experienced the situational awareness, and if they could gain trust in the system's ability to navigate when having the ability to see that the 360° image corresponds with the virtual 3D world. An example of the GUI, together with one of the participants from the user study, is shown in Figure 3.15.

The info-logical interfaces between the ship and the teleoperation tool are shown in Figure 3.16. The teleoperation tool receives heading, speed, estimated position, and images from the USV, and bearings to landmarks are sent to the TAN application onboard the USV.

3.3.1 Performance of the 3D GUI and VR GUI

The user studies to evaluate the GUI versions gave some interesting results, described in more detail in Papers IV and V. It was investigated how 3D and VR approaches could support the supervision of a USV with a low throughput con-

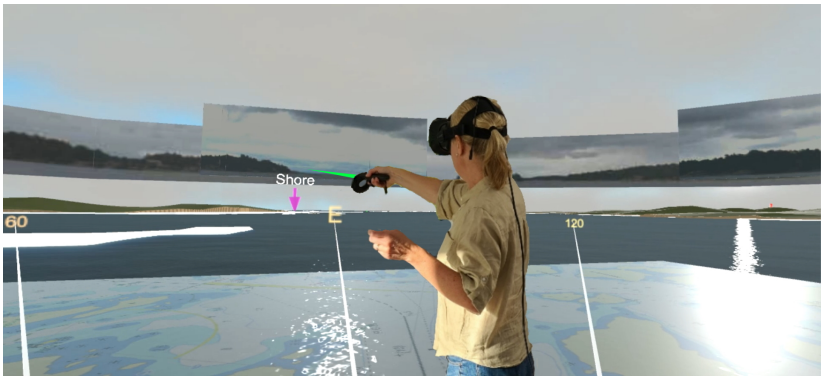

Figure 3.15: A participant of the user study taking a bearing by pointing towards an augmented landmark.

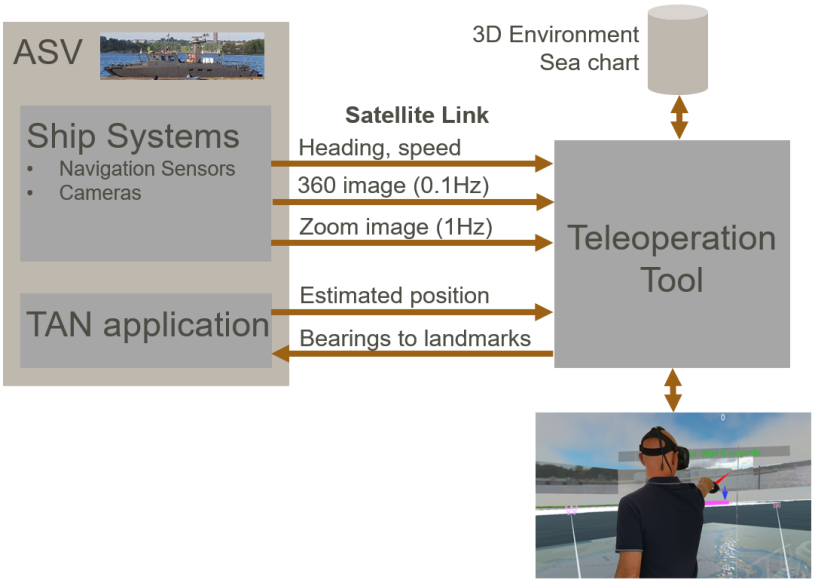

Figure 3.16: An architectural overview of the teleoperation tool in Paper V.

nection, by comparing respective interfaces with a GUI following the currently applied interfaces in such contexts. Our findings in Paper IV show that both the 3D and VR approaches outperform the traditional approach significantly. We found the users were calmer during the study and could keep track of the situation more accurately. They also reported they expected the *3D GUI*, and especially the *VR GUI* to be the best tool of the three choices for an expert user with many hours of training.

From the user study in Paper V, we found the users had a good overview of the situation despite the low-quality images. The users have experienced they could judge if the position was correctly estimated by easily matching the 3D environment with the 360° image. When it did not match, they could react quickly and tried to solve the problem by updating the positioning system with new bearings. We found the teleoperation tool to improve the accuracy of the TAN application, despite the low image quality.

4 Discussion and Conclusion

This chapter ends the first part of the thesis with a discussion and conclusions about the work.

4.1 Discussion

4.1.1 Future of Unmanned Ships

There is a long way to go before autonomous ships will be commonly used. Many research and development projects are going on, though, and as unmanned ships and ships with lean manning get more affordable, it is likely that the fleet will gradually reduce their manning. The shipping industry will not need to develop all building blocks themselves. They will need similar technology as, e.g., the automotive industry, which makes great efforts to produce fully autonomous cars within the next coming years. However, the building blocks still need to be adjusted to fit the naval domain. Some areas where the technology needs to be adjusted are:

- Positioning of a ship is normally not done in the same way as for cars. Ships need their own methods and algorithms for robust positioning systems.
- Traffic rules at sea are not the same as for cars. The ships need to obey these rules. Planning algorithms from the car industry might work as a basic tool to build from.
- Training data for, e.g., image recognition, is not the same. A large amount of data needs to be collected. The same algorithms as for cars can possibly be used.
- Teleoperation is probably more important for the shipping industry than for cars. An important difference between the domains is the relaxed latency requirements for ships, as ships have slow dynamics where dangerous obstacles typically are detected seconds or minutes before collisions instead of milliseconds.

4.1.2 GNSS free Navigation

In general, GNSS systems are easy to use and provide accurate position estimations. The problem is that they are not totally reliable, as the system can be jammed or spoofed. If the ship is autonomous, the ship lacks the crew that can act when something unpredicted happens. Hence, it is appropriate to complement the GNSS equipment with a GNSS-independent positioning system.

I propose a system that can be used without relying on high-resolution 3D maps, as these are limited to very few geographical areas. I also propose a system that normally uses the GNSS system, but where a TAN application evaluates the position in the background, ready to alert users and take over the function to provide the position to the navigation equipment. The following findings have been found in Papers I, II, and V:

- If there is a need for an accurate position, a PF relying on a high-accuracy INS system provides better position estimation than a PF relying on compass and speed log. The high-accuracy INS system is expensive, though.

- Paper I showed the accuracy is better when using the bottom depth lines from the sea chart, which is reasonable, as wrongly placed particles then can be discarded with better precision.

- Papers I and II show that the algorithm benefits from the fusion of data from multiple domains. By using PDFs created by using both depth and magnetic field measurements in Paper I, the performance increased. Paper II also showed that the robustness increased.

- Papers II and V show that the use of bearing measurements to landmarks increases the positioning performance further. In Paper II, the bearings were measured off-line manually from recorded video. In Paper V, the users in the user study instead measured the bearings in real-time via VR. Another alternative is to use image recognition to detect landmarks or terrain autonomously.

As can be seen, there are many alternatives to GNSS systems when navigating. By combining multiple sources, it is possible to construct a robust and accurate positioning mechanism. Other sources such as celestial navigation, radar, and multibeam sonars can also be used to increase the performance and robustness even further.

4.1.3 Teleoperation of USVs

Teleoperation is a crucial technology for the implementation of autonomous ships. The most well-used teleoperation GUI today is to use one or multiple computer screens, where a 2D GUI is shown along with at least one GUI part dedicated to streaming real-time video from the vessel. We hypothesize a 3D GUI, especially when presented in VR, would increase the operator's ability to uphold an overall understanding of the surrounding situation, and thereby the safety. This hypothesis was proven to be true, as the user study presented in Paper IV showed that the VR GUI and the 3D GUI presented on a computer screen increased the performance compared to the traditional GUI on a computer screen. Persons that already had experience in 3D games or VR had even higher scores, indicating that expert users would benefit even more from this new technique. Furthermore, I believe the 360° image of the surrounding real-world increased the user's immersive experience, and we showed the user could get a good overview of the situation and see if the vessel was correctly positioned.

One of the benefits of VR is that the surrounding world can be presented in a way that reminds of how humans normally perceive their environment. Another benefit is that there are hardly any limitations regarding how the GUI can be presented for the operator. The human can have various surrounding worlds; the GUI can be placed anywhere in the space and, e.g., hover above an object or present multiple virtual screens. A virtual control room can be created for the specific operator's task, and other relevant human operators can be placed nearby as avatars.

The GUIs presented in Papers III, IV, and V are intended to showcase functions applicable for user-interaction with autonomous ships. The GUIs have not been intended to be perfect, but be used to evaluate specific functions and designs to gain experience and learn. When conducting a user study in academia, it is also challenging to use a too complicated tool. It will be too time-consuming for the user study if all participants first need to learn how to use all tools before being able to conduct the user tests.

If the goal is to develop a GUI for the teleoperation of autonomous ships, I believe it is essential to guide the operator by augmenting objects directly in the surrounding. A 360° image is also a great tool for helping the operator understand the surrounding environment, and to gain trust in the system's ability to navigate. 3D is a visual technique that is easy for a human to perceive, and VR guides the user effectively when it comes to the perception of directions. Still, I am not sure of the best way to construct a shore control center. It is perhaps not ergonomic or healthy

Figure 4.1: A control station of Saab's *Remote air traffic control systems*. In the figure, two simulated airports are traffic controlled simultaneously by a single operator.

to use VR for 40 hours per week, and it is difficult to look at objects behind the back. An alternative is to stitch together many large screens, creating a huge screen covering a wall. This technique has been used in Saab's *Remote air traffic control systems* for remote operation of airports via a digital tower [121], see Figure 4.1, and also by Rolls Royce Commercial Maritime when remote controlling the tug in Copenhagen, shown in Figure 2.7 on page 37. More research is probably needed to find which solution is best.

4.2 Future Work

Even though the process of creating an autonomous ship has rapidly progressed during the last years, there is much more research that needs to be done. I believe that the tasks conducted onboard a ship can be modularized into building blocks, where each block is easier or harder to automate. In the beginning, the task of a building block is most often best performed by a human. Nevertheless, as technology evolves, the machine can gradually do a larger portion of the task, first supporting the human operator, then doing the task supported by the human operator, and finally doing the whole task by itself. So far, I have investigated how two of these building blocks can be enhanced, and there are many more of those to be studied further:

- **Image recognition at sea.** Semi-autonomous cars are gathering data to train neural networks to recognize objects in the traffic. The technique needs to be also evolved at sea. A big difference is that not as much data can be easily collected, as there are fewer ships than cars. The images will mainly consist of water and sky, so it should be possible to do fairly robust object detection. On the other hand, there can be more problems with glare, reflections, mist, snow, and rain, partly due to the longer distances at sea. To remedy the lack of a large training set, *transfer learning* might be used in combination with simulated images and data augmentation for creating the first layers in the network.

- **AR or VR on manned ships.** Currently, we have created a VR GUI for remote supervision of a small USV with a throughput constraint. Comparable solutions can be constructed for manned ships as well. Then the throughput constraint would be removed, and all the sensors onboard the vessel could, together with smart fusion techniques and AI, contribute to the ultimate situational awareness experience for the human operator. The GUI can be constructed for AR with the operator on the real-world bridge or for VR, where the operator is placed in a virtual control room, giving more flexibility to the GUI. These GUIs could be compared to a state-of-the-art GUI for ship navigation. This project can also use various types of fusion methods to compile what should be shown for the human operator.

- **Enhanced GNSS-denied positioning.** The GPS-denied positioning algorithm could also be enhanced. Currently, it only uses either the INS or compass and speed log for the *Prediction step*. Combining compass, speed log, and INS would give a better velocity estimation for a longer time, which would boost the algorithm's performance. The performance of the *Correction step* could also be enhanced. Currently, it only uses the magnetic field, bottom depth, and bearings to landmarks. It would be interesting to combine the algorithm with an autonomous technique to match elevation maps with visual images or radar data [83, 84]. In my opinion, the GNSS-denied positioning system should not run as a separate program, but should be combined with GNSS data when available. It should alarm when it judges the GNSS to give false information or being jammed, and be ready to take over. Research on how to combine these sources in the best way would be valuable.

4.3 Conclusion

Much work remains to be done in the quest for autonomous ships. Many building blocks need to be developed. In this thesis, two of these blocks have been studied.

In our first sub-project, we have seen that smart techniques can be used as a complement to positioning systems relying on satellites. During a 20h long test, the mean of the position error was measured to be 10.2m when using the bottom depth measurements, the magnetic field measurements, and high-accuracy INS. This is probably accurate enough for most navigation purposes (research question 3 RQ3), but has only been tested from simulated data. The PF performance improved with more and better input data, as the PF then could discard particles placed in incorrect locations. We also learned that the technique works when replacing the INS with a compass and speed log, with a degraded position accuracy (RQ4). The robustness increased by using multiple domains for the PF. The performance also increased by using bearings to landmarks, even when the bearings were taken by a remote operator using low-quality images of the surrounding (RQ5). We reached a mean position error of about 40m, using a compass and a speed log and without bearings to landmarks, and 27.8m with 69 manual bearings. During the teleoperation user study, which used a higher drift speed that degrades the performance, the mean position error was 35.7m. The results show that a fairly accurate positioning tool is given by using bearings from the teleoperation tool (RQ5). To not risk groundings, it is important to complement with visual bearings so that a remote operator can trust in the position estimations. The route can also be adjusted to have larger margins.

The second sub-project investigated how 3D and VR approaches could support the remote operation of a USV with a low throughput connection. Our findings showed that both the 3D, especially when visualized in VR, significantly outperformed the traditional approach. We found the 3D GUI and VR GUI users to be better at reacting to potentially dangerous situations than the Baseline GUI users (RQ1). Choosing from the three GUI types, the users also expected the 3D user-interfaces, especially the VR GUI, to be the best expert user tool (RQ1). By augmenting objects directly in the surrounding world, the cognitive load is reduced, and the user gets a good overview of the situation (RQ1). By also adding a 360° image of the real-world terrain that corresponds to the virtual 3D world, the user can instantly see if the position is accurate or not. The operator can then gain trust in the system's ability to navigate (RQ2). Using the 360° image, the users could also, despite the low quality, enhance the positioning system's accuracy.

In summary, the research questions are answered below:

1. **RQ1**: How can a human operator teleoperate a USV through a low throughput connection, giving the user a good and safe overview of the situation while maintaining a low cognitive load?
   Answer: By creating a VE of the surrounding world from maps, and using it as a base for a 3D GUI, a data connection with a lower throughput connection is sufficient for most scenarios. By augmenting important objects and images, e.g., detected by sensors, directly in the surrounding world, the cognitive load is reduced at the same time as the user gets a good overview of the situation, aspects leading to increased safety.

2. **RQ2:** How can a human operator gain trust in the USV's ability to navigate when using a low throughput connection? How does the operator know the position is correct?
   Answer: On manned vessels, the ordinary way of ensuring that the navigation system has the correct position is to compare surrounding visual information (or radar) with what is seen in the sea chart. By having the ability to compare the virtual surrounding to a 360° image of the real-world terrain, the remote operator can ensure that the position is accurate. Our user tests show that this 360° image does not need to be streamed in real-time, but can be sent with a frequency of about one image every ten seconds, and have a low resolution, thereby adapting to available throughput.

3. **RQ3:** When not using a GNSS system, is it possible to estimate the position accurately enough for navigation purposes by using a high accuracy INS, and measuring the bottom depth and the magnetic field?
   Answer: How accurate the position must be depends on the situation. In general, lower position accuracy is needed far away from the coast, and higher accuracy is needed in the archipelago with dangerous grounds nearby. In our simulation using a high-accuracy INS, the PF had a mean position error of 10.2m, which in most cases is accurate enough.

4. **RQ4:** When not using a GNSS system, is it possible to estimate the position accurately enough for navigation purposes by using a compass and speed log, and measuring the bottom depth and the magnetic field?
   Answer: As the information is very sparse in both the sea chart and the used magnetic anomaly map, it is challenging to get an accurate position estimation by using the compass and speed log when supporting the PF.

In our tests, when using 0.25 knots of drift speed, we have gained a mean position error of about 40m, when only relying on depth, and not using the magnetic field. In many situations, this is not accurate enough, and should probably be complemented with other navigation techniques to improve the performance further.

5. **RQ5:** Can the human operator help the positioning system via a teleoperation system using a low throughput connection? Is the image quality sufficient for this?
   Answer: Our user tests clearly show that the accuracy of the positioning method is increased when using the 360° image to take bearings to nearby landmarks. Even though some of the users wished for better quality images, we conclude that the image quality is sufficient to increase the positioning performance significantly.

We believe these results to be valuable contributions to the development of technologies supporting autonomous ships.

5 Overview of Research Papers

The project started with the aim to create digital cognitive companions for marine vessels. This aim resulted in the two sub-projects, which have been finally combined into Paper V. In total, eight papers have been written. Five of these are included in the thesis, reformatted into the thesis format. Figure 5.1 shows the order of the papers, when they were created, and which papers belong to which sub-project.

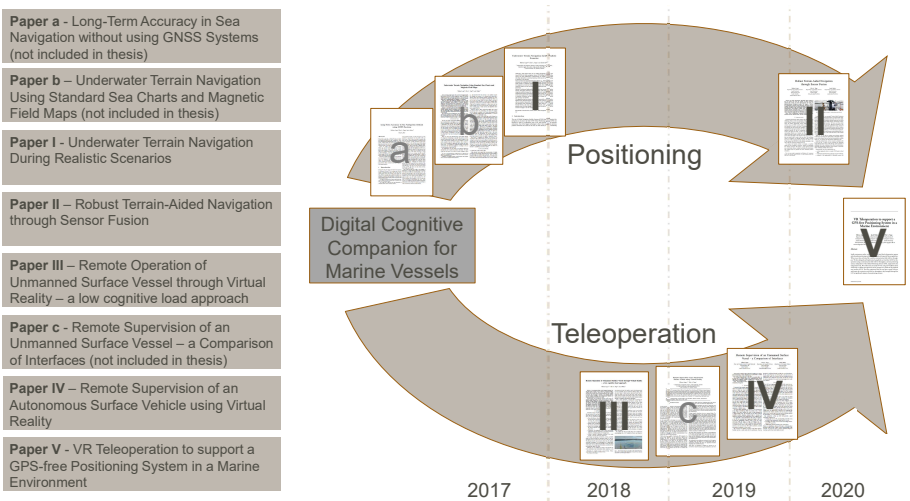

Figure 5.1: An overview of all eight papers, and which sub-project they belong to.

5.1 Summary of the Included Papers

Paper I

Underwater Terrain Navigation During Realistic Scenarios

M. Lager, E. A. Topp and J. Malec
Multisensor Fusion and Integration in the Wake of Big Data, Deep Learning and Cyber-Physical System - An Edition of the Selected Papers from the 2017 IEEE International Conference on Multisensor Fusion and Integration for Intelligent Systems (MFI 2017), Springer (pp 186-209)
DOI: 10.1007/978-3-319-90509-9_11

Summary:
The paper presents a method for estimating a ship's position at sea by comparing bottom depth measurements and magnetic field measurements with known sea charts and magnetic field maps. The method uses a particle filter that moves thousands of particles (position estimations) according to own INS. It then calculates the probability that each particle is correctly located by comparing the sensor measurements with the maps. After each iteration, more likely particles will survive and less likely such will be discarded, and the position is thereby continuously estimated. To increase the performance even further, a Kalman filter has been used. The paper also elaborates on how the performance is changed when weighing different sensor measurements differently or having various INS performances. The results from the simulated tests described in this paper, show that for the high-end INS, the mean position error is 10.2m, and the maximum position error is 33.0m during a 20h test.

Paper II

Robust Terrain-Aided Navigation through Sensor Fusion

M. Lager, E. A. Topp and J. Malec
2020 IEEE 23rd International Conference on Information Fusion (FUSION 2020)
DOI: 10.23919/fusion45008.2020.9190578

Summary:
The paper builds on the work regarding the particle filter from Paper I, but instead of using a high-end INS, the paper focuses on small affordable autonomous ships with a compass and speed log. It still uses the bottom depth and magnetic field for the particle filter, but also complements the design with visual bearings to landmarks to enhance the positioning accuracy. To validate the algorithm's performance, we have conducted a real-world field trial to collect data in a realistic scenario in the archipelago. The simulations, building on the field trial data, showed that the proposed fusion mechanism provides accurate and robust navigation. Furthermore, we showed that both the algorithm's performance and robustness increases when using multiple data sources instead of depth or magnetic field intensity individually.

Paper III

Remote Operation of Unmanned Surface Vessel through Virtual Reality - a low cognitive load approach

M. Lager, E. A. Topp and J. Malec
The first International Workshop on Virtual, Augmented and Mixed Reality for Human-Robot Interaction 2018 (HRI 2018)
DOI: 10.6084/m9.figshare.13537019.

Summary: The paper describes a VR GUI design for teleoperation of a USV, where there is a throughput constraint between the operator and the USV that makes it impossible to transmit high-resolution images or video streams. The intention has been to create a GUI that provides at least as safe navigation as when an operator navigates onboard a ship. To accomplish this, the strength of 3D and VR has been used, where surrounding objects are augmented directly in the 3D world, giving a user experience that resembles how humans normally perceive their environment. Three main views have been suggested, which all have their strength and weaknesses depending on the situation.

Paper IV

Remote Supervision of an Autonomous Surface Vehicle using Virtual Reality

M. Lager and E. A. Topp
Autonomous Intelligent Vehicles 2019 (IAV 2019)
DOI: 10.1016/j.ifacol.2019.08.104.

Summary: The paper presents a user study of the GUI, presented in Paper III, where 16 participants have supervised a simulated USV, going through the archipelago. The user study has studied how safety, situational awareness, and the cognitive load is changing depending on if the user uses a traditional GUI, a 3D GUI presented in VR, or a 3D GUI presented on a computer screen. Our findings show that both the 3D and especially the VR GUI outperform the traditional GUI significantly.

Paper V

VR Teleoperation to support a GPS-free Positioning System in a Marine Environment

M. Lager, J. Malec and E. A. Topp
Submitted

Summary:
The paper presents a system combining the positioning system from Paper II with the teleoperation system presented in Papers III and IV. The system is validated through a user study based on a field trial in the archipelago. The teleoperation system presents a virtual replica of the real-world terrain and the ship, along with augmented 360° images from the real-world ship. The user can then take bearings to nearby landmarks, sent to the positioning system to enhance the positioning accuracy further. We have intentionally highly compressed the 360° image, as a low throughput communication link limits the data transmission. The users in the user study experienced the tool provides a good overview, and despite the connection with the low throughput, they managed through the GUI to significantly improve the positioning accuracy.

5.2 Contribution Statement

Author and co-authors are abbreviated as follows: Mårten Lager (ML), Elin A. Topp (ET) and Jacek Malec (JM).

ML is the main author of Papers I–V. Papers I–III and V have been co-written with ET and JM, and Paper IV has been co-written with ET. For all these papers, ML provided an initial version of the paper, which was then revised to the final form in collaboration with co-writers. The overall project ideas presented in the papers have been proposed by ML, and have then been discussed and enhanced in collaboration with co-writers. ML has carried out all the implementation work. ML carried out both user studies (Papers IV and V).

5.3 Other Contributions

The following papers are related but not included in this thesis.

Long-Term Accuracy in Sea Navigation without using GNSS Systems

M. Lager, E. A. Topp, and J. Malec
In Proc. of the 30th Annual Workshop of the Swedish Artificial Intelligence Society (SAIS 2017), Karlskrona, Sweden.
Link[1].

Underwater Terrain Navigation Using Standard Sea Charts and Magnetic Field Maps

M. Lager, E. A. Topp, and J. Malec
In Proc. of the 2017 IEEE International Conference on Multisensor Fusion and Integration for Intelligent Systems (MFI 2017), Daegu, South Korea,
DOI: 10.1109/MFI.2017.8170410.

Remote Supervision of an Unmanned Surface Vessel - a Comparison of Interfaces

M. Lager, E. A. Topp, and J. Malec
In Proc. of the 14th ACM/IEEE International Conference on Human-Robot Interaction (HRI 2019), Daegu, South Korea, DOI: 10.1109/hri.2019.8673100.

[1]https://ep.liu.se/en/conference-article.aspx?series=ecp&issue=137&Article_No=1

Part II

Research Papers

Paper I

Paper I

Underwater Terrain Navigation during Realistic Scenarios

Mårten Lager
Department of Computer Science
Lund University
Saab Kockums AB
marten.lager@cs.lth.se

Elin A. Topp
Department of Computer Science
Lund University
elin_anna.topp@cs.lth.se

Jacek Malec
Department of Computer Science
Lund University
jacek.malec@cs.lth.se

Abstract

Many ships today rely on Global Navigation Satellite Systems (GNSS), for their navigation, where GPS (Global Positioning System) is the most well-known. Unfortunately, the GNSS systems make the ships dependent on external systems, which can be malfunctioning, be jammed or be spoofed.

There is today some proposed techniques where, e.g., bottom depth measurements are compared with known maps using Bayesian calculations, which results in a position estimation. Both maps and navigational sensor equipment are used in these techniques, most often relying on high-resolution maps, with the accuracy of the navigational sensors being less important.

Instead of relying on high-resolution maps and low accuracy navigation sensors, this paper presents an implementation of the opposite, namely using low-resolution maps, but compensating this by using high-accuracy navigational sensors and fusing data from both bottom depth measurements and magnetic field measurements. A Particle Filter uses the data to estimate a position, and as a second step, a Kalman Filter enhances the accuracy even further.

In "Multisensor Fusion and Integration in the Wake of Big Data, Deep Learning and Cyber Physical System", Springer, (MFI 2017), (pp 186-209), DOI: 10.1007/978-3-319-90509-9_11.

The algorithm has been tuned and evaluated using both a medium and a high-accuracy Inertial System. Comparisons of the various tuning methods are presented along with their performance results. The results from the simulated tests, described in this paper, show that for the high-end Inertial System, the mean position error is 10.2m, and the maximum position error is 33.0m during a 20h test, which in most cases would be accurate enough to use for navigation.

1 Introduction

The use of Global Navigation Satellite Systems (GNSS) has revolutionized the navigation at sea since the first GNSS Global Positioning System (GPS) was launched in 1994. It is affordable, easy to use, and provides accurate position estimations. One of the biggest advantages is that it does not use the previous position estimation as a base for the next one and thereby avoids accumulating position errors, which happens when dead-reckoning the position using a compass or an Inertial Navigation System (INS). With this advantage, a GNSS system can maintain an accurate position no matter how long time it was since leaving the harbor with a known position.

There are still some disadvantages with GNSS though. One important disadvantage is that the ship needs to rely on external information from the GNSS satellites which is sent to the GNSS receiver onboard. It is quite simple to jam the radio reception from the GNSS satellites, which results in that it is not possible to determine the position anymore. Even worse, it is possible to spoof the GNSS transmission information with advanced equipment, resulting in that an incorrect position is provided [65].

If a dependency on the GNSS is not desired, Bayesian calculations can be used for position estimation. The technique has been used for decades for some airplanes, where, e.g., [70] describes how the systems on an airplane measure the altitude and compare it to a known terrain map with a *Particle Filter* (PF) algorithm, thereby estimating the position. There are also many papers describing how ships can use the same technique, where the bottom depth is measured by an echo sounder system or a sonar system [77, 122–124]. More specifically, Autonomous Underwater Vehicles (AUVs) have a big need for position estimations, as they cannot use any GNSS, which has led to much research covering this topic, where various types of sonar systems and algorithms have been studied [67, 68, 71–74, 122, 125, 126].

However, there is other information which can be used by particle filters for positioning. [81] and [82] suggest how to estimate a position in an indoor environment with a PF comparing magnetometer measurements to a known magnetic map of a particular room.

The current research in this field has mainly focused on achieving good performance of the positioning systems when having a limited performance of the sensor suite, but nearly unlimited accuracy of the map. The available research for ship navigation has also mainly focused on one sensor type at a time. In this paper,

we propose a solution where we do it the other way around, which is more inline with a real-world scenario on bigger ships than on AUVs. The main research question is, therefore: **Is it possible to navigate accurately enough without GNSS systems, only relying on high-performance navigation sensors, normal sea charts and standard magnetic maps?** In this paper, we show, that by using both depth data and magnetic data at the same time and fusing this information, the position accuracy is increased, and it is possible to overcome the difficulty with poor map accuracy in either the depth or magnetic domain. As the last step to boost the position accuracy even further, we also propose to use a Kalman Filter (KF).

The algorithm has been evaluated using various configurations, both when using a medium and a high accuracy inertial system.

This paper is an extended version of an already published paper [115], and is organized as follows: In Section 2, an overview of other related work is given focusing on PF estimating the position by measuring bottom depth and magnetic field. Based on the currently available research, limitations and opportunities of this approach are described in Section 3. Sections 4 and 5 describe our contributions. First, the software is described, and then the simulation results and tuning are discussed. In Section 6, concluding remarks are given.

2 Related Work

As our system is based on the fusion of different measurement data types, each of which being used in similar or related contexts and approaches, we describe related work organized by these data types and their appearance in filtering techniques.

2.1 Depth Data in the Particle Filter

It has already been named that in possession of a high-resolution bottom map PF can be used for position estimation by measuring the bottom depth [67, 68, 71–74, 77, 122, 122–126]. There are some problems with the technique though. There are not that many areas where high-resolution maps have been created. Another problem is that the bottom terrain needs to vary enough for the PF to work, and in some areas, the bottom terrain is quite flat [77]. A solution to these two problems would be to use normal bottom sea charts and to complement the depth measurements with other measurements.

2.2 Magnetic Data in the Particle Filter

Earth is surrounded by a magnetic field, where each ferromagnetic element disturbs this field. These disturbances can for indoor environments be even greater than the natural magnetic field of Earth [81]. For indoor environments, numerous ferromagnetic elements create a complex magnetic field where the magnetic vector varies greatly depending on the location. The magnetic field is also quite stable if no major furniture or iron walls are moved. This information can be compared to a magnetic map using a PF, and in conjunction with some sort of odometry, such as wheel encoders or inertial sensors, it has been possible to localize a human or robot [82]. In [81] only cheap smartphone sensors are used, and the magnetic field and acceleration are used for determining the position of the human user.

Although [81] and [82] have explored indoor environments, the same technique is applicable for outdoor environments. The magnetic field does not fluctuate as fast as in indoor environments, but on the other hand, it is more stable, because no furniture or building parts are moved around as in the indoor environments. There are satellite maps available covering the entire magnetic field of Earth, and in some areas of the world, higher resolution maps have been created, e.g., by low flying airplanes. Hence, the magnetic field has been used in our PF algorithm for estimating the position of the ship. Our implementation shows that the magnetic field intensity serves as a good complement to bottom depth measurements when it comes to improving the accuracy and robustness of the position estimation.

2.3 Using Other Data in the Particle Filter

The bottom depth and the magnetic field are good candidates to use for the PF algorithm when estimating the position, but there are other alternatives. In addition to the bottom depth, [68] also uses range measurements to land objects in another PF algorithm. This range is measured by a radar and is compared to a sea-chart database.

It is also possible to not only use the depth measurement directly vertically to the bottom. If the ship is equipped with a sonar system, it is also possible to use multiple bottom depth measurements covering a larger area at once. This increases the performance of the PF, as it is possible to evaluate if the bottom readings match the map with better precision [73]. Another way to improve the performance is to use the sediment layers of the bottom, where the lower layers' depth most often varies more than the sea floor [77].

The strength of the PF algorithm is that it is very flexible when it comes to which measurements to use. The important thing is that the measurements shall vary enough when changing position and that it shall have varied in the same way (or in a predictable way) when the map was created, and when doing the PF measurements. Other candidates which could be used for the PF algorithm are:

- Celestial navigation items such as star positions, where a star either is present in a proposed direction or is not.
- Gravitation, which varies depending on where the ship is located on the earth.
- Various types of available bearing measurements, depending on which sensors the ship is equipped with. For instance, bearing measurements to visual objects, radio and radar sources with known map locations can be used, if the ship's sensors are able to estimate the bearing to that kind of sources.

3 Limitations with Current Research

The referred papers show that it is possible to do accurate position estimations if high-resolution maps are available to compare new measurements with. Many of the studies also evaluate how accurate the position estimation can become when these high-resolution maps are available. However, there are some limitations with these approaches, as it is rather rarely the case that such maps exist, even in coastal areas. The reality is that different areas have been mapped with various accuracy, where high-traffic areas more often have better accuracy and resolution than less-traffic ones. The algorithm for positioning in, e.g., [82], assumes that it can get the true bottom depth in any position of the map, but from a normal sea chart it is more likely that it is possible to compute some sort of likelihood distribution of the bottom depth for each position.

Excluding AUVs, the user platforms that are most likely to have a need for a system for accurate position estimation techniques which eliminates the need for GNSSs, are not cheap ones with moderate navigation systems. The most probable platform is instead an advanced vessel with accurate and expensive navigation sensors, where the RD (ship reference data), speed, bottom depth and magnetic field can be measured with high accuracy.

In this paper, a scenario more fit to the real world is investigated; namely, a platform estimating the position using high accuracy sensors, normal sea charts

and magnetic field maps. The purpose of combining depth and magnetism is that the condition for estimating the position by using solely depth data or magnetic field data varies depending on location. By combining the data, it is possible to increase the performance and overcome large position errors where one of the maps has lower accuracy.

The algorithms used for the high accuracy INS can also be used for a medium accuracy INS, which is an INS more in line with an INS that are normally being used on high-end AUVs. The algorithm performance has been evaluated also for these platforms.

4 Combining Depth and Magnetic Data

The key problem we have is that we would like to estimate the ship's position (denoted by x_t), but we are only measuring other related information such as how the ship is moving, bottom depth and magnetic field (denoted by y_t).

If the measurements and transition functions were linear and the measurement and process noise Gaussian, the immediate application of a KF would have been the optimal choice to compute the position [127]. In our case the transition functions are non-linear and the measurements have no Gaussian distribution, but instead a highly multi-modal distribution. There are some non-optimal extensions to KFs to handle the issues with non-linearity and not having a Gaussian distribution [128]. However, PFs are more flexible and have a built-in capability to handle multi-modal distributions. Therefore, the PF algorithm has initially been used for our implementation. However, as indicated above, we improve the accuracy of our method by applying a KF in a second filtering step, as is described later.

On a ship, the Inertial Navigation System (INS) uses accelerometers and gyroscopes to continually calculate the ship's orientation and velocity with high accuracy, without the need for external references. The INS outputs this data as the ship's Reference Data (RD) which is used in the state model.

The state can contain different variables depending on what sensors are available and how complex we want the algorithm to be. Because our currently developed implementation is made for simulation purposes, variables for compensating sensor directions and ship drifts can be left out. Therefore the state (I.1) contains solely the position, where X_t and Y_t are coordinates in some suitable coordinate system.

$$x_t = \begin{bmatrix} X_t \\ Y_t \end{bmatrix} \tag{I.1}$$

The model of the state change, with the discrete sample time Δ, is given by (I.2).

$$x_{t+1} = f(x_t, u_t, w_t) = \begin{bmatrix} X_t + v_t \Delta sin(\varphi_t) \\ Y_t + v_t \Delta cos(\varphi_t) \end{bmatrix} + w_t \tag{I.2}$$

In this equation $u_t = [v_t \ \ \varphi_t]^T$ is the input signal, which consists of the speed v_t and compass angle φ_t. The w_t is the process noise.

We now have the model for how to go from one state to the next one, and from the sea chart and magnetic field map, we can get information about how the depth and magnetic field y_t depend on the position in the state x_t. In this setting, the PF can be used for estimating the position.

4.1 Kalman Filter for Enhancing the Performance

The PF provide position estimations as well as quality attributes of the measurements, which can be acquired from the covariance of the particle cloud. Due to the map dynamics, the PF's position estimation can change rapidly around the true position.

The dynamics of how the position error increases with time is modeled as the *Process Noise* of the KF, and by feeding the KF with the position estimations as the *Observed State*, the KF is able to estimate a smoother and more accurate position of the ship.

4.2 High Level Algorithm

The model has been implemented in Python in order to investigate how the performance of a PF is influenced by using depth measurements, magnetic field measurements and a combination of those. For depth calculations, a standard sea chart has been used from outside the city of Karlskrona in Sweden, see Figure I.1. The program can read the bottom depth measurements and bottom depth lines from the sea chart. The simulated ship is, on the other hand, reading depths from a manually created high-resolution map, see Figure I.2, which has been created to as far as possible mimic the real terrain at the seabed. In a comparable way, a simulated magnetic field map has been created, along with a low-resolution magnetic map, comparable to publicly available magnetic field maps.

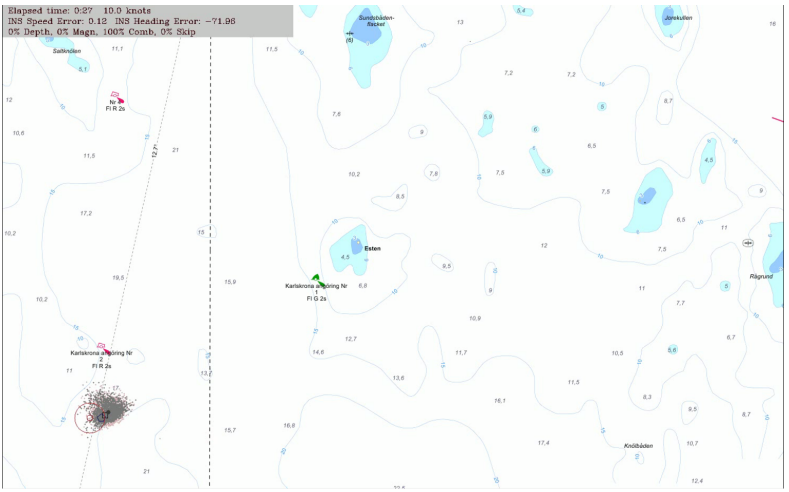

Figure I.1: A screen-shot from the program. As an underlay, the used sea chart is shown. In South-west, the particles are following the simulated ship's position. (The area is about 2 Nautical Miles (NM) wide.)

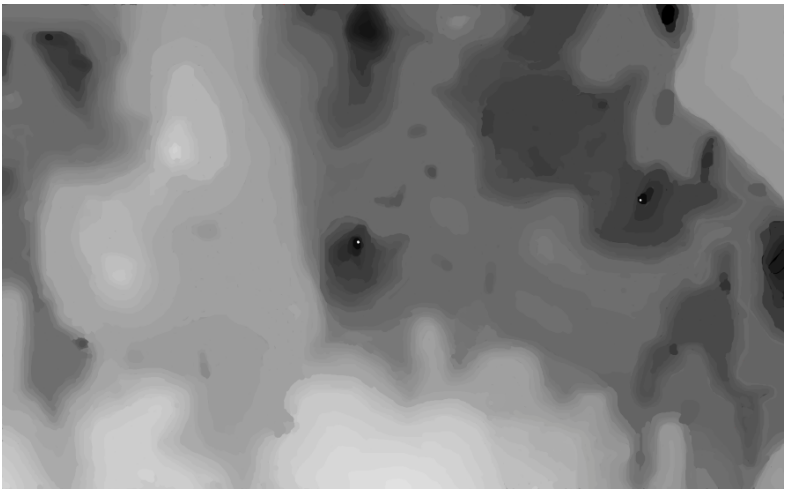

Figure I.2: A corresponding high-resolution map, manually created. The aim has been to as far as possible estimate how the terrain is formed in real life. The simulated ship is measuring bottom depth by reading a value from the current position from this image.

The high-level behavior of the model using the PF algorithm (see Figure I.3) is as follows:

1. **Initialization** - Generate N particles and give them a random starting position around a manual estimation of the starting position.

2. **Prediction** - Move each particle according to the velocity vector predicted by the INS. Then move each particle according to a random velocity vector, in order to simulate the velocity vector error of the INS.

3. **Correction** - Calculate the weights for each particle given the maps and each particle's position. The weights are calculated for depth, magnetic field and a combination of those two. Normalize the weights.

4. **Re-sampling** - The particles are re-sampled according to a predefined distribution from subsets defined as in Table I.1.

5. **Iteration** Go to step 2.

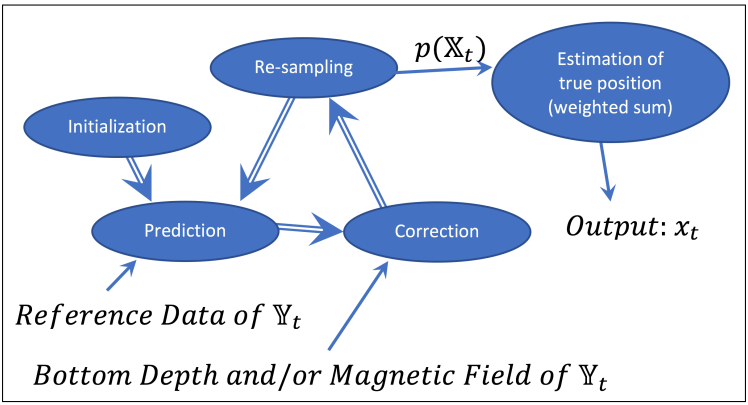

Figure I.3: A block diagram of the Particle Filter used in our implementation. After initialization, the particle filter iterates between *Prediction*, *Correction* and *Re-sampling*. After the *Re-sampling Step*, a probability of each state $p(\mathbb{X}_t)$ is estimated from the particles. From this, a weighted sum of all particles can be used as an estimation of the true position.

The *Correction Step* needed some tools in order to operate, which are described below:

Table I.1: Example distribution of particles

Subset	Distribution of particles
PF with bottom depth	20%
PF with magnetic field	10%
PF combining depth and magnetic field	50%
No PF, just move particles according to RD	20%

Map Data

To make the *Correction Step* operable, there must be data supporting the likelihood calculations, which estimate how likely it is that the current measurement has been performed at a given location. If a high-resolution sea chart is available, where it is possible to see the exact depth at every location, this is easy. On the other hand, we cannot assume that high-resolution and high accuracy maps will be available for every possible area. Therefore, a combination is desirable, using high accuracy maps (either depth or magnetic) where available and normal sea charts for bottom depth information if only those are available.

To support the PF algorithm for the case when high-resolution maps are not available, two functions have been created; one for bottom depth estimation from sea charts, and one for magnetic field estimation from magnetic maps.

The function for bottom depth estimation first reads the position of a particle and then gathers the closest bottom depth measurements from the sea chart. These measurements are then weighted according to the distance from the particle ($weight = 1/distance$). In Figure I.4, an example is shown where the bottom depth in a particle's position indicated by the star, is to be estimated. The depth measurement of 10.6m will be given higher weight than the other measurements. From these values, a weighted mean and a weighted standard deviation are calculated, which is used for creating a probability density function (PDF) with a normal distribution. The 10m-bottom depth line specifies that there is not less than 10.0m in the star's location. The 15m-bottom depth line specifies that there is probably not a depth of more than 15m (but there might be in some rare cases). In our implementation, we have set an (arbitrary) margin of 2.0m, and will approximate it as there cannot be any depth greater than 17.0m. Therefore, the PDF for the position in the image will be truncated below 10.0m and above 17.0m.

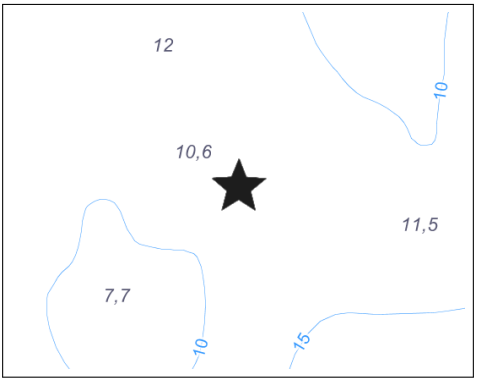

Figure I.4: A sample detail of a sea chart. The position of a particle is indicated with a star. Bottom depth measurements are available as well as bottom depth lines. These values and lines are used for creating a probability density function.

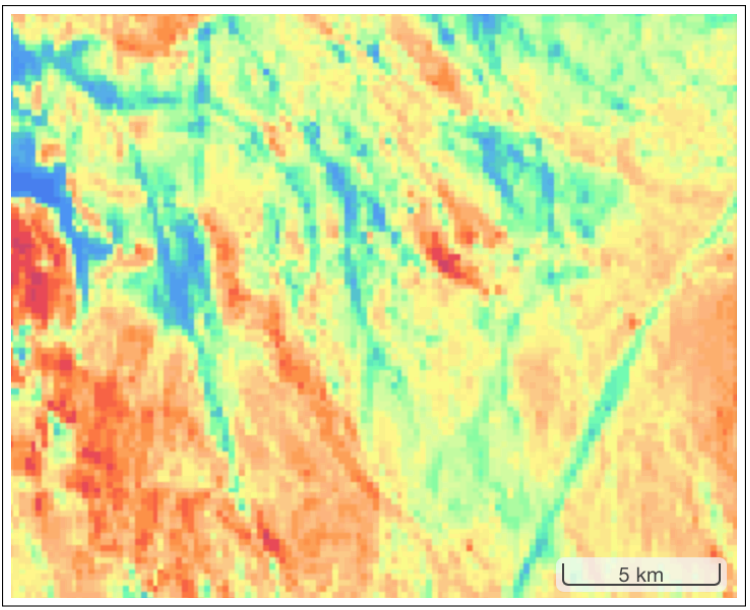

Figure I.5: The figure shows a publicly available magnetic field map. Each pixel corresponds to a square with a size of 185m×185m.

A magnetic chart does not look in the same way as the depth charts. Figure I.5 shows a publicly available map of an area in Sweden, which has been created by flying on low altitude measuring the magnetic field. Each pixel in the map corresponds to an area of 185m×185m. The function that estimates the magnetic field in the position of a particle, first interpolates the low-resolution image, creating a high-resolution image. Then it is possible to estimate the magnetic field directly by reading the magnetic field value from the position in the image. By comparing the estimated magnetic field with the values in the surrounding area, a standard deviation can be estimated. This is used for creating a normal probability distribution also for the magnetic field.

Fusion of Sensor Data

On an advanced ship with high-precision navigation sensors, it can be acceptable to use the navigation sensors for dead reckoning without using global positioning techniques for some time. It will take a long time before the drift of the INS has become large enough for resulting in a completely inaccurate position. When using the PF algorithm to correct the position, it is therefore important not to spoil the advantages of the already well-working navigation system by leaning too much towards estimation of the position based on the PF compared to the dead-reckoning algorithm. The worst thing that could happen was if all particles at the correct position eventually were discarded, which can happen if the local measurements are not accurate enough, the maps are not accurate enough, the particles are too few, or the map measurements have been changed, e.g., due to some external effect. To meet this challenge, we propose dividing the particles into subsets at the beginning of each Re-sampling step. Then the particles in each subset are corrected according to the correction rule for the particular subset. There are different alternatives of how to divide the particles into subsets, when using magnetic and bottom depth data for the PF algorithm. We propose the following four subsets:

1. One subset of particles is weighted according to bottom depth measurements compared to a sea chart.

2. One subset of particles is weighted according to magnetic field measurements compared to a magnetic field map.

3. One subset of particles is weighted according to a combination of the bottom depth and magnetic field measurement (obtained by multiplying the

probabilities). By combining both magnetic fields and bottom depth distributions into a single one, $\mathbb{Y}$, the PF has a better ability to calculate the probability density $p(x_t \mid \mathbb{Y}_t)$. The drawback is that particles can be discarded incorrectly if any measurements or the maps from the two subsets are inaccurate.

4. The last subset of particles has equal weights, where only the dead-reckoned position changes from the RD matters.

By letting various portions of particles be evaluated by the different subsets, the advantages can be taken from each solution. The size of each subset can then be determined by the quality of the bottom depth and magnetic maps/measurements compared to RD accuracy. The advantage of using multiple subsets is that, e.g., bad magnetic measurements or maps will not damage the subsets where magnetism is not taken into consideration. The drawback is that it will take a longer time before the PF converges to the correct position.

If bottom depth gives a better performance than the magnetic field in some area, the particles can be divided, e.g., according to Table I.1.

In this way, the strength in combining data to support the PF is used by half of the particles. The other half of the particles are more carefully used so that some particles will survive even if local measurement errors occur or maps are inaccurate.

5 Evaluation and Tuning of the Algorithm

The program is written in Python, running on Ubuntu Linux in VirtualBox, on a high-end PC laptop. Even though the program is getting limited resources in the virtual environment, it still manages to simulate one hour of simulated time with 10000 particles, in one real hour. Each iteration lasts for 7.2 seconds. During the test runs, 500 particles were used for the high-accuracy INS and 5000 particles for the medium-accuracy INS. The algorithm is today made for simulation purpose and has not been tested in real-world conditions.

The following test runs first examine the performance of the algorithm when correcting 100% of the particles according to a single source of data. Then the performance is investigated when various combinations of these data sources are used. The last investigation is to see what happens when a portion of the particles are dead reckoned instead of using the PF. KF enhancement is used during all the tests, to see how this influences the performance. All the tests are being done using both a medium-accuracy INS and a high-accuracy INS.

5.1 Test Setup

In the test runs, a normal sea chart and a magnetic map with the same resolution as publicly available magnetic field maps (comparable with Figure I.5) were used. Echo sounder data and magnetometer data were simulated by reading values from manually created high-resolution maps, see Section 4.2.

The particles are evaluated if they are within the map area. If any particle is outside the map, they survive to the next iteration and are just dead-reckoned. By not being able to evaluate these outliers in a correct way, the performance of the algorithm is reduced. Hence, the route is chosen in a way so that particles seldom end up outside the map, especially for the high-accuracy INS.

During each test run, a ship was going around on the map for either 60min or 24h, depending on which INS that were being used. A predefined trajectory was used, so that multiple runs could be done using the same trajectory, thus making it possible to compare the performance in between. After the journey, the test was restarted using another configuration of subsets. When all runs were completed, the mean position error and covariance was calculated, and the PF position error, KF position error and INS position error were plotted. The INS in the tests was set to have an error of either 1NM (1852m) after 1h or 1NM after 24h, which is what some INS manufacturers guarantee for their medium and high-performance products. In the performance plots, see Figures I.8 and I.15, it is shown that this error dramatically increases with time.

A typical example of the symbols used in the program can be seen in Figure I.6. The symbols are summarized in Table I.2.

5.2 Example Images from Running the Program

The images in Figure I.7 show how the ship moves in the west direction. After passing the 20m-bottom-depth line, the PF is able to discard many of the wrongly positioned particles (to the south-east) and is thereby able to estimate the position more accurately.

5.3 Test 1 - Comparing Subset Methods

In the three runs in this 60 minutes test, 100% of the particles have been corrected using one of the subsets; bottom depth, magnetic field and a combination of those, see Figure I.8. The test has been done using the medium-accuracy INS. Because the INS's ability to estimate the velocity of the particles is rather limited, because of the INS's poor performance, the PF has trouble following the correct

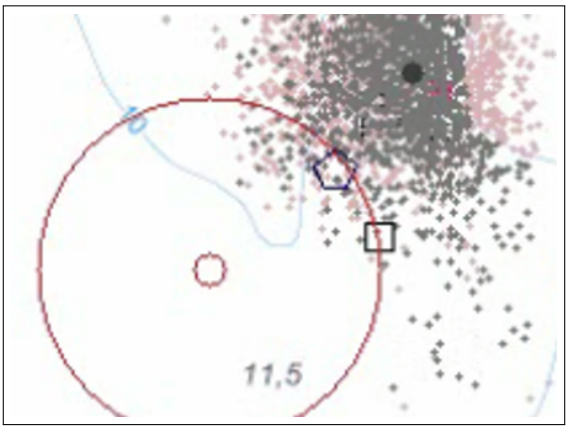

Figure I.6: The symbols in the program is summarized in Table I.2. The particles are indicated with small dots, where the brighter dots are discarded during the current iteration. The big dot marks the mean of the particle cloud. The INS position estimation is indicated by a circle, where the bigger ring grows with time to show the position uncertainty; the INS manufacturer guarantees that the ship is located inside the bigger circle. The correct position is indicated with a square, and the KF position estimation is indicated by a pentagon. Thereby, the wanted behavior is that the pentagon comes as close as possible to the square.

Table I.2: Legend for figure I.6

Symbol	Meaning
Small grey dot	Surviving particle
Small bright dot	Discarded particle
Large grey dot	Mean of particles
Square	True ship position
Pentagon	KF position estimation
Circle	INS position estimation with uncertainty area

position. This can be seen especially for the depth in the graph (1) and (2), but also for the magnetic field in the graphs (3) and (4). By combining the depth and magnetic field, so that the PF is corrected according to the subset where both the depth and magnetic field match the measured values, the particles are not to the same extent fooled to incorrect locations. The combined graph (5) has better performance, and by further enhancement of (5) by using a KF, (6) has a mean position error of only 79m. More information about the configuration and performance can be found in Table I.3. A video of (5) and (6) in Figure I.8 can be seen on `https://youtu.be/4m8AsuuYhF0`.

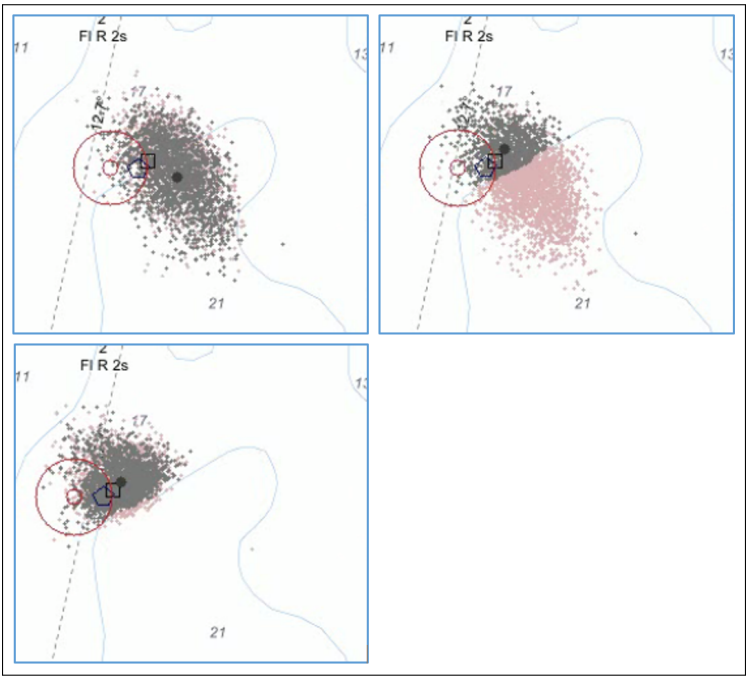

Figure I.7: For symbol legend, see Table I.2 on page 94. In the left upper image, the particle cloud is spread to the east from the true position. The right image shows how the particles to the south-west of the 20m bottom depth line are discarded, when the echo sounder system onboard the ship measures a depth of below 20m. In the left bottom image, the discarded particles are no longer showing.

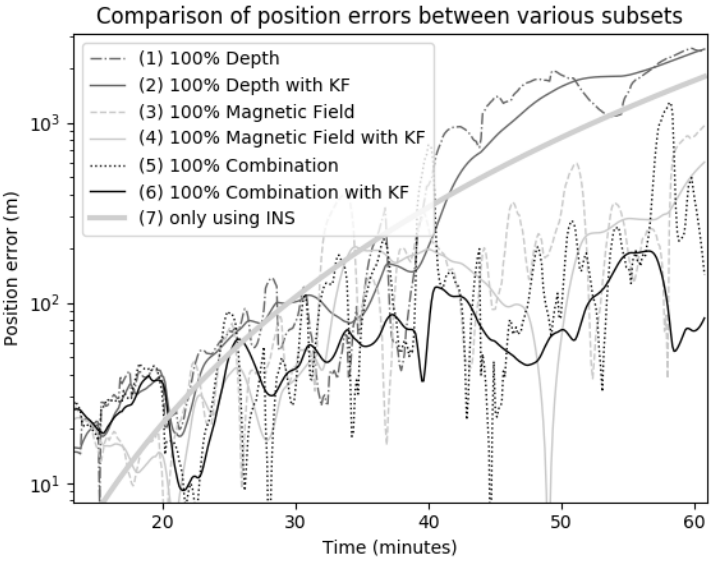

Figure I.8: Test 1: The PF with the correction from depth does not manage to track the correct position, seen in the graph (1) and (2). The performance is also rather limited for the magnetic graphs (3) and (4). By combining depth and magnetic field, the performance is increased in (5). The performance is enhanced even further by using a KF, seen in the graph (6). More information about the configuration and performance can be found in Table I.3.

Table I.3: Test setup for graphs in Figure I.8

Evaluation method	**(1)**	**(2)**	**(3)**	**(4)**	**(5)**	**(6)**	**(7)**
Depth	100	100	0	0	0	0	0
Magnetic Field	0	0	100	100	0	0	0
Depth ∩ Magnetism	0	0	0	0	100	100	0
Skip PF (Only INS)	0	0	0	0	0	0	100
PF Mean (m)	917	-	221	-	176	-	-
PF Covariance	677k	-	42k	-	50k	-	-
KF Mean (m)	-	860	-	164	-	**78.9**	-
KF Covariance	-	681k	-	15k	-	1740	-

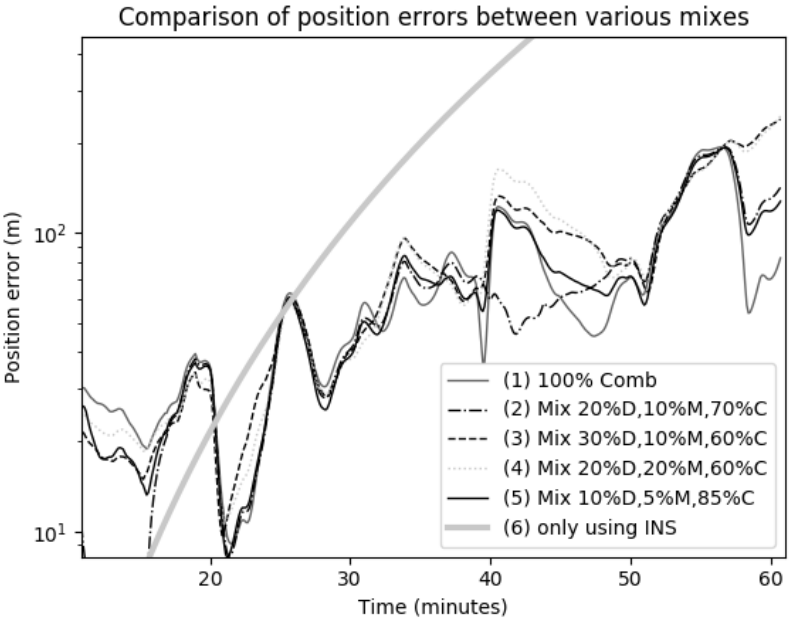

Figure I.9: Test 2: Various mixes of the subsets have been evaluated. There is no clear difference between the distributions though. (1) gives the best mean by using the KF, but (5) seems more robust due to the lower covariance. More information about the configuration and performance can be found in Table I.4.

Table I.4: Test setup for graphs in Figure I.9

Evaluation method	**(1)**	**(2)**	**(3)**	**(4)**	**(5)**	**(6)**
Depth	0	20	30	20	10	0
Magnetic Field	0	10	10	20	5	0
Depth ∩ Magnetism	100	70	60	60	85	0
Skip PF (Only INS)	0	0	0	0	0	100
PF Mean (m)	176.3	**155.2**	167.2	165.9	167.4	-
PF Covariance	49800	37500	45451	43000	43000	-
KF Mean (m)	**78.9**	80.7	99.6	102.0	**83.4**	-
KF Covariance	1737	1740	2830	3020	**1700**	-

5.4 Test 2 - Comparing Various Mixes of Subset Methods

In the five runs in this 60 minutes test with the medium-accuracy INS, various distributions have been used for the 3 subsets, investigated in Section 5.3. The idea is that by having a portion of the particles corrected by various subsets, they are more likely to overcome difficult areas in the map where the particles can get lost from the correct position. By studying the behavior of the PF, no major difference is found though. Various distributions seem to be beneficial in different situations. Because of the lack of a clear result, a distribution somewhere in the middle has been chosen. This gives the distribution of 85% from the subset *Combination*, 10% from *Depth* and 5% *Magnetic Field* for the next step for further studies. More information about the configuration and performance can be found in Figure I.9 Table I.4.

5.5 Test 3 - Comparing Various Mixes of Subset Methods for a High-Accuracy INS

In the five runs in this 24-hour test, the 3 subsets investigated in Section 5.3 has been tested with the high-accuracy INS instead, which guarantees a position error of less than 1NM after 24h. In the first three runs in this test, 100% of the particles have been evaluated using only one subset; bottom depth, magnetic field and a combination of those, see Figure I.10. The sea chart has greater accuracy and resolution than the magnetic field map, and it is, therefore, the expected result that bottom-depth correction should give better performance, which is also the result. The third test run is correcting 100% of its particles according to a combination of the two first. This increases the performance even further. In the fourth and fifth run, a portion of the first three evaluation methods are used. The size of the various portions are first based on the performance of the individual methods, and the subset sizes have then been adjusted after empirical tests to gain the best performance. This method gives even better results than the third one. The reason is probably that sometimes the PF benefits from handling the particles in a smoother way. The most important thing when having a high-performance INS is not to let the particle cloud lose track of the correct position, and by having used multiple suggestions from various subsets, it is less likely to lose track. One example where the particle cloud loose track of the correct position will be presented later in Figure I.14.

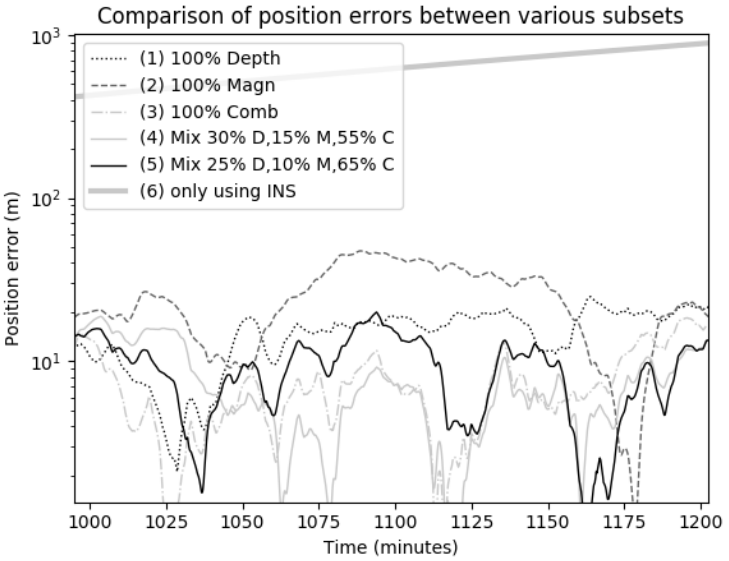

Figure I.10: Test 3: The graph presents 200min of the second half of a 24h test. By using the high-accuracy INS, the particles can follow the correct position with good accuracy. By combining the subsets from (1) and (2), the accuracy is increased even further. It is not until after 22h, the mixed subsets have a position error greater than 42m. More information about the configuration and performance can be found in Table I.5.

Table I.5: Test setup for graphs in Figure I.10

Evaluation method	**(1)**	**(2)**	**(3)**	**(4)**	**(5)**	**(6)**
Depth	100	0	0	30	25	0
Magnetic Field	0	100	0	15	10	0
Depth ∩ Magnetism	0	0	100	55	65	0
Skip PF (Only INS)	0	0	0	0	0	100
PF Mean (m)	23.8	38.7	25.6	22.2	21.3	-
PF Covariance	635	720	304	279	317	-
KF Mean (m)	22.5	28.9	19.8	17.0	**16.8**	-
PF with KF Covariance	539	217	204	160	227	-
KF max error during 24h (m)	120	72.9	77.9	74.0	84.9	-

Comparing of PF Performance With and Without KF

In this section, the subset (5) in Figure I.10 and Table I.5 is studied further. In Figure I.11 the position error can be seen when using and when not using a KF to enhance and smoothing the performance. 200 minutes from the second half of the 24h test are studied. The graph shows the position error of the INS, which is around 600m. The PF gives a position error of around 40m during these 200 minutes, while the KF enhancement of the PF gives a mean error of around 10m.

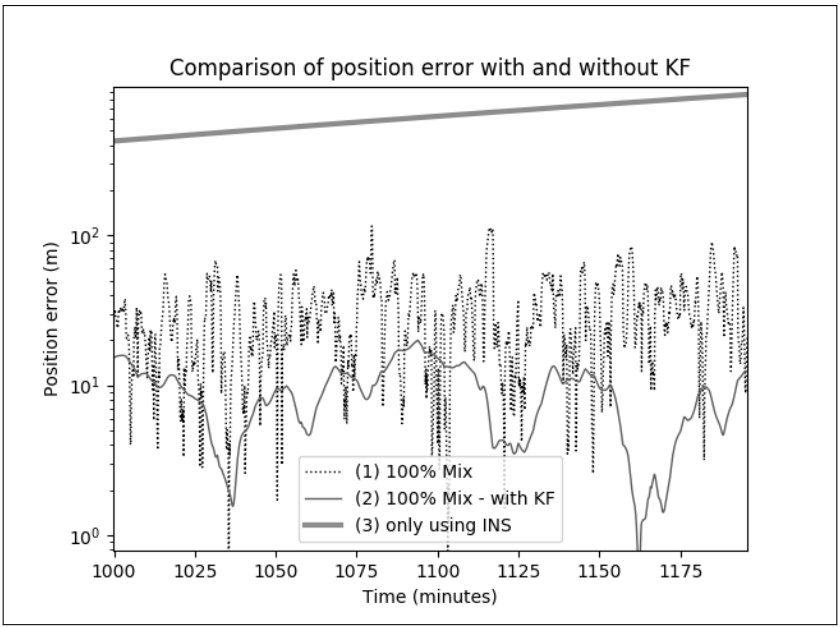

Figure I.11: The graph presents around 200min in the second half of a 24h test from the subset (5) in Figure I.10. The PF with the mix of evaluation methods significantly increases the position accuracy, compared to the position estimation from INS. The position accuracy is enhanced even further with the KF, by lowering the mean position error from around 40m to around 10m, during these 200 minutes.

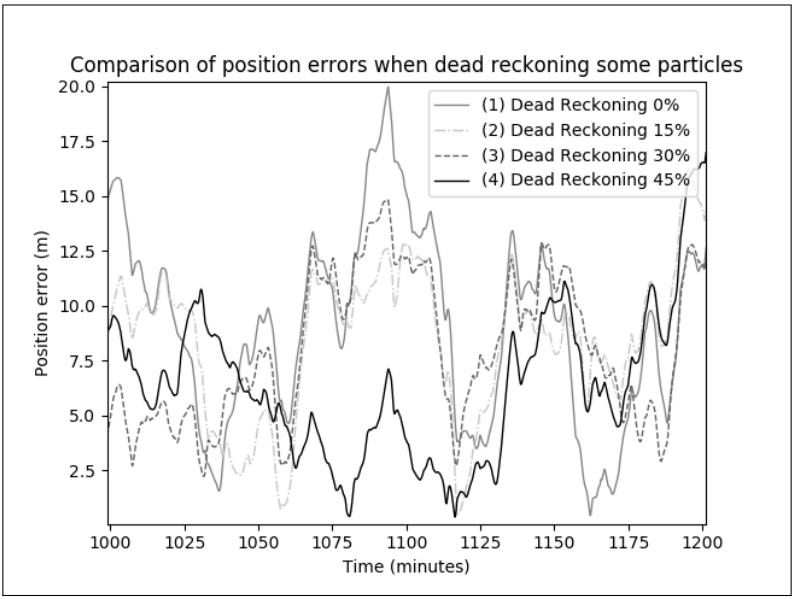

Figure I.12: Test 4: The graphs show that the performance of the algorithm is actually increased, when a large amount of the particles are dead reckoned, instead of using the PF. By dead reckoning 45% of the particles, the position error is maintained less than 33m for 23h. The mean position error during the first 20h is 10.2m. More information about the configuration and performance can be found in Table I.6.

Table I.6: Test setup for graphs in Figure I.12

Evaluation method	**(1)**	**(2)**	**(3)**	**(4)**
Depth	25	21.25	17.5	13.75
Magnetic Field	10	8.5	7	5.5
Depth ∩ Magnetism	65	55.25	45.5	35.75
Skip PF (Only INS)	0	15.0	30	**45.0**
PF Mean (m)	21.3	24.8	22.5	18.3
PF Covariance	320	240	255	212.6
KF Mean (m)	16.8	20.2	17.7	**14.9**
KF Covariance	226.6	197	190	197.5

5.6 Test 4 - Investigating the Performance when a Portion of Particles are Dead Reckoned

When having a high-accuracy INS, it is possible to maintain the position during long periods of time without using GPS, PF, or other methods. In this test, the performance is evaluated when a portion of the particles are not using the PF, but instead are dead reckoned by the velocity from the INS. Figure I.12 shows that by dead reckoning a large portion of the particles, the algorithm performance can be increased. This is probably happening because the ability to lose track of the correct position is lowered by trusting more in the INS. The mean position error during the first 20h is 10.2m. More information about the configuration and performance can be found in Table I.6. A video of (4) in Figure I.12 can be seen on `https://youtu.be/EFamUSUsIOs`.

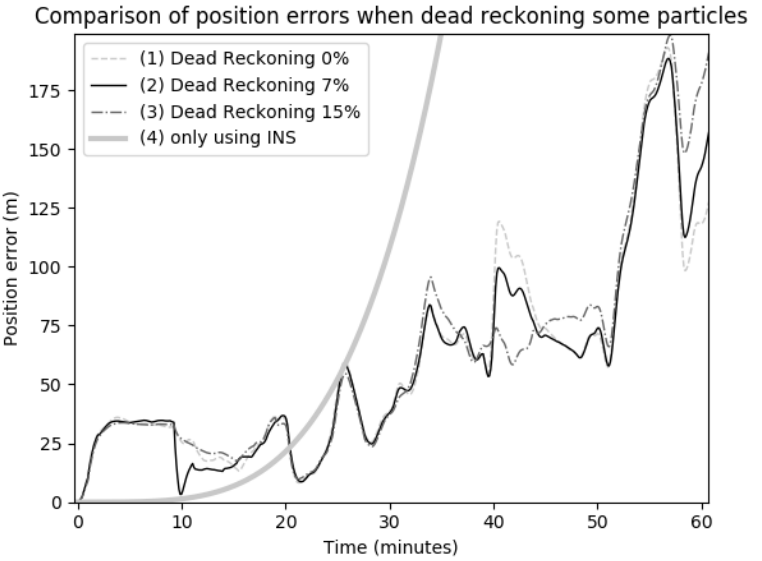

Figure I.13: Test 5: The graphs show that the performance of the algorithm is increased a bit when 7% of the particles are dead reckoned, but there is no clear difference in contrast to the difference received when using the high-accuracy INS. By dead reckoning 7% or 15% of the particles, the position error is maintained below 100m for 50min. More information about the configuration and performance can be found in Table I.7.

Table I.7: Test setup for graphs in Figure I.13

Evaluation method	**(1)**	**(2)**	**(3)**	**(4)**
Depth	10	9.3	8.5	0
Magnetic Field	5	4.65	4.25	0
Depth ∩ Magnetism	85	79.05	72.25	0
Skip PF (Only INS)	0	**7.0**	15.0	0
PF Mean (m)	167.4	161.4	150.7	-
PF Covariance	43000	41700	36000	-
KF Mean (m)	83.4	**82.4**	86.9	-
KF Covariance	1690	1700	2225	-

5.7 Test 5 - Investigating the Performance when a Portion of Particles are Dead Reckoned

When instead using the medium-accuracy INS, it is no longer possible to rely as much on the performance of the INS. As in Section 5.6, this test evaluates the performance when a portion of the particles are dead reckoned instead of using the PF. The test shows that it is more beneficial to trust more in the PF than the INS, even though there is no clear difference. The best performance was acquired when dead reckoning 7% of the particles, see Figure I.13, which also can be seen on a video on `https://youtu.be/OVVO53qduWg`. More information about the configuration and performance can be found in Table I.7.

5.8 Test 6 - Comparing Performance when not Using the Bottom Depth Lines

The bottom-depth lines provide the PF with accurate information about which depth interval there is in an area. This helps the PF discarding particles with an incorrect depth value, increasing the performance of the PF. On the other hand, it will in some cases delete particles in the vicinity, pushing the mean away from the correct position. This phenomenon can be observed in Figure I.14. When not using bottom depth lines, it is, therefore, converging slower and the particles are spread in a larger area, but the mean of the particles is still located near the correct position.

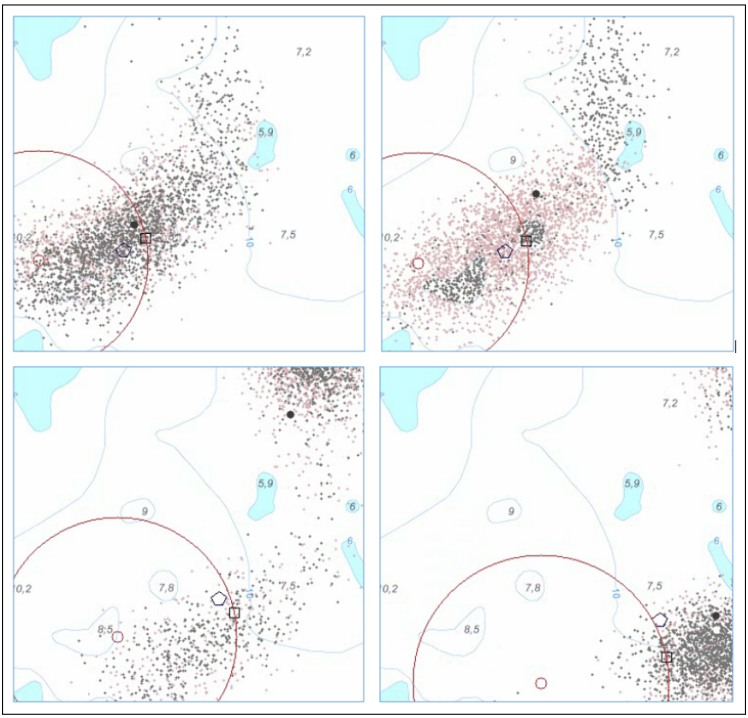

Figure I.14: In this image, the particle cloud is initially (top left image) spread around the ship (indicated by the square). When passing a grounding (top right image), most particles are discarded and split into smaller sub-clouds. The mean of the particle cloud moves to the biggest sub-cloud (bottom left image), far from the correct position. A few moments later (bottom right image), the particles located in the wrong location, has been discarded after further evaluation of the particles. A position has been estimated by a KF, using the position estimation from the particle filter along with the INS data. The Kalman position estimation is indicated by a pentagon. In the four images, it can be seen that the KF gives a more stable and accurate position estimation, as it does not respond to the fast position variations from the particle filter.

In many areas, the sea charts are not equipped with bottom-depth lines. With this in mind, it is interesting to evaluate the performance also without using them, which has been done in these two test runs. The first test run compares the performance of the high-accuracy INS during a 24h test, see Figure I.15 and a video on `https://youtu.be/v2H26Olyr6c`. Even though the position error is larger when not using the depth bottom lines, the mean position error from when using the KF enhancement still is maintained at 34.0m, and the position error does not overshoot 70m until the very last minutes of the test.

The algorithm for the medium-accuracy INS also shows a good performance. It maintains a position accuracy comparable to when using the depth lines until 40min, see Figure I.16 and a video on `https://youtu.be/p69zQzMSciU`. After about 45min, it has problems tracking the position due to the big velocity error in the INS.

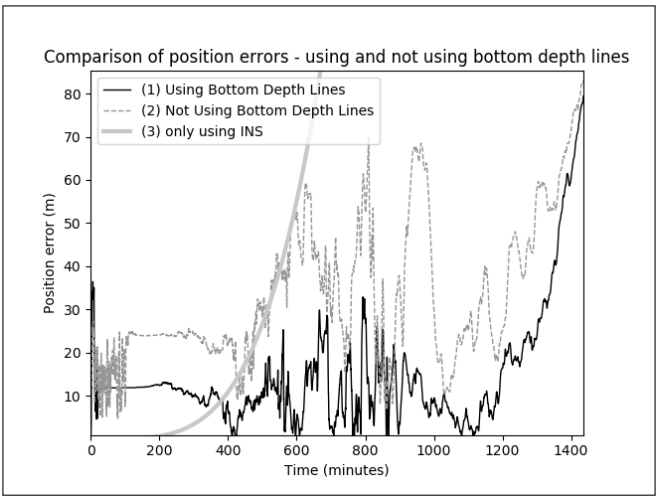

Figure I.15: Test 6:1: The high-accuracy INS is used. The performance is influenced by using or not using the bottom depth lines in the sea chart. Even though the performance is lower, it still manage to track the correct position during the 24h test. A mean position error of 34.0m is maintained.

5.9 Further Development and Testing of the Algorithm

The algorithm has only been tested with simulated data so far, but the plan for the future is to test it on a ship, using digital sea charts and magnetic maps. The

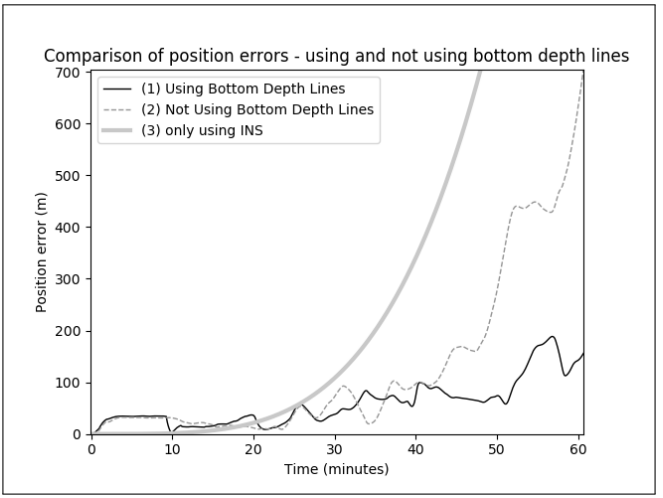

Figure I.16: Test 6:2: The medium-accuracy INS is used. It shows a good performance during 45min, even though the bottom depth lines are not being used. After this time, it has problem tracking the correct position.

position can then be compared to a GPS position. When testing at sea, it will also be important to keep track of the water level, as the tide will influence the performance significantly due to the importance of correct bottom depth measurements.

6 Conclusion

It has already been shown that PF algorithms can be used for estimating positions [70, 82, 127, 128], and it has even been shown that it is possible to accurately estimate a ship's position if high-resolution maps are available [67, 68, 71–74, 77, 122, 122–126, 129]. This paper describes how this technique can be used in solutions more suitable for real-world scenarios, where only normal sea charts and magnetic field maps are available. The paper has shown how the performance varies depending on only using one or multiple inputs to the PF, and how the performance can be enhanced by using a KF. It has also been shown how the performance of the INS influences the position accuracy when using the PF.

When fusing the different PF methods in a 20h long test, the mean of the position errors for the high-end INS has been calculated to be 10.2m when using the bottom depth lines, and 30.5m when not using them. This is not as

good as GNSS-based accuracy, but probably accurate enough for most navigation purposes. When using the medium-accuracy INS, the mean position error for a 40min long test was 35.4m when using the bottom depth lines, and 37.1m when not using them.

Whether it is possible to navigate accurately enough without GNSS systems, only relying on high-performance navigation sensors and normal sea chart and magnetic charts, still remains unclear. Further testing with real ship data in multiple areas is therefore necessary.

ACKNOWLEDGMENT

This work was partially supported by the Wallenberg AI, Autonomous Systems and Software Program (WASP) [1] funded by Knut and Alice Wallenberg Foundation.

Paper II

Paper II

Robust Terrain-Aided Navigation through Sensor Fusion

Mårten Lager
Department of Computer Science
Lund University
Saab Kockums AB
marten.lager@cs.lth.se

Elin A. Topp
Department of Computer Science
Lund University
elin_anna.topp@cs.lth.se

Jacek Malec
Department of Computer Science
Lund University
jacek.malec@cs.lth.se

Abstract

To make autonomous, affordable ships feasible in the real world, they must be capable of safely navigating without fully relying on GPS, high-resolution 3D maps, or high-performance navigation sensors. We suggest a method for estimating the position using affordable navigation sensors (compass and speed log or inertial navigation sensor), sensors used for perception of the environment (cameras, echo sounder, magnetometer), and publicly available maps (sea charts and magnetic intensity anomalies maps). A real-world field trial has shown that the proposed fusion mechanism provides accurate and robust navigation, applicable for affordable autonomous ships.

In "2020 IEEE 23rd International Conference on Information Fusion (FUSION 2020)", DOI: 10.23919/fusion45008.2020.9190578

1 Introduction

Unmanned autonomous ships (surface and sub-surface) face challenges when it comes to navigating safely at sea. Today mainly Global Navigation Satellite Systems (GNSS) are used, where the Global Positioning System (GPS) is the most common one. As GNSS systems easily can be jammed or even spoofed [65], and do not work if submerged or objects are blocking the path towards the satellites, it is essential to complement the navigation ability with other solutions. Human operators typically do this by comparing the surrounding world to the digital sea chart, as well as by watching out for surrounding obstacles as a lookout, see Figure II.1. Humans are skilled in having a good overview of the navigation, and can reason about and adapt to the situation if the surrounding area does not match what is seen in the sea chart. The reasoning comes at a cognitive cost, though, and after a while, a human loses focus with increased risks for mistakes [130]. This is one of the reasons why 90–95% of all collision accidents at sea since 1999 are caused by human errors [14].

Figure II.1: The main author is acting as a lookout during the field trial.

To surpass the human's ability to navigate, a machine should use the strength it possesses, instead of mimicking how humans navigate. We believe a good approach should use several data sources weighted according to performance and combine them to generate the best statistical position estimation.

In previous work, we presented Terrain-Aided Navigation (TAN) and evaluated the performance of a Particle Filter (PF)-based approach using simulated data only [131]. It used a high-performance INS and compared standard map data with fused data from depth, magnetic field intensity, intersection of those, and the dead reckoned position. We have used that earlier work as a baseline for

our new approach presented in this paper. Here, we have refined the approach by using, instead of the high-performance INS, affordable sensors such as compass and log. We have also extended the underlying algorithm to use Kalman Filter (KF) feedback, as well as bearings to landmarks. Instead of evaluating the performance using simulated data, we have collected data in a real-world field trial in the Swedish Archipelago.

With this, we are able to combine and evaluate standard technologies regarding their applicability in affordable ships in a real-world scenario that can use data from publicly available maps (e.g., sea charts) and still perform sufficiently well.

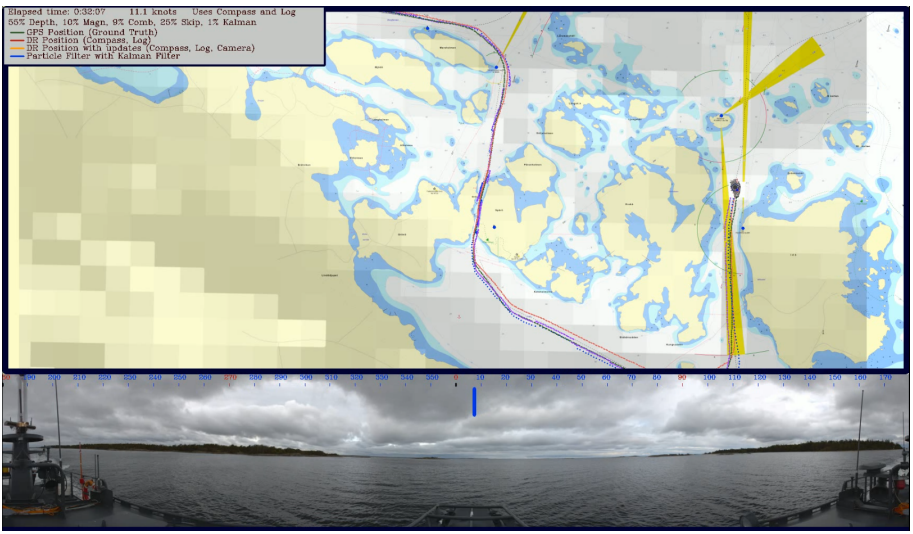

Figure II.2: Screenshot of the GUI. At the bottom is the 360°-video presented, wherein this case the ship has course 7°. The top part is showing the sea chart, and the current route, where the ship and surrounding particles currently are to the right in the image. The overlayed magnetic intensity anomalies map is seen as squares in various greyscale.

Using the collected data, we have created a simulator with a GUI, see Figure II.2, where we have evaluated our algorithm using different fusion mixes while having various amounts of simulated drift. Our evaluations show that the performance, especially regarding the robustness of the system, is increased, when combining multiple data sources.

Summarising, our main contributions are:

- a robust approach where we conduct TAN based on fused data,
- a thorough evaluation of the approach on real-world data,
- evidence of the applicability of affordable sensors for reasonable results, instead of high-accuracy sensors,
- evidence of the applicability of regular sea charts and publicly available magnetic intensity anomaly maps, instead of high-resolution 3D terrain maps.

The paper is organized as follows. In Section 2, related work is described regarding how bottom depth and magnetic intensity have been used by PFs to implement TAN. Section 3 describes the algorithm and how the maps are interpreted, followed by Section 4 that describes the sensors that have been used on the boat. The tests are described in Section 5, with the Conclusion in Section 6.

2 Related Work

We discuss in the following related work based on TAN using different types of sensory data available at sea.

2.1 Particle Filter using Depth Data

Our approach to TAN uses bottom depth measurements and compares these with a known map. Because it uses distributions that are highly nonlinear, non-Gaussian, and multimodal, classical methods with low computer power needs, such as KF perform poorly [66]. By this, KF implementations, which were more common before the year 2000, have nowadays mainly been replaced by implementations of PFs and Point Mass Filters (PMF) [67]. We apply the multi-hypothesis filtering method PF, with the ability to tackle the mentioned difficulties [68, 69].

It has been shown many times that a PF can estimate the position by comparing the bottom depth with a known high-resolution 3D terrain map [68, 69, 71–76]. Many of these references focus on a use-case for Autonomous Underwater Vehicles (AUV) [69, 71–76], where it is of particular importance to be able to navigate without a GNSS system. An AUV is typically equipped with a multibeam sonar in order to map the seabed, and as the equipment is already available, it has also been used for the PF [69, 71–74]. We use a single-beam echosounder instead, which makes the use-case relevant for a more substantial portion of ships.

There are still problems to be solved in order to make the technique applicable to most real-world scenarios. The first problem is that there are almost no areas in the world with high-resolution 3D terrain maps. Because of this, AUV deployments are typically preceded by a ship-based multibeam bathymetry survey of the operating area, followed by processing of the data (outliers are removed), and the construction of the gridded bathymetric reference map [78]. This puts a considerable limitation to the usage of the TAN technology. Hence we instead restrict ourselves only to use publicly available sea charts, which cover most coastlines.

The performance of the PF also increases with varied terrain, but in some areas, the terrain is quite flat, resulting in poor accuracy [77, 79, 80]. In symmetric terrain, there can also be a problem with sample impoverishment, which can occur when the particle cloud is divided to follow paths that give similar measurement values. Teixeira et al. reduce this problem by using three different types of PFs to different terrains types [75]. Another difficulty that generally is not mitigated is that a PF is vulnerable to outliers in the maps or depth measurements. Peng et al. point out that these outliers can occur in many ways, and they describe how to alleviate the effect by using the Huber function when setting the importance weights for the PF [69].

To mitigate all these types of problems in our work, we do not rely on depth measurements alone, but instead, use a combination of different measurements. By relying on multiple domains, we make our algorithm less susceptible to sample impoverishment and to outliers.

2.2 Particle Filter using Magnetic Intensity

A magnetic field surrounds Earth, where each ferromagnetic element disturbs this field. These disturbances can for indoor environments be even greater than the natural magnetic field of Earth [81]. For indoor environments, numerous ferromagnetic elements create a complex magnetic field where the magnetic vector varies greatly depending on the location. As long as no major furniture or iron walls are moved, the magnetic field is also quite stable. Frassl et al. use a PF combining the magnetic field with a magnetic anomaly map together with odometry, to localize a mobile robot [82]. In [81] the position of a human user is estimated by measuring the magnetic field and acceleration by only using cheap smartphone sensors.

In our approach, we use the magnetic intensity as a second input to the PF, together with the previously mentioned depth measurements. The magnetic field

does not fluctuate nearly as much as for indoor use, and each pixel in the available map corresponds to 185m×185m. Still, this is enough to improve performance.

2.3 Using other data for the Particle Filter

Other measurements than depth and magnetic field intensity have been used in research to support a PF. Karlsson et al. used radar to measure bearings and ranges to land objects [68]. Some echosounder systems measure not only the bottom depth, but also the range to different sediment layers below the bottom. The benefit of using lower layers of the bottom is that these layers tend to have more variations [77]. The downside is that there are few maps available.

It is also possible to compare the current gravity with a gravity anomaly map, which Musso et al. show can be beneficial for navigation [85]. Other candidates that can be used together with a PF are:

- Celestial Navigation, where, e.g., a star in a specific direction, is present or not [68],
- Bearings to landmarks from, e.g., visual sensors [68].

We have used bearings to landmarks in our project as a third data source to increase the robustness and the performance of the system.

3 TAN with a Mixture Re-sampling Step

In the following, we explain our PF based Terrain-Aided Navigation algorithm, and how it has been extended with a mixture function for the re-sampling step for increased robustness. It has been fed by data about depth, magnetic field intensity, and bearings to known landmarks.

3.1 Transition Model

The ship goes on a surface route, where its state is estimated with N particles, with ($\mathbf{X}_t$) denoting all the N particles in time t yielding:

$$\mathbf{X}_t = [x_t^{(1)}, x_t^{(2)}, ..., x_t^{(N)}]^T \tag{II.1}$$

Each particle contains the state representation according to:

$$x_t^{(p)} = \begin{bmatrix} \lambda_t^{(p)} \\ \Phi_t^{(p)} \end{bmatrix} \tag{II.2}$$

where $\lambda_t^{(p)}$ is the latitude of the position for particle p in time t, and $\Phi_t^{(p)}$ is the longitude for the same particle.

At the beginning of each test, N particles are initialized around an initial, known position (x_0) using (II.3), where the superscript states the particle index and the subscript the time.

$$x_0^p = x_0 + \mathcal{N}(0,\, \sigma^2) : p = 1, 2, ..., N \tag{II.3}$$

The state changes over time, with the discrete sample time Δ, and is modeled by:

$$x_{t+1} = f(x_t, u_t, \eta_t) = \begin{bmatrix} \lambda_t + v_t \Delta \sin(\varphi_t) \\ \Phi_t + v_t \Delta \cos(\varphi_t) \end{bmatrix} + \eta_t \tag{II.4}$$

where $u_t = [v_t, \varphi_t]^T$ is the input signal, which consists of the speed v_t and the compass angle φ_t. The η_t is the process noise.

We now have the model to go from one state to the next state. For the particle filter to work, information about how the measured values depth and magnetic intensity y_t depend on the state x_t is also needed. For this, we use the sea chart and the magnetic intensity anomalies map.

3.2 Maps

As we use a standard sea chart (see Figure II.3) and a low-resolution magnetic intensity anomalies map (see left part of Figure II.4), it is not possible to look up the depth and magnetic intensity value directly in the location of one particle. Instead, for each particle, we create a Probability Density Functions (PDF) of the depth and the magnetic intensity estimation.

For creating the PDF^{depth}, we gather the bottom depth indicators closest to the specific particle from the sea chart. For the right part of Figure II.3, where the location of a particle is indicated with a star, these are $\{7.4,\ 1.9,\ 8,\ 5.4\}$. We then weight these indicators according to $weight = distance^{-1}$. From these values, we calculate a weighted mean and a weighted standard deviation, which we use for creating the PDF with a normal distribution. The 6m bottom depth line in the right part of Figure II.3 specifies that the minimum bottom depth by the star is 6m, hence the PDF is truncated below 6.0m. The 10m bottom depth, on the other hand, does not provide any more information for the PDF, as the bottom depth is allowed to be more than 10.0m.

The left part of Figure II.4 shows a publicly available magnetic intensity anomaly map overlayed over the sea chart over the area near Västervik in Sweden. As

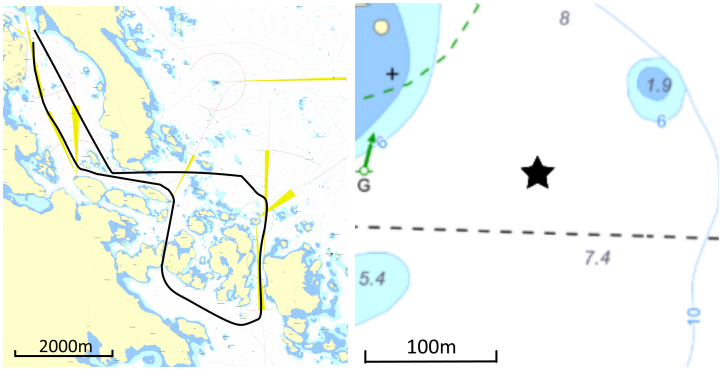

Figure II.3: The left image shows a sea chart over an area outside Västervik in Sweden. The route of the field trial is drawn in black. The right image shows an enlargement of a specific part of the map. The 6m bottom depth line indicates that it is at least 6m deep by the star. The 10m bottom depth line indicates that it is at least 10m deep to the right of the bottom depth line, but does not indicate anything to the location of the star. We have used the bottom depth lines, together with the bottom depth indicators (7.4, 1.9, 8, 5.4) for the creation of a PDF of the bottom depth.

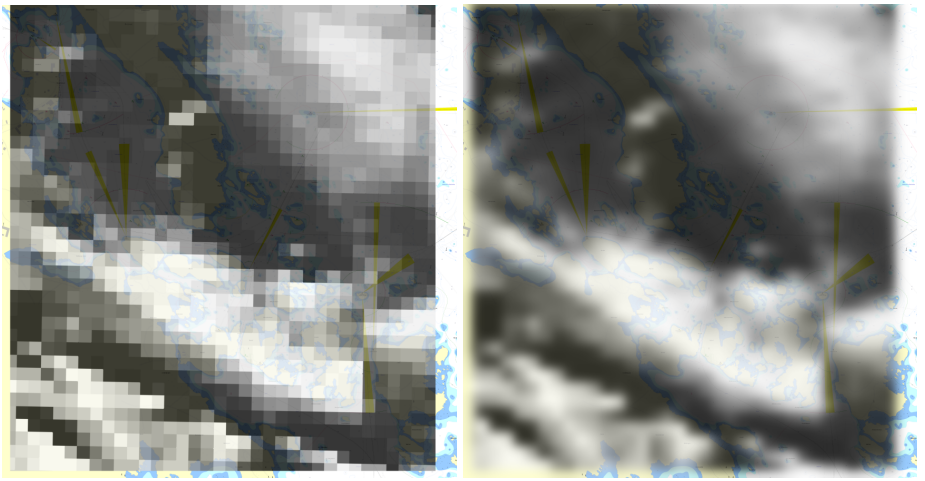

Figure II.4: The magnetic intensity anomalies map is overlayed over the sea chart. From the original map, each pixel has the size of 185m×185m, see the left image. To get a map that better corresponds to the real world, this low resolution map has been interpolated into a high resolution map, see the right image.

can be seen, the anomaly map has low resolution, and each pixel corresponds to an area of 185m×185m. To estimate the magnetic field with greater accuracy, the map has been interpolated into the right part of Figure II.4, creating a high-resolution image. We then use nearby values for creating a PDF^{Magn} in a similar way as for creating the PDF^{Depth}.

3.3 Algorithm

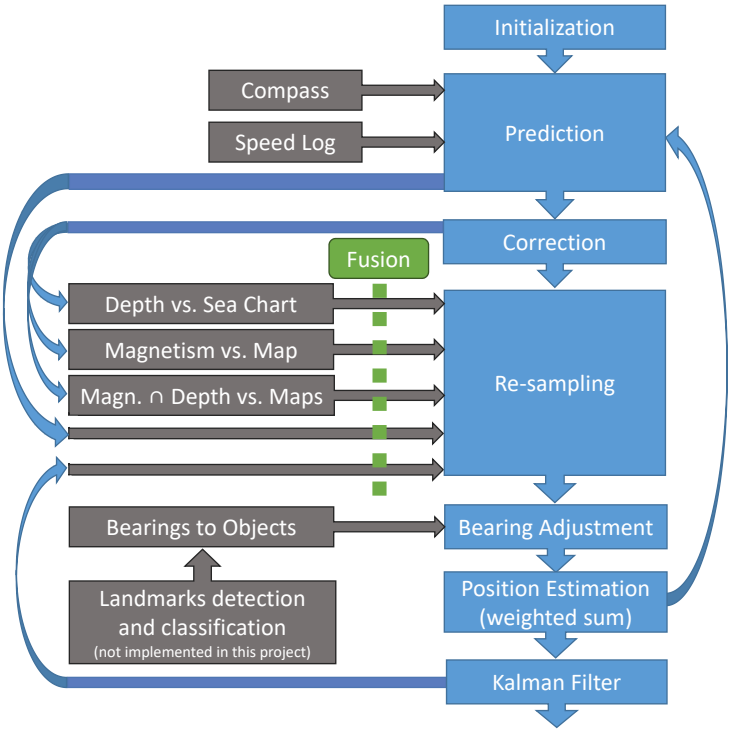

Figure II.5: The PF algorithm used in the project.

The specific PF algorithm used for this project is the Sampling Importance Resampling (SIR) [132], which we have slightly adjusted to enhance the robustness by fusion of various measurements. The high-level behavior (see Figure II.5) is as follows:

1. **Initialization** - Generate N particles and give them a random starting position around the initial starting position x_0 using (II.3).

2. **Prediction** - Move each particle according to the velocity vector measured by the compass and speed log, as well as an additional random velocity vector (see (II.4)).

3. **Correction** - Calculate weights for each particle given the maps and each particle's position. The weights are calculated for depth, magnetic field, and a combination of those two. Normalize the weights.

4. **Re-sampling** - The particles are resampled according to a distribution from subsets defined in Section 3.4.

5. **Bearing Adjustment** - If a bearing to a landmark is detected, all particles that are outside a 2° corridor to the landmark are moved to a normal distribution around the bearing line.

6. **Iteration** Go to step 2.

To further enhance the performance, we used a KF for the final position estimation.

3.4 Fusion by Evaluating the Particles by Using Various Data

The Resampling Step creates particle subsets of defined sizes to benefit from the different available data. The weights created in the Correction Step can be based on either the intersection $Depth \cap Magnetic\ Intensity$ or $Depth$ or $Magnetic\ Intensity$ separately. We denote a PF that re-samples fully from only one of these subsets as PF^{Depth}, PF^{Magn}, or PF^{Comb}, and we denote a PF that re-samples from all the subsets as PF^{Fusion}. The particles can also just be dead reckoned using the compass and speed data (DR). The KF gives a good estimation of the correct location. Hence a small portion of the particles can be recreated at the KF estimation.

The subset sizes of the PF can be set arbitrarily, and we hypothesize that a well balanced PF^{Fusion} will perform better and especially be more robust compared to the other PFs using a single subset.

4 System Setup

Our overarching goal is to provide insights from the evaluation of navigation tools for future affordable autonomous ships that can not rely on GNSS navigation

alone due to safety constraints. The position accuracy gained when navigating is dependent on the performance of each navigation sensor. There are many possibilities to use better sensors, but these often come at a higher cost. A very expensive *Inertial Navigation Sensor* (INS) system can be used, which often has a drift of less than 1852m (1 Nautical Mile, NM) after 24h. In our previous work, we evaluated a PF using an INS like that, using simulated data [131]. A speed log that measures the *Speed Over Ground* (SOG) instead of *Speed Through Water* (STW) can also be used, as well as a *Multibeam Sonar* (MBE), which makes it possible to create an accurate 3D terrain of the bottom. These types of sensors have not been used for the presented work, as the high cost would limit the practical usage significantly.

Figure II.6: The boat of type CB90 used in the field trial.

We have based our algorithms and evaluations on the sensors used in the field trial, which we believe corresponds to the setup of a typical future affordable autonomous ship. The boat used in this project is of type *CB90* (see Figure II.6), and has been complemented with some additional sensors to support the Swedish Universities via the WASP program[1] with a research platform for developing tools for autonomous ships. Data is collected from the digital compass onboard, but the ship is not equipped with a speed log. Instead, a virtual speed log has been created by using data from the GPS and adding an error of 0.2 knots (i.e., NM/h) (see Table II.1). In the last step, we add a drift (0.0–1.5 knots) to mimic the drift from the wind and current that can not be detected by the compass and speed log.

We mounted the magnetometer on the non-magnetic aluminum hull. Its purpose was to measure the anomalies of the magnetic intensity. As these anomalies are small, it is essential to know how the own ship disturbs the values when, e.g., a windshield wiper motor is started. During the data collection, this knowledge

was not available, which unfortunately made the magnetic intensity values less accurate. The echo sounder system, on the other hand, was already installed and calibrated. Hence the data matched the sea chart well.

For obtaining the bearing information to landmarks detected in a video stream from a 360° camera, the intention was to mimic a system that would be able to detect, classify, and measure the bearings to visual landmarks. As we have not integrated this AI technology into our system yet, the bearings were measured manually from the video feed available on board.

Table II.1 presents the data that we collected. We downsampled all the data to 0.5Hz, as it was collected with a higher frame rate than needed. Also, the data from the GPS, which we used as ground truth, was downsampled to 0.5Hz. With the used speed of the boat, 0.5Hz implies that we get data every 9m, which can be considered as relatively dense readings at sea. It should be pointed out that limitations of our approach are not due to limited sensor readings, as the bottleneck is the sparseness of information in the maps. In the right part of Figure II.3, it can be seen that there can be easily a distance of about 200m between two bottom depth measurements in the sea chart.

Table II.1: Sensors used during field trial

Sensor	**Description**
Digital Compass*	Heading (Accuracy 0.5°) - 1Hz
Speed Log*	STW (Accuracy 1% + 0.1knots) - 1Hz
Echosounder	Depth from surface to sea bed (Accuracy 0.1m) - 1Hz
Magnetometer	Magnetic Intensity measured as a vector - 100Hz
360° camera	Provides visual image of the horizon around most of the ship. Can alternatively be multiple cameras. Images from 6 cameras were compiled into an image with a resolution of 16384×8192 - 15Hz

*The digital compass and speed log could be exchanged to an INS.

The boat traveled a 17km long route in the Swedish archipelago for 54min. The route is shown in Figure II.3, where the weather conditions can be seen in one of the videos, accessed from one of the links, presented, e.g., in Figure II.7.

We gathered 69 bearings to landmarks from the videos with at least a time of 30 seconds between each measurement.

5 Test Runs for Evaluating the Positioning Algorithm

We conducted a series of tests with various mixes of subsets used evaluation and optimization of the PFs. Every such subset mix is denoted as:

$$Depth\ A\%, Magn\ B\%, Comb\ C\%, DR\ D\%, KF\ E\% \tag{II.5}$$

This should be interpreted as A% of the particles are re-sampled using weights from the Correction Step created by comparing $Depth$ with the sea chart, B% from $Magnetic\ Intensity$, C% $Depth \cap Magnetic\ Intensity$, D% Dead Reckoned (DR), and E% from KF.

Each of the following tests is based on the same 54min long data collection from the field trial, and has been conducted with a PF with 1000 particles. Different amounts of drifts have been added to stress test the algorithm. We present the main tests from this evaluation in Section 5.3; however, we start out with presenting evaluations of tests for KF and DR.

5.1 Resampling from KF subset

In the following tests, we evaluate whether performance is improved by resampling 1% of the particles from the KF position estimation. We conducted a total of 12 tests, where half of the tests had a drift of 0.25 knots and the other half a drift of 0.75 knots. Various mixes were used according to Table II.2.
As can be seen in the table (the best value for each comparison is marked with bold text), the KF estimations seem to slightly improve the performance for most tests, especially for the tests having lower accuracy due to the weaker performance of the magnetic corrections. As we prioritize robustness, and we assume that the usage of the KF position will decrease our risk of starvation of particles at the correct location, we decide to use 1% KF for the rest of the tests.

5.2 Re-sampling from Dead Reckoned particles

In the following tests, we evaluated whether the performance is improved by each iteration randomly selecting 29% of the particles, and dead reckoning them instead of using the PF functionality. The benefit is that some particles will survive

Table II.2: Test using KF positions

Drift	Depth	Magn	Comb	DR	KF	Mean Pos Error (m)
0.25	100	0	0	0	0	41.9
0.25	99	0	0	0	1	**37.5**
0.25	0	100	0	0	0	135.9
0.25	0	99	0	0	1	**130.6**
0.25	0	0	100	0	0	**85.6**
0.25	0	0	99	0	1	90.6
0.75	100	0	0	0	0	**92.9**
0.75	99	0	0	0	1	101.8
0.75	0	100	0	0	0	182.6
0.75	0	99	0	0	1	**176.1**
0.75	0	0	100	0	0	102.8
0.75	0	0	99	0	1	**99.5**

starvation during the specific iteration, even if the PF points the cloud in the wrong direction. The drawback is that the performance of the DR will decrease as the drift increases. We conducted a total of 12 tests, where half of the tests had a drift of 0.25 knots and the other half a drift of 0.75 knots. We used various mixes according to Table II.3.

The results were somewhat ambiguous, as only 2 tests out of 6 indicated that the performance increased by using DR. Our main comparison, presented in Figure II.9, will, by this, compare the PF^{Fusion} to mixes with both 29% DR and 0% DR.

5.3 Fusion of Sensor Data to Increase the Robustness of the PF

We assume that the depth measurements are more valuable compared to magnetic intensity when it is possible to keep track of the position accurately. This is due to the magnetic intensity sensor being less accurate, and these maps being more diffuse and of lower resolution than the sea chart. As the position estimation worsens, e.g., due to higher drift or outliers, we predict the magnetic intensity to increase in value. When depth and magnetic intensity give similar position accuracy, the combination (intersection) probably gives higher accuracy than each of them individually.

Table II.3: Test using DR

Drift	Depth	Magn	Comb	DR	KF	Mean Pos Error (m)
0.25	99	0	0	0	1	**37.5**
0.25	70	0	0	29	1	42.6
0.25	0	99	0	0	1	130.6
0.25	0	70	0	29	1	**124.2**
0.25	0	0	99	0	1	90.9
0.25	0	0	70	29	1	**73.9**
0.75	99	0	0	0	1	**101.8**
0.75	70	0	0	29	1	197.0
0.75	0	99	0	0	1	**176.1**
0.75	0	70	0	29	1	194.8
0.75	0	0	99	0	1	**99.5**
0.75	0	0	70	29	1	100.5

The challenge when having low accuracy is that a PF corrected by one type of data easily suffers from sample impoverishment when some outliers impair the calculations. By letting some of the particles be dead reckoned, and some particles regenerated from the KF position estimation (in our case set to 1%), we suspect the robustness to increase.

After a structured series of tests that we based on these assumptions, where we, e.g., assumed $Depth$ to be more valuable than $Magnetic\ Intensity$, we have found that (II.6) expresses a well-balanced mix for PF^{Fusion}.

$$Depth\ 40\%, Magn\ 15\%, Comb\ 25\%, DR\ 19\%, KF\ 1\% \tag{II.6}$$

The tests were conducted using various amount of drift to find a mix that could perform well during various conditions. We will use this mix as a reference throughout the following evaluations of the PF performance.

For these tests, we used various mixes for the re-sampling step while having a various amount of drift. PF^{Depth}, PF^{Magn}, PF^{Comb}, and PF^{Fusion} were compared while having 0.0–1.5 knots of drift. The simulations were made using both 29% DR and 0% DR for PF^{Depth}, PF^{Magn}, and PF^{Comb}, giving a total of 49 tests.

Figure II.7 shows four of these 49 tests, where we have used 0.25 knots drift speed and 29% DR. For this modest drift, PF^{Depth} performs best, PF^{Fusion} next best, PF^{Comb} a little worse, and PF^{Magn} the worst, due to the lower accuracy of the magnetic map and sensor.

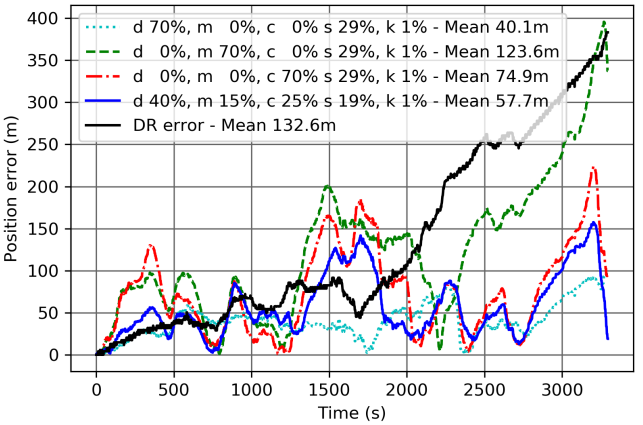

Figure II.7: PF^{Depth} gives the best performance when having 0.25 knots driftspeed. PF^{Fusion} gives the next best performance. (See videos on https://youtu.be/5wXou74isso.)

When having a higher drift speed, see Figure II.8, both PF^{Depth} and PF^{Comb} lose track of the position, which results in poor performance. In these prerequisites, PF^{Fusion} has the best performance.

We show all 7×7 test results in Figure II.9. The data shows that PF^{Depth} performs well when there is a slow drift, but as the drift increases and the position estimation diverges from the correct location, the performance of the PF^{Depth} quickly weakens. The PF^{Fusion}, on the other hand, has quite good performance over all evaluated drift speeds.

5.4 Using Landmarks to Increase the Performance and Robustness

If the ship is equipped with a system that can detect bearings to known landmarks, these can be used to adjust the particles' positions. In the tests presented in Figure II.10, we evaluate how the performance improves by the usage of bearings. We have set the drift speed to 0.25 knots. In the first test, we use no bearings to land-

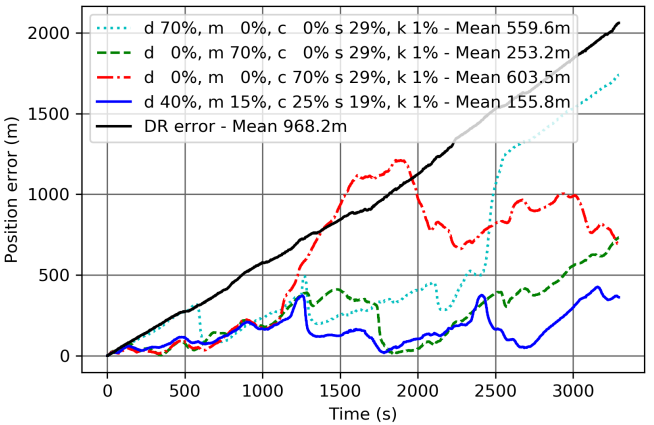

Figure II.8: When having 1.25 knots driftspeed, PF^{Fusion} gave the best performance. (See videos on https://youtu.be/ELi7ALXImm4.)

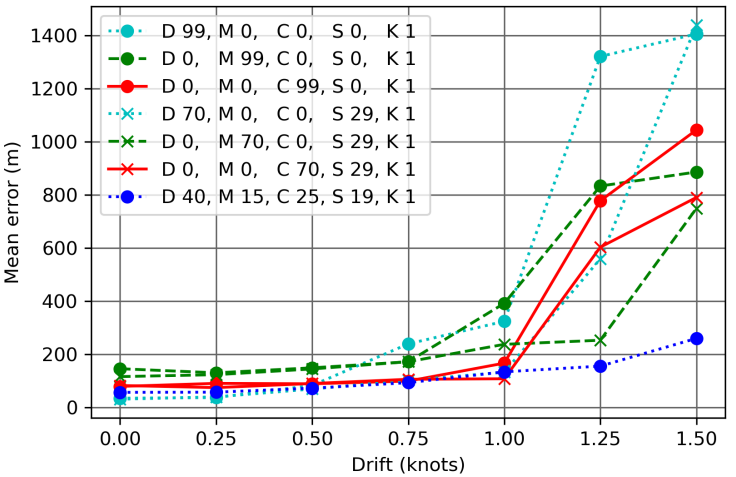

Figure II.9: The diagram shows the results from 49 simulations when using various mixes during various drift speeds. The PF which re-samples from multiple subsets (PF^{Fusion}) has the best robustness, and performs well during all drift speeds. It has a good accuracy for all drift speeds.

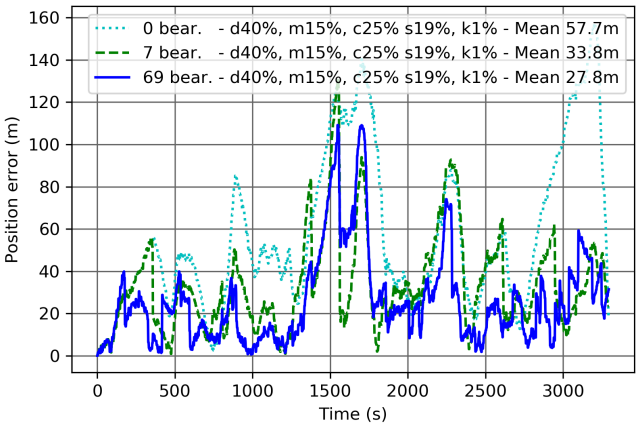

Figure II.10: Tests that show how bearings to landmarks can reduce the position error when having a low drift and using the PF^{Fusion}. (See videos on https://youtu.be/8nHf7cuIyGA.)

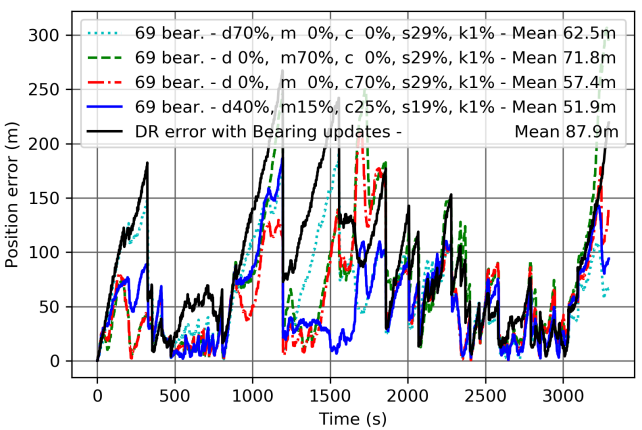

Figure II.11: Tests that show that the fusion mix outperform the other mixes while having the high drift speed 1.5 knots, and using all 69 bearings. (See videos on https://youtu.be/ZJG-CyMcWpI.)

marks. In the second test, we use seven, which results in a substantial performance gain. In the last test, 69 bearings are used, which increases the performance slightly more. As can be seen in the linked video, the particles are continually adjusting to the bearings, thereby maintaining the position accuracy. By at least occasionally updating the particle position from bearings, the risk of particle starvation at the correct position is lowered.

In Figure II.11, we present tests with a higher drift, where we compare different mixes where the particles are updated from all the 69 bearing updates. As can be seen, the PF^{Fusion} performs best also in these tests.

6 Conclusion

Other research has already shown that PFs can be used for position estimations when a high-resolution 3D terrain map is available. In our study, we have a broader use-case where we instead use publicly available maps, such as sea charts. We have shown that low-accuracy maps can be used, and more importantly, we have shown that by fusing measurement evaluations based on several such low-accuracy maps, the robustness of the system can be increased. In our study, we have used an increased position drift as a stress-test for our algorithm. Nevertheless, it should be noted that the algorithm will also be more resilient to outliers in sensor measurements or map accuracy, to flat terrains, and symmetric terrains, as long as these difficulties do not arise in all domains at the same time.

Humans mostly use GNSS systems as the primary way of determining the position but are also monitoring terrestrial navigation as a redundancy. We propose that autonomous ships could use GNSS systems, but for safety reasons also should cross-reference with a system such as a TAN with multiple data sources. All this can be achieved with affordable sensors, which we have used in this work. Our future efforts are targeting the integration of our positioning approach into an earlier presented VR based visualization and control tool for remote supervision of (semi-)autonomous vessels [130]. We also plan to develop an ML-based tool for evaluation of the current seabed and magnetic field anomaly map. This evaluation data will then be used by the algorithm to dynamically adjust the subset sizes of PF^{Fusion} to optimize the performance even further.

Paper III

Paper III

Remote Operation of Unmanned Surface Vessel through Virtual Reality - a low cognitive load approach

Mårten Lager
Department of Computer Science
Lund University
Saab Kockums AB
marten.lager@cs.lth.se

Elin A. Topp
Department of Computer Science
Lund University
elin_anna.topp@cs.lth.se

Jacek Malec
Department of Computer Science
Lund University
jacek.malec@cs.lth.se

Abstract

An unmanned ship can be designed without considering human comfort, and can thus be constructed lighter, smaller and less expensive. It can carry out missions in rough terrain or be in areas where it would be dangerous for a human to operate. By not having to support a crew, lengthy missions can be accepted, enabling, e.g., reconnaissance missions, or reducing emissions by lowering the speed.

Breakthroughs with autonomous systems enable more advanced unmanned surface vessels (USVs), but to be able to handle complex missions in a dynamic environment, a human operator is still assumed an effective decision maker. Thus, we propose a method for remote operation of a USV, where the operator uses (VR) to comprehend the surrounding environment. Great importance has been given

In "The Inaugural International Workshop on Virtual, Augmented and Mixed Reality for Human-Robot Interaction", (VAM-HRI 2018).

to the ability to perform safe navigation, by designing a Graphical User Interface (GUI) that guides the operator through the navigation process, by presenting the important information at the right place in the right orientation.

1 Introduction

Autonomous Surface Vessels (ASV) have evolved during the last decades [133], and have now reached a maturity level where they are starting to be used commercially. We believe there are many potential benefits, including:

- Cost-effectiveness, where the expensive human operator can be removed. By removing the operator, the ship will no longer be constructed for human comfort, and the cost can thereby be reduced even further.
- Human work environment. By reducing the crew size, the risk of a shortage of seafarers is reduced.
- Safety. By developing algorithms for safe navigation, the ship can operate continuously without making human errors.
- Persistence. An unmanned vehicle can be used during long periods of time when there is no humans on-board who have a limited amount of working hours.
- Ability to operate in hazardous conditions, e.g., rough weather or during anti-piracy operations.

Even bigger oceangoing commercial container and bulk ships are being developed for unmanned usage [48], and are anticipated to be in commercial service in 10-15 years [2]. The foreseen benefits are increased safety, but also reduced workload for humans. As a consequence of a significantly reduced crew-size, it will also be possible to reduce the speed of the ships, lowering the fuel consumption, and thereby the environmental impact [2, 18].

Compared to car traffic situations, traffic at sea is often characterized with more available time for decision making. Many ships also travel most of their route at open sea, where there is hardly any traffic at all. On the other hand, when entering a highly trafficked harbor during bad weather, many complex situations arise, which gives a need for either human decision making or intelligent autonomous algorithms.

Also in other situations, it might still be beneficial or even crucial to allow for human decision making. Hence, we assume that allowing a human operator to have both an insight into the situation an unmanned, maybe to a certain degree autonomously navigating vessel is, and the opportunity to take at will control over

the vessel, can be very beneficial to overcome the gap between manned and fully autonomous vessels.

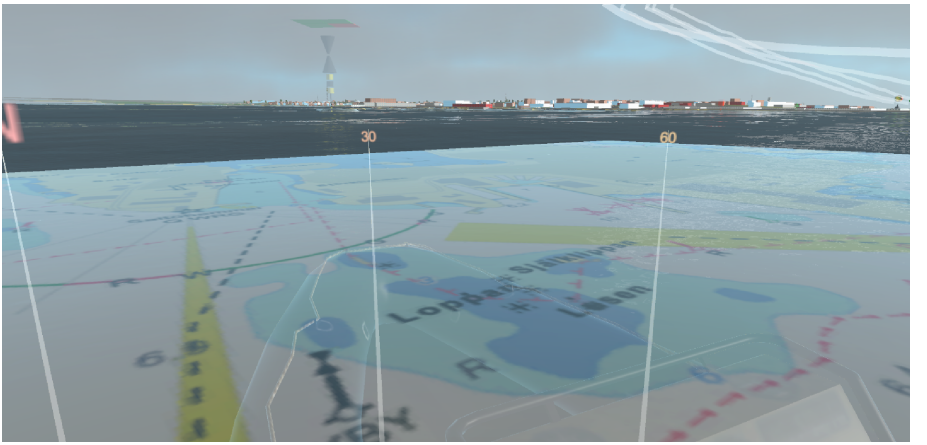

Figure III.1: The GUI from the project, presented in the Virtual Environment. The sea chart is rotated to fit the surrounding world, and the sea marks are increased in size to be simpler to detect.

However, during complex situations at sea, it can be hard for even a human to interpret and match the surrounding environment with the information from the navigation equipment. There are several situations where the navigation operators, due to the high cognitive load, have mixed up sea marks, directions or landmarks, which in many cases have led to fatal accidents [87].

We propose thus a Graphical User Interface (GUI) developed for remote operation of an Unmanned Surface Vessel (USV). The GUI is created for VR utilization so that the operator can experience being situated on board the ship. The real world environment is re-created from sea charts into the Virtual Environment (VE). The GUI is then placed in another layer in the VE, where, e.g., seamarks augment directly the operators' view of the environment, making it easy for the operators to interpret them, see Figure III.1.

To evaluate the GUI, sea trials have been conducted in an archipelago by a USV called *the Piraya*, developed by *Saab Kockums AB* [120].

Naval officers have been involved in the implementation and have given a brief initial evaluation of the GUI.

This paper is organized as follows: In Section 3, an overview is given of how other research has investigated how the cognitive load can be reduced during nav-

igation. These learnings have been used in our GUI created in our project, presented in Section 4. Section 4.6 presents a brief operator evaluation, concluded by a discussion in Section 5.

2 Scope

There are many scenarios where VR and (AR) can be used in order to enhance Situational Awareness (SA) at sea. On a bridge, AR can be used for augmenting the surrounding environment with information from the ship's sensors. In a control room on board a ship where there are no windows, VR can be used in the same way, but in this case, the surrounding environment also needs to be created virtually, or by streaming video from all available directions. In this scenario on board the ship, sensor information such as video can be added directly to the Virtual Environment (VE).

In order to bound the scope of our study, we have chosen to focus our work on a GUI with the task to control a USV, where the USV has a limited bandwidth connection to the GUI which inhibits video or high-resolution images to be sent. The implementation can easily be extended to also fit the other scenarios. For these, however, features in the GUI need to be added or changed, and an AR HMD (Head Mounted Display) needs to be used for the bridge scenario.

3 Related Work

Much research has investigated how the operators can interact with the navigation systems, in order to increase safety. There has also been done a lot of research regarding USVs, where remote control often is an essential part. However, we have not found any research done in the combination of these two areas.

3.1 Safe Navigation with Low Cognitive Load

The traditional way to navigate at sea is to use a paper sea chart, showing an abstracted map of, e.g., islands, groundings, depths measurements and sea marks. The paper sea chart is constructed with north facing up. During the last two decades, there has been a transition on bigger ships to use electronic chart systems, where the sea chart is instead visualized digitally on a computer screen. The main benefit is that the own ship's position, normally received from the GPS, is

visualized at the correct location on the sea chart. The sea chart can be presented with north-up or head-up reading rotation.

The human ability to mentally rotate a map or sea chart, so that the symbols in the map can be matched with surrounding real-world objects, is rather limited. Shepard et al. [86] showed that the time to recognize that two perspective drawings are showing the same three-dimensional shape is linearly increasing to the angular difference of the perspectives. This means that a human can match the ship's surrounding quite well when steering in north direction when reading a north-up oriented sea chart, but will need more time reading the same north-up oriented sea chart when steering in the opposite direction. Operators often choose to present the sea chart with north-up and radar with head-up [87] rotation, thus mental rotations are needed both between those two systems, and between the systems and the surrounding real world.

Another way of presenting a map is to view it from the driver's perspective. This is normally done in a GPS navigator for car drivers. The benefit is that the driver can quickly understand which roads and buildings on the map match the roads and buildings in the real world surrounding. By letting the machine do the mental rotations instead of the human operator, valuable time is saved, and many accidents are thereby likely to be avoided.

Porathe [88] compares these four map views in a simplified indoor environment where persons navigate on a floor trying to navigate fast but striving to avoid groundings. The compared views are the already mentioned:

1. Traditional paper sea chart (north-up)
2. Electronic chart system (north-up)
3. Electronic chart system (head-up)
4. 3D map with Ego-centric View

The results of this test show that (4) gives the fastest decision makings, least groundings, and is perceived as the most user-friendly. The results also clearly show that using an electronic chart system gives better results than using paper charts.

Some persons are more skilled than others when it comes to interpretation and mental rotations of maps. Porathe [89] has divided the persons into subgroups depending on previous map experience, gender, and age. Persons with map experience, males, and younger persons generally perform better, but disregarding which group that compares the four different map views, the results remain the

same; (4) gives the best results, followed by (3), (2) and (1). An interesting finding is that although persons have a great experience from using an electronic chart system, they still perform better when switching to 3D maps, despite that they are not used to it.

With the results in mind, Porathe [87] suggests using a 3D map with the ego-centric view as a navigation aid, viewed on a computer screen or tablet. Witt [90] has also proposed a similar solution with a tablet where the ego-centric view helps the operator reducing the cognitive load. Our GUI is influenced by these results, as we place the operator directly into the 3D world where the surrounding world easily can be matched with the sea chart.

Much research has also been done investigating how AR can reduce cognitive load when navigating. In these applications Head Mounted Displays (HMDs), normally with see-through technology, augment important information, such as sea lanes, conning information or AIS information. [109–113]. We use the same technique to augment important information in the VE instead of overlaying it on top of the real world.

3.2 Remote Control of USV

Since there is no fully autonomous USV developed yet, USVs in general still need some remote operation. Respective GUIs often contain a map where the USV is positioned, along with functions for describing the status of the USV [134, 135]. We have not been able to find any research describing remote operation in VR though.

4 Navigation and Control in Virtual Reality

4.1 Platform Description

The Piraya boats used in the project have a length of 4m and a maximum speed of approximately 20 knots [136]. They are equipped with GPS for position measurement and a PTZ-camera (Axis Q6155-E) for video streaming. During operation, the position and attitude data are sent to the GUI, so that the GUI is positioned in the correct location in the VE. Sea-trials have been carried out to log entire trips, which have been used during the development of the GUI, along with simulations of comparable scenarios.

4.2 Architectural Description

There are two main parts in the architecture; the *Shore System* and the *USV (Piraya)*, see Figure III.2. The main contribution of this paper is the *VR GUI* in the *Shore System*. It is integrated with the *Unity world* that provides the VE, including the simulated ships. The VE is updated according to the *Simulation kernel*.

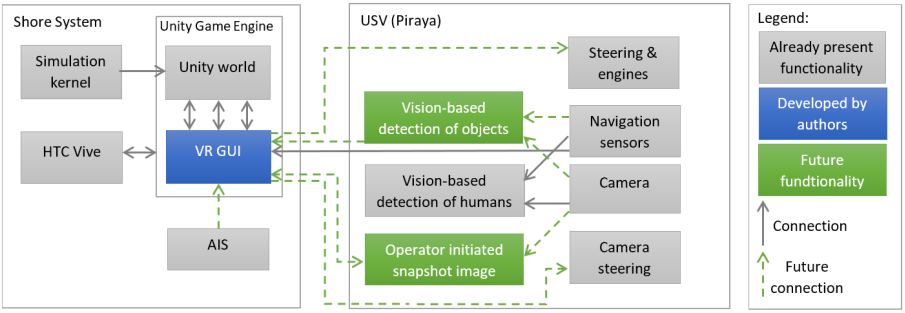

Figure III.2: Architecture Overview. The VE with the GUI is created ashore (left part of the image). The USV (right part of the image) has functionality for steering the ship and camera, and sends cropped camera images, USV position and USV orientation to the GUI.

In the *USV*, already present functionality was used for steering the USV as well as the camera. These functions are planned to be integrated with the *VR GUI* in the future. A function that has been developed for detecting persons in the water (simulated by orange buoys) was also used. When this function detects a buoy, it sends a small cropped image to the *VR GUI*, where the real world image can be visualized in the VE. In the future, functionality for controlling the camera directly from the GUI is foreseen to be added. Another valuable function is to be able to detect other objects than buoys. Cropped images from other detected objects, e.g., boats could then be sent to the *VR GUI*.

4.3 Goals with the GUI Implementation

The intention is to create an easy-to-use GUI for remote operation of a USV. It is important to uphold a safe navigation, and the goal is to create a system which is at least as safe as a comparable ship of its size. Thereby, the USV and the GUI must have functionality for creating a good understanding of the vessel's environment and the USV needs to have functionality for making some decisions

about what information that should be sent to the GUI. The GUI also needs to give the operator better navigation tools than normal ships, to compensate for the operator not being on-board.

In this paper, the first baseline of the GUI is presented, which will be evaluated so that it can be evolved to finally meet the goals.

4.4 Main Operational Views

Two different main views have been created; *Egocentric view* and *Tethered View*. These will in the future be complemented with the *Exocentric View*, which will show the USV in the middle of a north-up sea chart. Each of the views has their own benefits and shall be seen as a complement to each other.

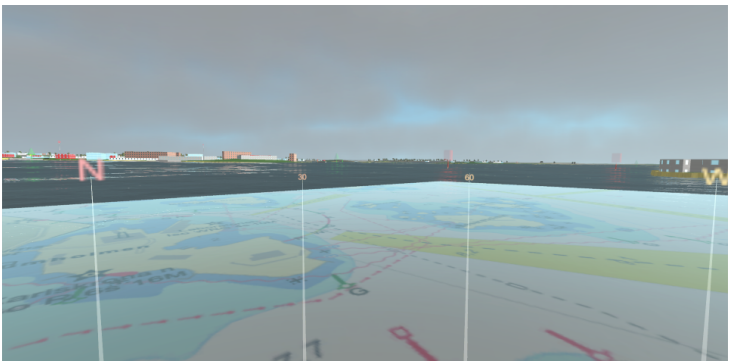

Figure III.3: In the ego-centric view the camera is placed on-board the USV so that the operator experience being on-board. The center of the sea chart is placed in the operator's location and rotated so that it is consistent with the orientation of the world.

Egocentric View

The *Egocentric View* in Figure III.3 visualizes the world from the USV's (ego) perspective, hence it simulates what the surrounding environment looks like. The camera has good bearing accuracy but poor range accuracy. From the egocentric view, the range is of lower importance, hence information from passive sensors such as cameras are well visualized in this view. By capturing real-world images of landmarks and comparing the bearings to the sea chart, it will be obvious if the

current GPS position diverges from the correct position, as the landmark bearings will not match the chart.

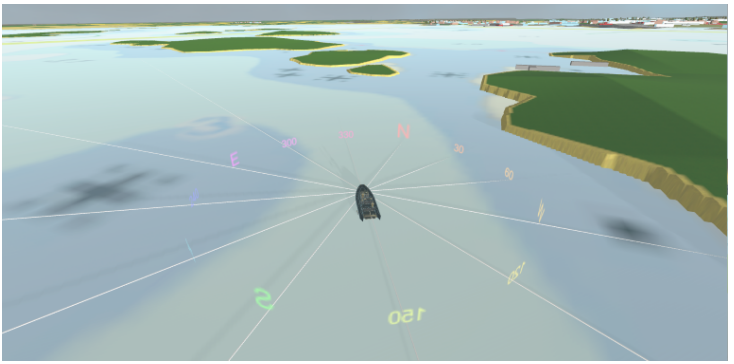

Figure III.4: The USV is visualized from above in the *Tethered View*.

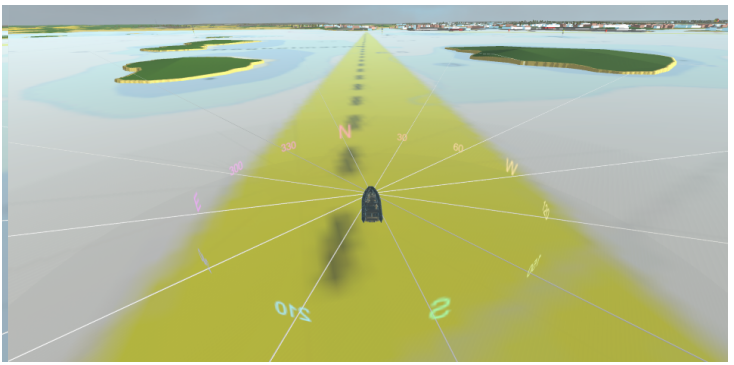

Figure III.5: *Tethered View.* The USV is going in the yellow light segment from a lighthouse.

Tethered View

The *Tethered View* is created by a camera hanging after the USV up in the air, viewing the USV from above, see Figure III.4. The operator has a good overview of the USV and what is around it, and can at the same time see where the USV is situated on the sea chart. In Figure III.5 the USV is going to the right in the sea lane in the direction towards a lighthouse where yellow light is emitted.

4.5 Features to Reduce the Cognitive Load

Several features have been implemented to support navigation and situational awareness, while still limiting the cognitive load.

Sea Chart

A sea chart is visualized both in *Egocentric View* (see Figure III.7 and III.1 and in *Tethered Veiw* (see Figure III.4 and III.5). In the *Tethered View*, the sea chart is shown instead of the water. The operator can see where groundings or sea marks are located and adjust the steering to adjust to the map.

In the *Egocentric View* the viewing camera is located at the center of the sea chart, showing the surrounding area of the USV. The sea chart is always arranged in the correct orientation so that the operator easily can match surrounding objects and islands to the symbols in the sea chart.

Orientation and Compass Rose

It is important to be able to uphold an orientation at all time. To help the operator, the following clues are given:

- The sea chart is quadratic and is always heading north, together with all text and numbers on the chart.
- The sun is visible at all time in a direction that matches the time and day of the year.
- The *Compass Rose* is visible at all time

The *Compass Rose* is visible both during *Egocentric View* (see Figure III.3) and *Tethered View* (see Figure III.4 and III.5). Other research has shown that the usage of different colors can increase the orientation capability, and by overlaying colors, the time to translate to a rotation can be shortened [137, 138]. Thus, the *Compass Rose* has been colored according to a circular rainbow pattern, with the potential benefit that the operators in time will learn to associate the different colors with the related orientations. The *Compass Rose* can be seen in Figure III.6.

NoGo-Areas

There are many parameters which influence under-keel clearance. First, the accuracy of the current position needs to be estimated, resulting in an area in where the

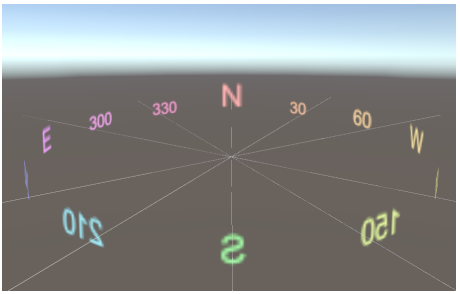

Figure III.6: The angle indicator on the compass rose shown above the sea chart, have been color coded according to a rainbow. By doing so, the intention is that a human operator will eventually learn which color corresponds to which orientation.

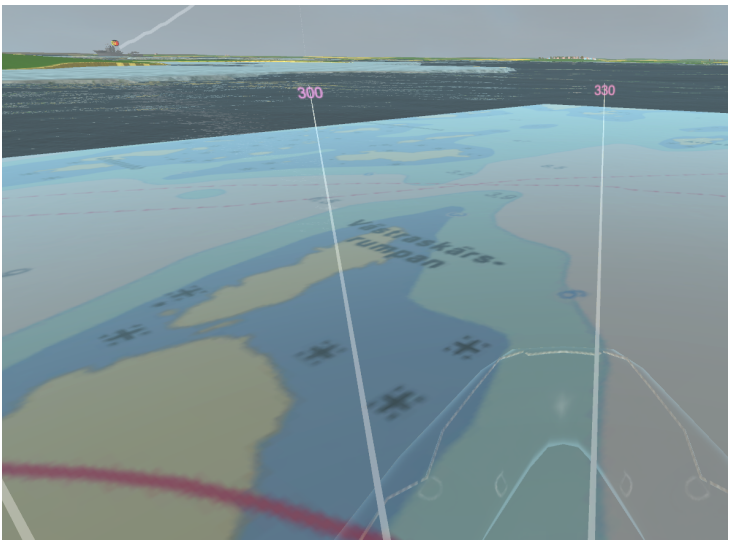

Figure III.7: The area in the sea chart with depth below 3m are lifted up above surface as icebergs, so that the operator easily understands that it is a dangerous area.

USV is located. Then this area is compared with the bottom topography of the same area. The last step is to compensate for current draught and for the current water level. All these steps are time-consuming and hard to do for a human. A computer can instead perform the calculations. Porathe [87] suggests coloring the water in his proposed 3D-images so that the operator knows where not to go. We have proposed a comparable way, by showing icebergs where it is too shallow. In the images, the operator is warned when shallower than 3m, see Figure III.7.

Sea Marks

Seamarks are in general hard to detect at sea. The problem is that they are small, and in rough weather, it is time-consuming to first find the seamark in the sea chart, then try to estimate in what direction they are located in, and then finally trying to detect it when still far away.

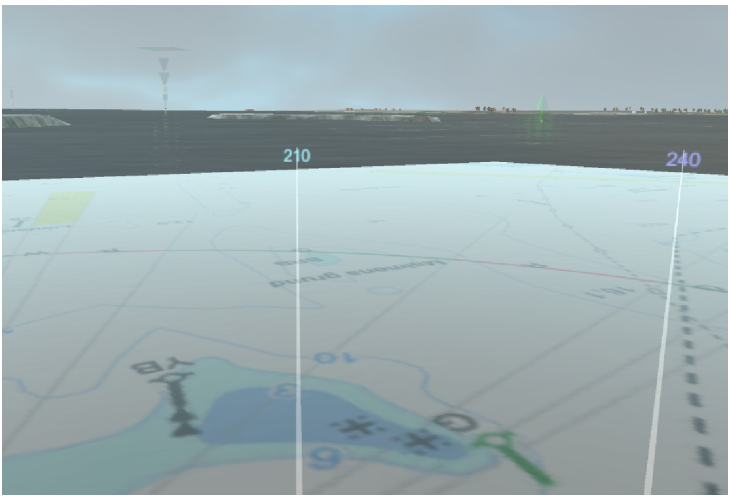

Figure III.8: The sea marks are increased in size to be more easily detected. By following the lines from the compass rose, it gets easier to find out which sea marks that match which symbols in the sea chart.

By having a sea chart that is always rotated in the correct way, it is easy to estimate which sea marks that belong to which in the sea chart, see Figure III.8. The sea marks are also ten times bigger than reality, which makes them easier to detect.

Cardinal marks are sea marks which mark out in what compass direction there is a grounding. In the VR GUI, they are complemented with a red-green area above them, indicating in which direction the grounding is located. This is shown in Figure III.9, as well as that the iceberg marks the same grounding.

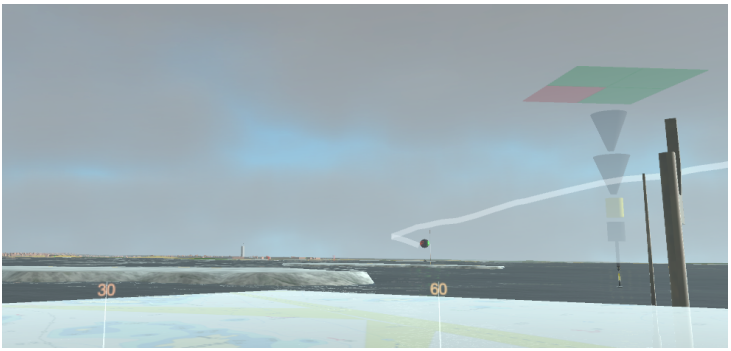

Figure III.9: The South Cardinal Mark marks the grounding north from the Cardinal Mark (to the left in the image). The grounding is also marked with an iceberg.

Tracking of Ships

The Automatic Identification System (AIS) is mandatory for bigger ships. The system provides information about, e.g., identification, position and heading, to nearby ships. By receiving this information directly to the GUI, it is possible to present real-time information about the bigger ships in the surrounding to the USV.

In the GUI, the information from the AIS is presented in three ways:

- The type of ship is translated into available 3D-models of various types of ships. The 3D-model is then presented in the VE, see Figure III.10.
- The heading from the AIS is used for coloring a sphere according to standard ship lantern configuration, see Figure III.10. If, e.g., most of the sphere is green, the operator can instantly conclude that the ship is moving to the right.
- A *Contact Evaluation Plot* (CEP) is normally used to present fused bearing tracks when at least one of the sensor data originates from passive sensors,

Figure III.10: From the AIS data, the ship type, position and heading is extracted. From the ship type, a suitable 3D-model is chosen. The sphere is positioned above the position, and is colored according to the heading.

Figure III.11: The bright bearing-lines in the sky indicates that both visual ships are steering to the right. The ship to the right is farther away, which is visualized with the thinner line. The ship to the left is going at a constant speed but has made a turn approximately 25 seconds ago. 30 seconds of history is presented in the CEP.

such as cameras or passive sonars [139]. The CEP presents the bearing tracks in a time-bearing format. In the VR GUI, the CEP lines at this time only originate from the AIS. The CEP provides the operator with an overview of all the surrounding ships, where the relative motion, as well as ship maneuvers, can be detected, see Figure III.11.

Presenting Real-World Images

An algorithm for detection of buoys has been developed for the USV, where the buoys simulate people in the water with life vests. The algorithm uses the camera images and can calculate the bearing and range to the detected buoys. By using this information, the images can be cropped to only contain the object of interest, and send this cropped image through the low bandwidth connection for presentation in the GUI, see Figure III.12. The operator can then study the image, and decide if the USV shall move closer to examine the object more carefully.

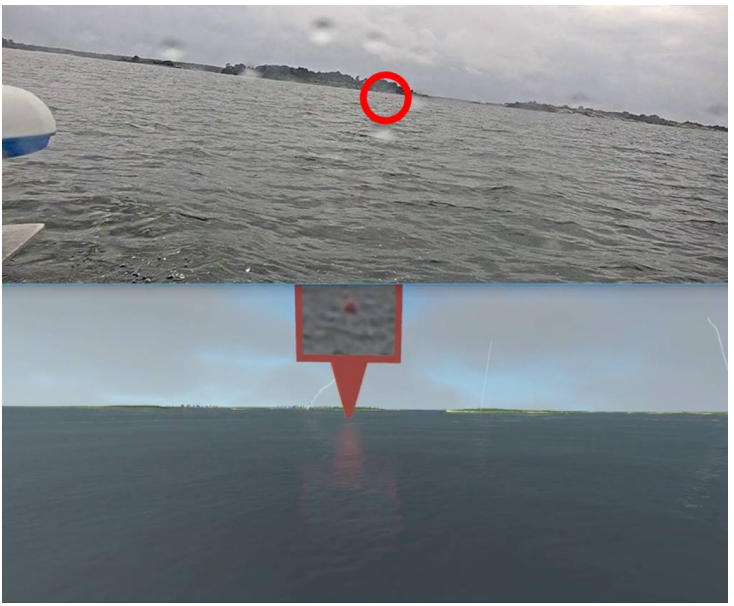

Figure III.12: Above, an image from the sea-trials is shown. From this image, the buoy was detected. Below, the cropped image is presented in the VR GUI.

4.6 Usability Evaluation

The GUI has been evaluated by two experienced naval operators. They both found the cognitive load to be reduced by serving the operator with all available information, as the operator, e.g., does not need to mentally translate an AIS target to the sea chart, and then to the real world. Other functions that were mentioned to reduce the load were the enlarged sea marks, the NoGo-areas, the spheres and the CEP-lines. The CEP-lines where pointed out to be able to serve the operator with valuable information, such as when passing the *Closest Point of Approach*. One of the operators was skeptical whether the colored compass rose would increase the orientation ability. More textual information from the AIS is also requested.

5 Discussion and Future Work

We have designed a GUI for remote control of a USV. Special attention has been given to reduce the cognitive load while maintaining safe navigation. It is important to have a good situational awareness, which is given by augmenting the surrounding ships and objects.

To be able to operate a USV remotely in a safe manner, it is important that the USV can detect all hazardous objects such as ships, and share this information with the GUI. By that, a function for automatic detection and classification of nearby objects would boost the functionality of the GUI.

In the near future, the GUI will be evaluated by experienced naval operators, in order to enhance the usability even further. New sea-trials will be conducted with new features to steer the USV directly from the GUI.

ACKNOWLEDGMENT

This work was partially supported by the Wallenberg AI, Autonomous Systems and Software Program (WASP) [1] funded by Knut and Alice Wallenberg Foundation. The simulation environment provided by Saab Kockums AB is gratefully acknowledged.

Paper IV

Paper IV

Remote Supervision of an Autonomous Surface Vehicle using Virtual Reality

Mårten Lager
Department of Computer Science
Lund University
Saab Kockums AB
marten.lager@cs.lth.se

Elin A. Topp
Department of Computer Science
Lund University
elin_anna.topp@cs.lth.se

Abstract

We compared three different Graphical User Interfaces (GUI) that we have designed and implemented to enable human supervision of an Autonomous Surface Vehicle (ASV). Special attention has been paid to provide tools for a safe navigation and giving the user a good overall understanding of the surrounding world while keeping the cognitive load at a low level. Our findings indicate that a GUI in 3D, presented either on a screen or in a Virtual Reality (VR) setting provides several benefits compared to a *Baseline GUI* representing traditional tools.

In "In 2019 10th International Conference of Autonomous Intelligent Vehicles (IAV 2019), DOI: 10.1016/j.ifacol.2019.08.104.

1 Introduction

As the autonomous vehicles are becoming more intelligent, the human's role of being in constant control can be relaxed. In many cases, the semi-autonomous vehicle can plan and execute missions that meet the human needs, while the human can still take control by teleoperating the vehicle, which is useful, e.g., when some situation occurs that the vehicle has not yet been trained for. Many car manufacturers will equip their cars with teleoperation capability, and Levander [2] sees teleoperation of ships as a key technology in the transferring process towards autonomous ships.

In this study, we are focusing on a small Autonomous Surface Vehicle (ASV) that is being remotely supervised by a human user via a low bandwidth connection. Murphy [140] believes small ASVs like this are likely to play an important role during future Search and Rescue (SAR) operations at sea. The reason for adding the low bandwidth constraint that prohibits video streams and high-resolution images to be sent, is that we want the Graphical User Interface (GUI) to work on open sea. In these areas, ASVs need to rely on radio communication normally used by ships, as mobile communication has to insufficient coverage, and satellite communication is too costly and has too bulky antennas.

There are many benefits of using an ASV instead of a normal ship. An ASV can be constructed lighter and cheaper. An ASV can also be used when it would be dangerous for a human to operate, e.g., during bad weather at sea. Multiple ASV fleets can be placed in various locations, and during accidents, the closest fleet can be dispatched from a centralized location with teleoperating experts. ASVs and drones can typically be dispatched far more quickly than manned vehicles, as there is no need for waiting on the human crew. Compared to flying drones, ASVs have good endurance and can be on a mission for many hours, while drones are typically faster and can get a good overview of an area from their high altitude.

Although cars and airplanes are hard to teleoperate due to the constraints that the dynamic traffic situations set on time delays and jitter (see d'Orey et al. [141] and Neumeier et al. [99]), traffic at sea is often characterized by more available time for decision making, making it ideal for teleoperation.

During complex situations at sea on manned ships, Porathe [87] shows that it can be hard even for humans to interpret and match the surrounding environment with the information from the navigation equipment onboard. There are several occasions where the navigators, due to the high cognitive load, have mixed up sea marks, directions or landmarks, which in many cases have led to fatal accidents.

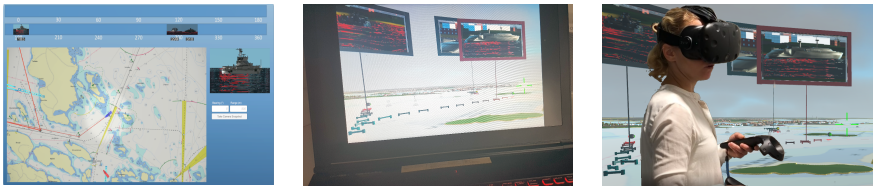

(a) Baseline 2D GUI (b) 3D GUI on a laptop (c) VR GUI

Figure IV.1: Three types of GUIs have been developed. (a) is a 2D GUI, that represents a traditional GUI. (b) and (c) are created in 3D, where (b) is presented on a laptop and (c) in VR.

This raises the question of how new types of GUIs can support remote supervision of an ASV with limited bandwidth. Of particular interest to us is to see how the user's *situational awareness* and *cognitive load* are affected when using such GUIs in comparison to using traditional ones. We use the term *situational awareness* to describe the ability of the user to assess the situation the vessel is in with respect to surrounding elements like other vessels, seamarks, or shallow areas.

To answer these questions, we propose a 3D-visualisation of the ship's surroundings either on a computer screen or in a Virtual Reality (VR) setup. We base this GUI on ideas from the available research regarding manned ships to increase the situational awareness while maintaining a low cognitive load.

We evaluated the two different versions of the GUI against a baseline GUI, see Figure IV.1, in a small study with 16 participants, showing that there are significant benefits regarding the mentioned factors.

This paper is organized as follows: In Section 2, an overview of related research is given followed by the GUI design in Section 3. Then the User Study is presented in Section 4, with related results and discussion in Section 5 and 6. Conclusion is given in Section 7.

2 Related Work

Teleoperation can be used for remote controlling vehicles and robots, e.g., cars (see Neumeier et al. [99]), drones (see Hedayati et al. [100]) or ships (see Nava-Balanzar et al. [102]). While teleoperating a vehicle, it is important to support the human's perception of what the vehicle's sensors detect of the surrounding world. Williams et al. [108] elaborate on how VR, Augmented Reality (AR) and Mixed Reality can strengthen visualization, and thereby the total communication

between the machine and the human, and how various viewpoints, e.g., the ego-centric view can be used. Hedayati et al. [100] explore how AR can be used for augmenting a drone's field of view for a user collocated with the drone. When not collocated, VR is often a better presentation technique compared to AR. Hosseini and Lienkamp [98] and Shen et al. [97] show how VR can enhance the situational awareness when driving a remote car.

When navigating onboard a ship, the traditional way is to use either a paper sea chart or an electronic chart system, showing an abstracted map of, e.g., islands, groundings, depth measurements, and sea marks. Research has shown that it is difficult for humans to match what they see on the chart or radar to what they see in the real world outside the bridge of the ship . Instead, it is a better approach to visualize a 3D map oriented in a way that matches the user's view of the surrounding world (see Porathe [88] and Witt [90]). Our GUI is influenced by these results, as we place the user directly into the 3D world where the surrounding world easily can be matched with the sea chart. We call this ego-centric view *First Person View* (*FPV*).

Some research has also investigated how AR can reduce cognitive load when navigating. In these applications, Head Mounted Displays (HMD), normally with see-through technology, augment important information, such as sea lanes and other nearby ships directly in the real-world environment (see Morgère et al. [110]; Mollandsøy and Pedersen [111]; Hugues et al. [112] and Jaeyong et al. [113]). In our application, we augment the important information directly in the virtual environment.

3 Design

In our study, we focus on a GUI for remote supervision of a small ASV via a limited bandwidth connection which inhibits video or high-resolution images to be transferred. The ASV is expected to be highly autonomous in order to handle a SAR mission, but still assumed to need some human supervision with the ability to take measure if something unexpected happens.

The GUI is developed for a small ASV with a computer capacity and sensor suite comparable to an autonomous car. The postulated sensors and capabilities are:

- Global Positioning System (GPS), or a satellite independent positioning system (see Lager et al. [115]);

- Application for autonomous route steering;
- Camera with 360-degree coverage and zoom capability;
- Radio communication with a small antenna with a bandwidth of around 10kbps;
- Application for image detection of ships; and
- Application for cropping and compressing images of ships, so that detected ship images can be transferred through the radio communication interface.

3.1 Architectural Overview

Figure IV.2 shows a summary of the communication interfaces to the GUI. To create the virtual surroundings and corresponding sea chart, the ASV transmits its position.

When the camera onboard the ASV detects ships, it transmits all tracks of them every second, as well as a small cropped image every 10 seconds. Some, mainly larger, ships have an Automatic Identification System (AIS) transponder, that transmits, e.g., their identity, position and steering direction. This is also received by the GUI and presented for the user along with the tracks from the camera.

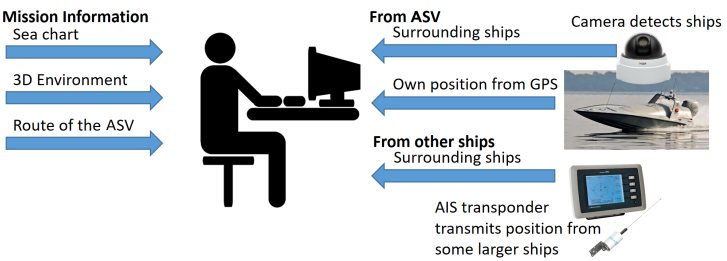

Figure IV.2: The GUI uses the position from the ASV's GPS to position the surrounding 3D world and the sea charts. The camera and AIS provide tracks to the GUI.

3.2 GUI Design

We have created two GUI versions in 3D to enhance situational awareness while maintaining a low cognitive load. In 3D, a virtual world is perceived in the same

way as humans normally perceive the real world. By combining a virtual world with the navigation GUI, our intention has been to give the user a better understanding of the environment, instead of just letting the user look at an electronic chart system. In the virtual environment, objects such as sea marks, surrounding ships, sea lanes, and routes are augmented for the user. To enhance the immersive experience even further, one of those GUIs are using VR. VR is a technique that presents a fully computer-generated simulated environment for the user, and the user is thereby fully left out from the visual physical world. In Figure IV.1c, a user supervises the ASV during the user study by using a VR HMD called *HTC Vive*.

The design of the different parts of the GUI has been developed in an iterative approach. First, a prototype was created based on research by, e.g., Porathe [88] about how the cognitive load of the user can be reduced for navigators. After a brief evaluation by navigation experts, an improved version of the application was developed, which has now been tested by a larger user group.

The GUI is implemented in Unity 3D (see [119]), which is normally used for creating 2D and 3D games. We have used a simulation kernel, received from the shipyard Saab Kockums AB, that simulates own and other ships in a predefined mission. It also creates a 3D replica of the real world, which has been used as a foundation for the implementation of the GUI.

Three different GUIs have been developed; one *Baseline GUI*, representing traditional navigation tools, one 3D tool presented on a laptop, called *3D GUI*, and one 3D tool presented in VR, called *VR GUI*. All these GUI types are presented in Figure IV.1.

3.3 Baseline - Traditional GUI

Navigators onboard manned ships use an electronic sea chart with north facing upwards. The own ship, positioned by the GPS, as well as other tracks of ships received by the AIS, are visualized directly on the chart. The *Baseline GUI*, see Figure IV.3 is created to mimic this design. A navigator normally needs to keep track of how the surrounding real world matches the sea chart, causing a large cognitive load. Because the ship in our application is controlled remotely, this matching is not needed, making it easier for the *Baseline GUI* users.

Optronic systems at sea often present a 360 view, split along two or four stripes with 180 degrees or 90 degrees each (see Maltese et al. [142]). As a compliment, normally an enlargement of one camera view can be seen. These features are also available in *Baseline GUI*. Because the received images have low resolution, we have been able to fit everything including the sea chart on one screen without

Figure IV.3: The *Baseline GUI* presents a 2D sea chart, as well as which images that the camera has photographed of the surroundings.

compromising too much with the size of the small images. When the camera on the ASV detects a ship, the large image in Figure IV.3 is shown at the same time as the image is placed in the correct location on the lower 180-degree stripe in the top of the GUI. At the same time, it indicates directly with a marker in the chart which area that has been photographed.

The users can manually take photos as well, by entering a bearing and a range. The camera onboard the ASV then takes a photo and transmits the compressed image when there is available bandwidth.

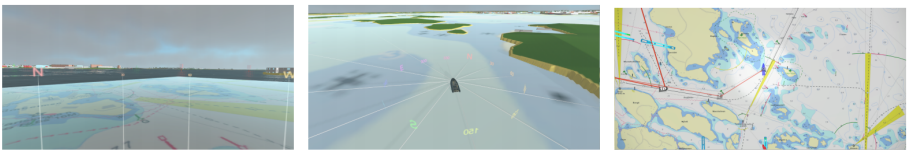

(a) First Person View (FPV) (b) Tethered View (TeV) (c) Exo-Centric View (ECV)

Figure IV.4: a) *FPV*: In the FPV the virtual user is placed onboard the ASV. b) *TeV*: The own ASV is situated in front of the virtual user, as the user was paragliding after the boat. c) *ECV:* This view provides a large sea chart for the user.

3.4 3D GUI and VR GUI

Our assumption is that we can create an easy-to-use GUI which provides a good situational awareness by:

- Creating the GUI in 3D, and present it in VR.
- Providing different views of the surrounding environment, optimized for various situations.
- Augment objects and information directly in the 3D world.

Our hypotheses are that a user operating a GUI built by these foundations will have a better overall understanding of the situation, and will observe potential dangerous situations earlier.

The GUIs seen in Figure IV.1b and IV.1c, named *3D GUI* and *VR GUI*, share most of the design and have three different views; *FPV*, *Tethered View* (TeV) and *Exo-Centric View* (ECV), see Figure IV.4. Each view has its own benefits so that the views complement each other.

First-Person View

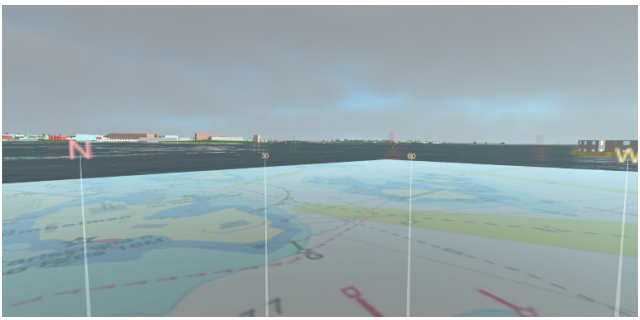

Figure IV.5: *FPV*: In the FPV the virtual user is placed onboard the ASV. The center of the sea chart is positioned in the user's location and is oriented to be consistent with the surrounding world.

The *FPV*, see Figure IV.5, visualizes the world from the ASV's (ego) perspective, hence it simulates what the surrounding environment looks like. A camera has good bearing accuracy but poor range accuracy. From the *FPV*, the range is of lower importance, hence information from passive sensors such as cameras is well

visualized in this view. By capturing real-world images of landmarks and comparing the bearings to the sea chart, it will be obvious if the current GPS position diverges from the correct position, as the landmark bearings will not match the chart.

Tethered View

The TeV is created by a virtual camera hanging above the ASV, viewing the ASV from above, providing a bird's eye view of the ASV in its environment, see Figure IV.6.

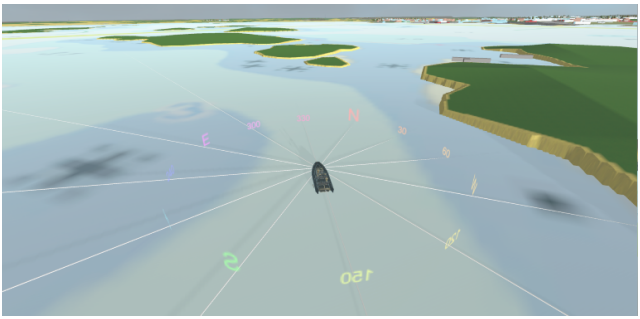

Figure IV.6: *TeV*: The own ASV is situated in front of the virtual user, as the user was paragliding after the boat. The dark blue in the sea chart indicates a dangerous area with a bottom depth less than 3m. In TeV, the user can easily get a feel for the own ASV's size compared to the passage between the shallow areas.

Exo-Centric View

The ECV, see Figure IV.7, is used for presenting a north-up facing sea chart for the user where the own ship is located in the middle, much resembling the *Baseline GUI*. The ECV has been implemented as a room with a large sea chart in front of the user. In the *3D GUI*, the user can zoom in and out, and in the *VR GUI*, the user can walk around freely in the room and look at other parts of the sea chart. The strength of this view is that the user can get an overview of the situation and plan a long way ahead. It is also easy to get an understanding of if the own route is well positioned according to the sea chart so that it does not pass any groundings.

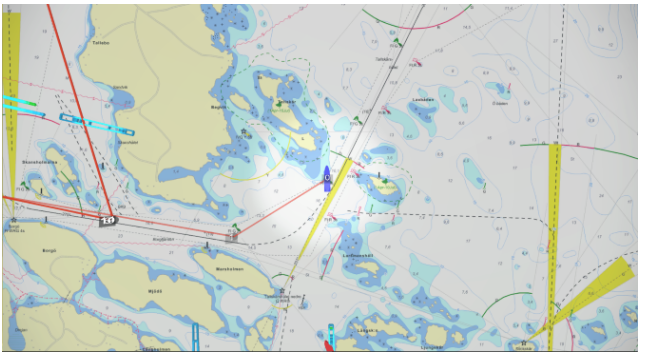

Figure IV.7: *ECV:* This view provides a large sea chart for the user, centered in the ASV's position.

3.5 The Differences Between the 3D GUI and the VR GUI

The main difference between the *3D GUI* and the *VR GUI* is how to interact with the GUI, see Figure IV.8. In the *3D GUI*, the switching between the various views and the zooming is done with keyboard buttons, and photos are taken by pointing and clicking with the mouse. In the *VR GUI* on the other hand, the associated HTC Vive hand controllers are used for the same interaction.

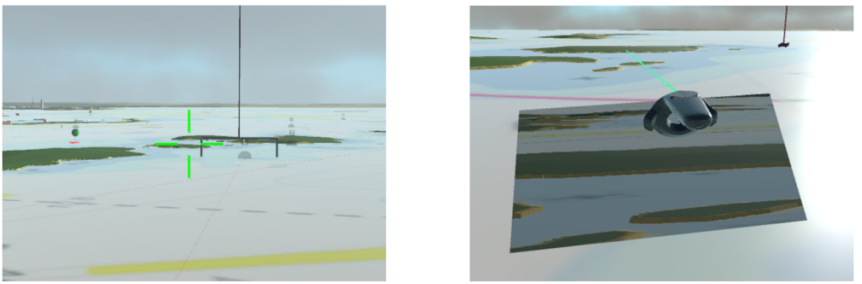

(a) (b)

Figure IV.8: a) In the *3D GUI*, photos are taken with a mouse click while pointing the green hair cross. b) In the *VR GUI*, photos are taken by pointing the green ray from the hand controller and then pressing a button. The image also shows a zoom-window below the hand controller, which enlarges what the hand controller is pointing towards.

3.6 Features to Reduce the Cognitive Load

Several features have been implemented to support navigation and situational awareness, while still limiting the cognitive load:

- A correctly oriented sea chart surrounds the user in FPV, see Figure IV.5.
- A sea chart is presented instead of the water in TeV.
- A rainbow-colored compass is shown in FPV and TeV, to guide the user with directions.
- Sea marks are augmented in FPV and TeV.
- Indications of surrounding ships are visualized in all views.
- Routes and waypoints are visualized in all views.

4 User Study

We evaluated our implementations with 16 participants, recruited mainly from Lund University and the shipyard Saab Kockums AB, in 50-minute long trial sessions (recorded on video) with the task and scenarios described below. We had the ethics board of our university check the study setup and were informed, that no supervision by the board or formal approval was needed to conduct the study. The participants were informed of the possibility to withdraw at any time and agreed upon the use of the recordings and other data for research purposes.

The user should, after an introduction phase based on written instructions and a slide show, use two different GUIs, either the *Baseline GUI* and the *3D GUI* (on screen), or the *Baseline GUI* and the *VR GUI* to supervise a ship that was passing through an archipelago on a predefined route in two different scenarios. The task was to observe potential dangerous situations and report them as soon as they were detected, and to keep track of the closest nearby ships. Also, they were asked to take pictures of surrounding islands when possible, assuming that we could measure their cognitive load by getting an idea of how much spare time (and mental capacity) they had to handle this secondary task. The participants were told that the safety tasks were most important, and the photo task was least important. A two minutes introduction to each GUI was given before each test.

From analyzing the video recordings of the user study, four final score values were given for each run (objective results) for *Collision Observations*, *Grounding*

Observations, *Situational Awareness* (closest ships correctly identified), and *Photos Taken* (Cognitive Load). The scores were computed as percentages of the respective possible values. After the experiments, the GUIs were evaluated subjectively by the participants by answering the following three questions for each GUI on a scale of 1–10 (10 was best):

1. Do you feel that you had a good overall picture of the situation? (Situational awareness rating)

2. Do you think that the GUI tool was easy to use?

3. If you had practiced 100 hours on this GUI, do you think it would be best for the task?

4.1 Objective Results

5 Results

The collected data from the user experiments have been summarized in the objective and subjective results below. The interpretation of the results is done in Section 6.

For the objective results from the user experiments, we found that both the *3D GUI* and the *VR GUI* gave significantly better results regarding the collision detection and situational awareness than the *Baseline GUI*, while there was no major difference regarding the detection of groundings. The *3D GUI* was significantly better than both the *Baseline GUI* and the *VR GUI* regarding the possibility to take photos, where the results for the *VR GUI* are somewhat inconclusive. Figure IV.9 summarizes the objective results, along with the p-values showing if there was a significant difference, computed in a series of one-tailed t-tests. The mean values are presented in Table IV.1. Even though it was a quite small user study, power tests (alfa=0.05, power>0.80) have shown that there were enough participants to support the significant results.

5.1 Subjective Results

For the subjective results from the user evaluation, we found that the users experienced a significant benefit of the *VR GUI* compared to the *Baseline GUI*, regarding having a good *Situational Awareness*. The users also experienced that both the *VR GUI* and the *3D GUI* were more *Easy to Use*. The users expected the *VR GUI* to

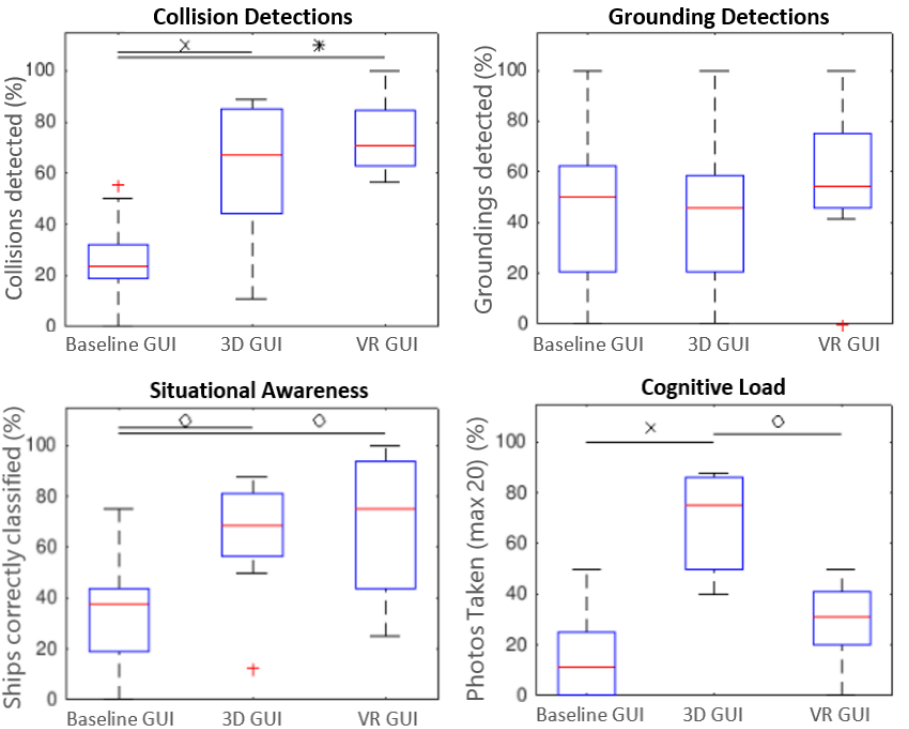

Figure IV.9: Objective results show that the situational awareness as well as the ability to detect collisions have been improved in both the *3D GUI* and the *VR GUI*. The users of the *3D GUI* have also managed to take more photos, which could indicate a lower cognitive load compared to the *Baseline GUI* and the *VR GUI*. (o), (x) and (*) denote comparisons with $p < 0.05$, $p < 0.01$ and $p < 0.001$ respectively.

Table IV.1: Objective Results Summary

	Baseline	**3D GUI**	**VR GUI**
Collision Detections	26.8%	61.5%	74.0%
Grounding Detections	42.2%	43.8%	56.3%
Situational Awareness	33.6%	64.1%	68.8%
Photos Taken	15.9%	82.8%	29.4%

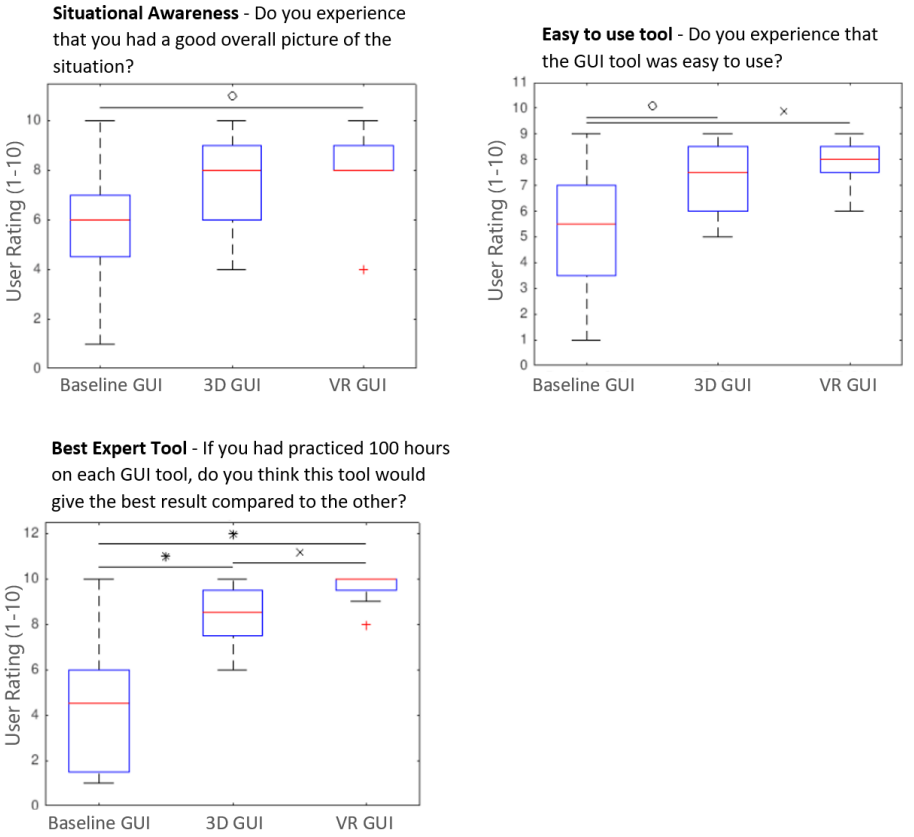

Figure IV.10: The evaluation score for *Situational Awareness*, *Easy to Use* and *Expert Tool* have been improved for the users of the *3D GUI*, and improved even more for the users of the *VR GUI*. (o), (x) and (*) denote comparisons with $p < 0.05$, $p < 0.01$ and $p < 0.001$ respectively.

be the best and the *3D GUI* to be the next best tool, for an expert user with many hours of training.

Figure IV.10 summarizes the subjective results, along with the p-values, computed in a series of one-tailed t-tests. The mean values are presented in Table IV.2. The power tests have shown that there were enough users to support the significant results with a p-value less than 0.01, but not the two results with a p-value between 0.01 and 0.05.

Table IV.2: Subjective Results Summary

	Baseline	**3D GUI**	**VR GUI**
(1) Situational Awareness	5.8	7.5	8.0
(2) Ease of use	5.3	7.3	7.9
(3) Best tool	4.3	8.4	9.6

6 Discussion

Our results show, that the users had better situational awareness when using 3D or VR, which can be seen in *Collision Detection* and (objective) *Situational Awareness*. They also said they experienced this in the question regarding the *Situational Awareness* and *Ease of Use* in the user evaluation. The *VR GUI* got a higher score than the *3D GUI* on all these four metrics, and the *3D GUI*, in turn, got a higher score on all these than the *Baseline GUI*, which is also reflected in the user ratings of the best tool for the task (given more training hours than they had experienced themselves). We think the good score for the *VR GUI* (and *3D GUI*) has to do with the fact that the perception in the GUI much resembles how a human normally perceives the world.

Regarding *Grounding Detections* and *Photos taken* (our assumed indicator for the cognitive load), our results are somewhat inconclusive, which we attribute to the relative unfamiliarity with the GUI as the users simply did not manage to switch into the optimal view (ECV) for this task reliably enough. We also observed a "fun factor" of taking photos of ships instead of islands in the VR setting, significantly reducing the scores for the *VR GUI* users.

Of the sixteen users in the user study, six persons considered themselves to be computer gamers (three used *3D GUI*, and three used *VR GUI*). These persons scored better in the experiments in general, indicating that the performance of the GUIs is increased with training. Table IV.3 shows a summary for each of the GUI

of how much better scores the gamers had compared to the persons that were not gamers. As can be seen, the gamers performed particularly well in the VR GUI. This finding goes in line with the user evaluation where the users suggested that the *VR GUI* and *3D GUI* would be a better expert tool after a long training.

Table IV.3: How much better gamers scored compared to non-gaming users.

	Baseline	**3D GUI**	**VR GUI**
Collision Detection	14.8%	6.9%	38.4%
Grounding Detection	88.6%	20.0%	93.9%
Situational Awareness	-19.5%	40.7%	52.2%

7 Conclusion

We investigated, how 3D and VR approaches could support the remote operation of an ASV with a low bandwidth connection, by comparing respective GUIs with a *Baseline GUI* following the currently applied interfaces in such contexts. Our findings show, that both the 3D and VR approaches outperform the traditional approach significantly. We found the *3D GUI* and *VR GUI* users to be better at reacting to potentially dangerous situations compared to the *Baseline GUI* users, and they could keep track of the surroundings more accurately. They also reported that they expected the *3D GUI*, and especially the *VR GUI*, to be the best tool of the three choices for an expert user with many hours of training.

As our investigations so far only have covered the supervision of a simulated ASV, we see the next step to be the integration of functionalities to control an actual ASV. This might potentially also mean looking at the integration of further information sources into the interfaces, which might entail new aspects for the user(s) to handle when interacting with the ASV.

ACKNOWLEDGMENT

This work was partially supported by the Wallenberg AI, Autonomous Systems and Software Program (WASP) funded by Knut and Alice Wallenberg Foundation. The simulation environment was provided by Saab Kockums AB.

Paper V

Paper V

VR Teleoperation to support a GPS-free Positioning System in a Marine Environment

Mårten Lager
Department of Computer Science
Lund University
Saab Kockums AB
marten.lager@cs.lth.se

Jacek Malec
Department of Computer Science
Lund University
jacek.malec@cs.lth.se

Elin A. Topp
Department of Computer Science
Lund University
elin_anna.topp@cs.lth.se

Abstract

Small autonomous surface vehicles (ASV) will need both teleoperation support and redundant positioning technology to comply with expected future regulations. When at sea, they are limited by a satellite communication link with low throughput. We have designed and implemented a graphical user interface (GUI) for teleoperation using a communication link with low throughput, and one positioning system, independent of the Global Positioning System (GPS), supported by the teleoperation tool. We conducted a user study (N=16), using real-world data from a field trial, to validate our approach, and to compare two variants of the graphical user interface (GUI). The users experienced that the tool gives a good overview, and despite the connection with the low throughput, they managed through the GUI to significantly improve the positioning accuracy.

Submitted.

1 Introduction

Autonomy and artificial intelligence are disrupting many sectors, including the marine industry. Many companies and academia are researching to evolve the field. Some companies have even started testing autonomy in real commercial routes (with safety drivers on board to meet current regulations). In late 2018 a ferry, developed by Finferries and Rolls Royce, went between two cities in Finland, first navigating autonomously and then remotely operated when returning [59]. In Norway, also in 2018, Kongsberg started testing autonomy on an autonomous ferry with passengers and cars on board, mainly to reduce the workload and to increase the safety [143]. To convince authorities to change regulations to permit using ships without a crew on board, it is of utmost importance to guarantee safety. A human onboard a ship is very flexible, and will in many situations discover if the ship is behaving strangely or if an unexpected event arises. When removing the crew, the vessel will need to incorporate this extra safety feature into the system instead.

When it comes to safe navigation, to have a correct position is vital. Nowadays, crew members rely heavily on the Global Positioning System (GPS) for this. A loss of the GPS signal, or a jammed or spoofed GPS, can for a crew-less ship result in hazardous situations. The global quality assurance and risk management company *DNV GL* believes unmanned ships may need alternative positioning methods to convince authorities that their safety is satisfactory [144]. Furthermore, they believe autonomous ships will not be fully autonomous for many years, but instead rely on autonomy and remote control in combination. Rolls Royce also believes this, as they see the teleoperation of ships as a key technology in the transferring process towards autonomous ships [2]. Moreover, they claim that the teleoperation of an autonomous vessel will increase reliability and performance. The communication link for the teleoperation system is vulnerable to downtime, though, and during this time, the system must solve the actions autonomously.

The work described by this paper has focused on how to use remote operation to improve positioning accuracy for small affordable vessels. Unmanned ground vehicles (UGV) have, for many years, been teleoperated to master harsh environments during, e.g., military or search and rescue (SAR) missions [94–96]. Small autonomous vessels at sea are also essential, and Murphy believes they will play an important role during future SAR operations [140]. The challenges with remote control and positioning are similar for small and large ships. However, the communication link's throughput sets a limitation on smaller, more affordable

vessels, as they can not have a large satellite antenna due to the size, weight, and cost constraints. This limitation makes the streaming of video and transmission of high-resolution images infeasible. For the positioning problem, we have, for the same reason, confined ourselves only to use affordable navigation sensors.

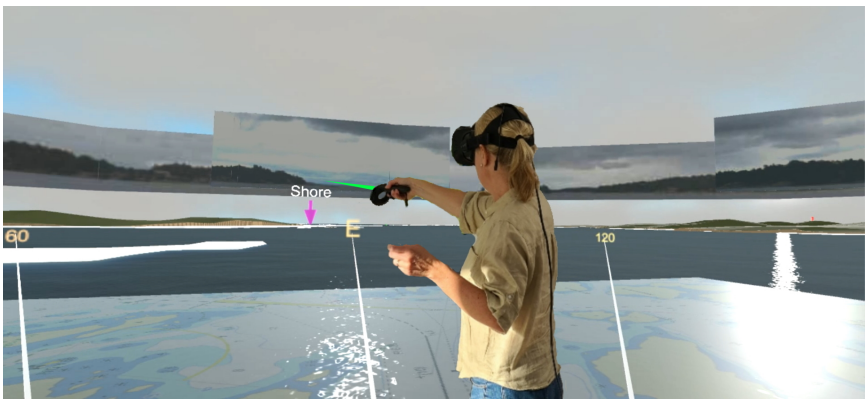

Figure V.1: A participant of the user study taking a bearing by pointing towards an augmented landmark.

The positioning system is built upon our previous implementation with terrain-aided navigation (TAN), presented in [145]. This paper estimated the position from a real-world field trial by comparing the bottom depth and magnetic intensity with available maps. To enhance the position accuracy even further, we manually measured bearings to landmarks from the recorded 360° image, making it possible for the positioning tool to adjust the position estimation accordingly. This is not possible to do manually on an unmanned ship. In this new work, a user instead measures these bearings from a teleoperation system in virtual reality (VR), see Figure V.1.

The teleoperation system also builds on our previous work, presented in [146, 147]. This work focused on developing a teleoperation tool with a low-cognitive load that could provide a good situational awareness (SA), leading to better safety for the vessel. In the work described in the latter paper, we developed a specific GUI to compare the performance when using VR, 3D visualization on a laptop, and 2D visualization on a laptop. In this earlier study, we observed that the longer available time for decisions at sea, measured in seconds or minutes, makes it ideal for teleoperation. This contrasts with the fast dynamics of the traffic situations

for cars and airplanes, often measured in milliseconds, reported as challenging teleoperation areas due to the vulnerability from mainly long latency [99, 103]. Several research papers propose methods to compensate or predict the teleoperated vehicle's pose to mitigate the latency problem [104–106]. We use this knowledge to predict our current position based on heading, speed, and the received estimated position from the remote vessel. We concluded in our previous study that 3D, and especially VR, gave the best performance. VR can strengthen the visualization, and thereby the total communication between the machine and the human [108]. It has also been shown that VR can enhance SA when driving a remote car [97, 98]. Because of our good results for VR in our previous work, we use only VR in this current work. Here we have re-built the GUI to evaluate how teleoperation can support navigation, and more specifically, the TAN application. We base the user evaluation on recordings from a field trial to make the user experience as realistic as possible.

One of our main objectives has been to provide the user with an immersive experience that provides good SA. To gain trust in the system's ability to navigate, it is essential that the user gets a good overview and instantly can determine whether the position is estimated correctly or not. When navigating onboard a manned vessel, the usual way of doing this is to try to match the real-world terrain with objects on the sea chart or radar and try to judge if the directions and ranges coincide. The mental rotations needed for this task are difficult for a human to perform [88, 90], and we believe it is even more challenging to do remotely, i.e., by comparing what is seen on a video screen with what is seen on the sea chart. Porathe concluded it is better on manned vessels to guide the operators by visualizing a 3D map oriented to match the user's view of the surrounding world [88]. Figure V.1 shows that we have built our GUI corresponding with this research, as the user will see if the real-world corresponds to the 3D-world, and thereby the position, easily and instantly. Moreover, if the system's position is not entirely accurate, the user can enhance the position accuracy by providing new bearing updates to the positioning system.

Our main contribution is to provide a GUI design for ship teleoperation providing good situation awareness, which meets the limitation of ships with a low throughput connection. We have shown that the users experienced the GUI to be simple to use while having a good overview of the situation. When the positioning system estimated an inaccurate position, the users could react upon this instantly. Furthermore, we have shown that our TAN application can be supported remotely by an operator taking bearings to landmarks.

This paper is organized as follows: Section 2 describes the Implementation and Method of the project, including the design of the applications in Subsection 2.1, the Field Trial in Subsection 2.2, and the User Study in Subsection 2.3. The results are given in Section 3, followed by Discussion and Conclusion in Section 4 and 5.

2 Implementation and Method

This section describes how the software for the *teleoperation tool* and the positioning tool, called *TAN application*, have been designed and implemented, followed by a description of the field trial and user study.

2.1 Design

In our study, we focus on a GUI for teleoperation of a small ASV via a connection with limited throughput, which inhibits the transfer of video or high-resolution images. The ASV is expected to be semi-autonomous to handle a SAR mission but is still assumed to need some human supervision to take measures if something unexpected happens.

We have developed the GUI to suit a small ASV with a computer capacity and sensor suite comparable to an autonomous car. The postulated sensors and capabilities are:

- Global Positioning System (GPS), (only used for ground truth in the study, as we want to test the system using the redundant navigation system).
- A redundant navigation system, which can estimate the global position. In our case, this has been accomplished by fusion of compass and speed log data with data from a particle filter (PF) comparing available maps with bottom depth and magnetic intensity [145].
- Camera with 360° coverage.
- Satellite communication system with a small antenna, providing a bandwidth of 256kbps.
- Application for cropping and compressing images, so that the ship can transmit panoramic images with a frequency of 0.1Hz, as well as an image with enhanced quality in the operator's direction, with a frequency of 1Hz.

System as a whole – Architectural Overview

An autonomous ship contains multiple sub-systems, all interacting with each other to create a smart system that can perceive its environment and act upon it. In this project, we focus on two sub-systems, the *teleoperation tool* to remote control an ASV, and the *TAN application*, which is used as a redundant positioning source to complement the GPS. The two sub-systems are important on their own, but we evaluate how they can interact and benefit from each other in this project. How does the position estimation influence the user experience of the teleoperation tool, and how can the teleoperation tool strengthen the TAN application's performance?

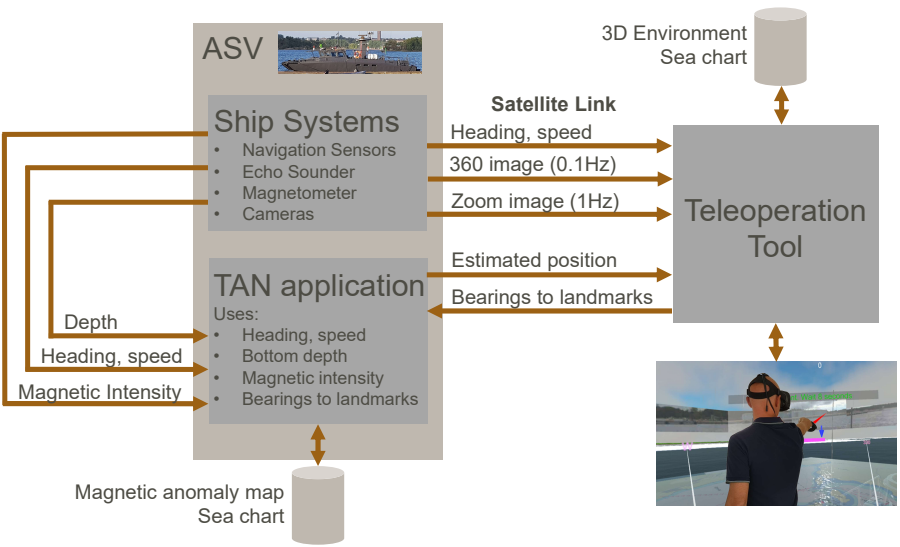

Figure V.2: An architectural overview of the system.

Figure V.2 shows the information flows between the sub-systems. The TAN application will run on a computer onboard the ASV, making it possible to receive all ship data in real-time. The teleoperation tool receives heading and speed together with cropped and compressed images. The TAN application sends the estimated position to the teleoperation tool, which transfers bearings to landmarks in return to the TAN application. The TAN application uses these bearings together with the heading, speed, depth, magnetic field, and the pre-loaded sea chart and magnetic anomaly map. All the interfaces between the TAN application and the teleoperation tool will be transmitted through a satellite link.

Terrain-Aided Navigation

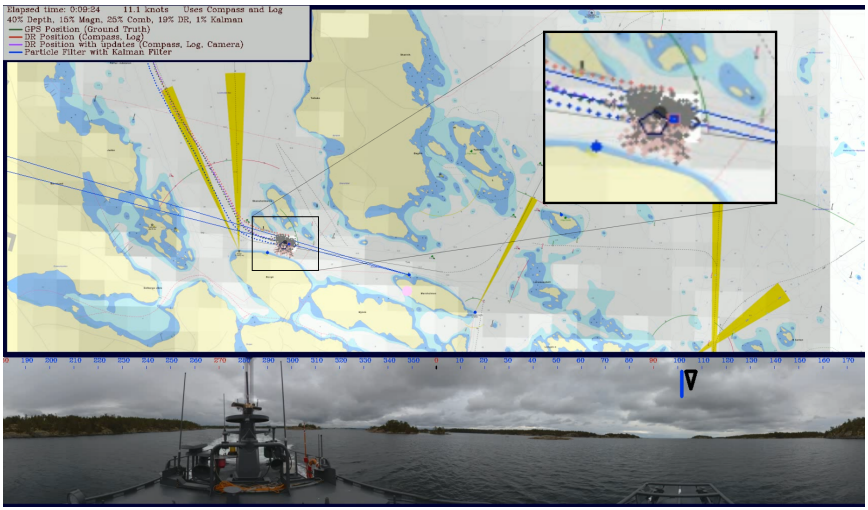

Figure V.3: The GUI of the TAN application. The upper right corner shows an enlargement of the current operation area. The ship is going in the east direction. The particles are visualized as grey and pink dots, where the pink dots have just been discarded due to being outside of the bearing's cone towards the lighthouse in bearing 107°. The blue dot in the middle of the enlarged image indicate ground truth, which comes from the GPS. The large grey dot indicate the mean of the particles, and the pentagon the estimated position from the Kalman filter.

The project described in this paper builds upon our previous work with a TAN application, which estimates the position by using a particle filter (PF) to compare known maps to depth and magnetic intensity measurements [145]. We concluded that the position estimation gains accuracy when using multiple information sources instead of only using either depth or magnetic intensity separately. Figure V.3 shows a screenshot of the GUI. For a better understanding, a video recording from the user study can be found on YouTube[2]. The upper part of the figure shows the sea chart with an enlargement of the image showing the particles estimating the ship's position. The lower part shows the 360° image. In the bearing 107° in the 360° image, a bearing to a landmark has just been detected.

[2]https://youtu.be/zu40PEsk5cQ

This is shown in the sea chart as a long blue cone originating from the landmark in the middle of the figure and stretching towards the ship. To satisfy the bearing measurement, the particles outside the cone are discarded, indicated as pink dots. In the user study, this GUI has been used for evaluating the TAN application's performance. The participants have not used it.

Tests showed that the positioning gained in performance from using the bearings to landmarks. These bearings were measured offline manually from the high-resolution images, which will not be possible in an unmanned vessel. A more realistic scenario is to use either image recognition software to detect landmarks, or that a human marks the landmarks from a remote location using low-quality images. In this project, we use the latter approach, where the user detects the landmarks in VR from a remote location.

Graphical User Interface for teleoperation

We have implemented the GUI for the teleoperation tool in Unity 3D [119], which game developers usually use for creating 2D and 3D games. We have used a 3D replica of the real world as a foundation for implementing the GUI. This 3D environment has been developed from maps and sea charts by the shipyard Saab Kockums AB [120].

The operator teleoperating the ship is virtually placed on board the virtual ship, positioned in the 3D environment according to where the TAN application is estimating the position. The tool receives speed and heading from the remote ship, which are used to move the vessel between each GUI frame. The 360° image is updated only six times every minute to minimize the bandwidth usage. The zoom image, which is an image with better quality in the pointing direction, is updated every second. The GUI presents the images with some latency to simulate the slow satellite communication link.

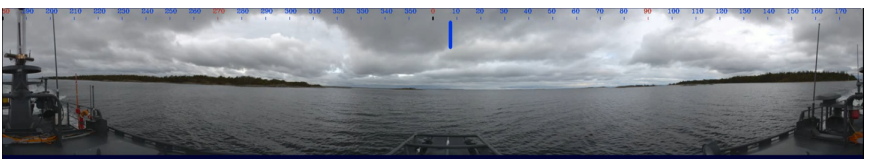

Figure V.4: A frame of the high resolution (16384×8192) 360° video, recorded during the field trial.

The GUI uses the panoramic video from the field trial both to create the zoom image and the 360° image. The video quality is high, with 16384×8192 pixels of resolution. Figure V.4 illustrates this with an example image. The problem is that the size of the images that build up the video is large and can not be transmitted in real-time over a satellite connection with low throughput. To meet the limitations, we have cropped and compressed the images. Figure V.5 shows both the zoom image and the 360° image in the teleoperation GUI, where the 360° image surrounds the user and the zoom image is in the direction of the pointing device. The zoom image is presented in front of the 360° image so that the better quality image covers the lower quality image. It slowly moves away from the user and vanishes behind the 360° after a few seconds. If, e.g., holding the pointer steadily towards a specific object, one new image in that direction will appear every second.

To minimize the throughput, the 360° image is sent with 0.1Hz and the zoom image is sent with 1Hz. The compressed panoramic image has a size of around 30kB, and the compressed zoom image with higher quality has a size of 3kB. This results in a throughput of 6kB/s, or 48kbps, which is a lot less than the 256kbps capacity of the communication link, leaving room for more user interface features.

Two variants of the Graphical User Interface

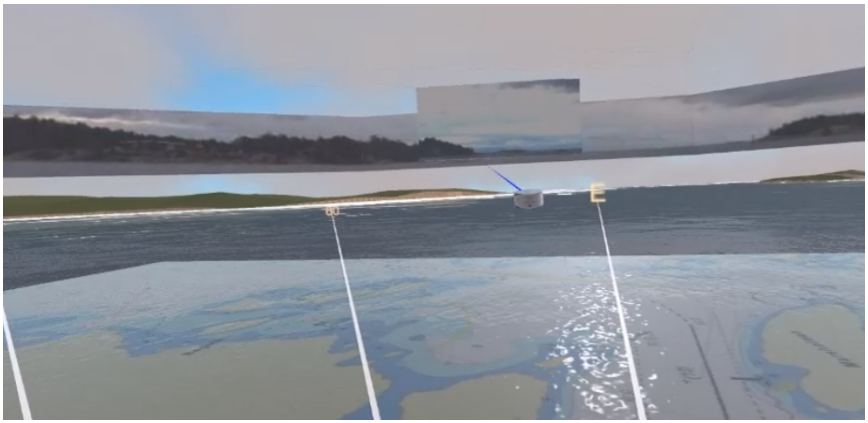

Figure V.5: The GUI version called $GUI^{without}$, without augmented landmarks. In the image the user is to take a bearing towards the shore.

There are two variants of the GUI, $GUI^{without}$ and GUI^{with}, each variant tested by half of the user study group. Figure V.5 shows the variant without augmented landmarks called $GUI^{without}$, where the user shall try to match objects between the upper 360° image with objects in the lower 3D environment, without any augmented landmarks that guide the user. In the figure, the user is pointing towards the shore, which is also found below in the 3D environment. By first shooting the laser towards the specific point of the shore in the 3D environment and then towards the 360° image, the application knows the ship is located in the opposite direction from the shore's specific position. This information is sent to the TAN application, which adjust the PF's position estimation accordingly.

This benefit of the $GUI^{without}$'s design is that the user is free to use all landmarks that can be found. The disadvantage is that it is quite difficult to point the laser pointer to the exact location in the vertical direction. If pointing a little bit over the intended direction, the user is pointing towards a position further away, which will result in the wrong position estimation. Another disadvantage with $GUI^{without}$ is that the users must be more creative and find the landmarks themselves.

Figure V.6: The GUI version called GUI^{with}, with augmented landmarks. (The user is overlaid over the image.)

Figure V.6 presents the other variant of the GUI with augmented landmarks, called GUI^{with}. The difference is that GUI^{with} shows proposed landmarks as large pink markers, often with arrows, that turn blue when the user point towards them. The user in the image first shoots the laser towards the arrow (that points towards the right part of the house), and then directly at the right part of the house in the 360° image. The tool then knows the landmark's exact position, in contrast to $GUI^{without}$, where the user could slightly miss the target. A disadvantage is

that the user is limited to the usage of only the proposed landmarks. Another screenshot from GUI^{with} is shown in Figure V.1.

2.2 Field Trial

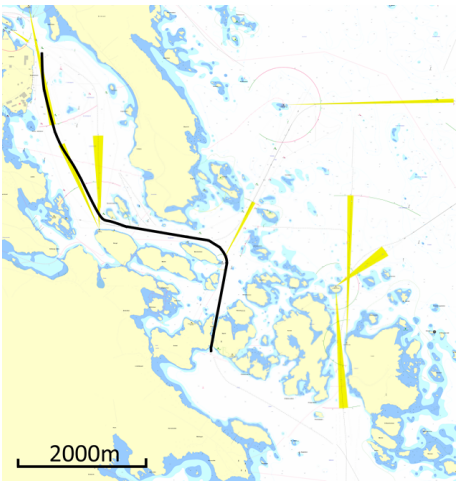

Figure V.7: The route of the field trial overlaid on the sea chart. The boat went in the south-east direction.

We conducted a field trial in Västervik archipelago in Sweden to validate our approach, see Figure V.7. We have used this field trial to collect data, which we have used for simulations and teleoperation tests. By using simulations for the user study instead of running the user study on the real-world ship, we have had the exact same scenario for all participants, making the results comparable. The boat used in the field trial is of type *CB90*, see Figure V.8. It has been complemented with additional sensors to support the Swedish Universities via the WASP program [1] with a research platform for developing autonomous ships. We believe that the sensors onboard, see Table V.1, correspond to a sensor suite of a typical future affordable autonomous ship. We collected data from the digital compass onboard, but the ship was not equipped with a speed log. Instead, a virtual speed log was created using data from the GPS and adding an error of 0.2 knots (i.e., NM/h) to simulate a worst-case scenario. In the last step, to study the robustness of the algorithm's ability to navigate, we added a drift of a constant 0.5 knots to

mimic the drift from the wind and current that can not be detected by the compass and speed log. The drift speed can, in general, be estimated with quite a good accuracy, and these 0.5 knots should be seen as the error between the estimated drift and the correct drift. If we can show that the TAN application can manage an inaccuracy of the drift speed of 0.5 knots, we believe the system is very robust. As the particle filter is estimating the position and not velocity nor the drift speed, the algorithm's results are not helped by a constant drift. The boat traveled a 9.2NM (17km) long route in 54min, but to make the user-study more manageable, we only used the first 20 minutes for the study.

Figure V.8: The boat of type CB90 used in the field trial.

Table V.1: Sensors used during field trial

Sensor	Description
Compass*	Heading (Accuracy 0.5°) - 1Hz
Speed Log*	Speed Through Water (STW) (Accuracy 1% + 0.1 knots) - 1Hz
Echosounder	Depth from surface to sea bed (Accuracy 0.1 m) - 1Hz
Magnetometer	Magnetic Intensity measured as a vector - 100Hz
360° camera	Provides visual image of the horizon around most of the ship. Can alternatively be multiple cameras. Images from 6 cameras were compiled into an image with a resolution of 16384×8192 - 15Hz

*The digital compass and speed log could be exchanged to an INS.

More information regarding the data collected from the field trial can be found in our earlier work [145], where we used the data to evaluate the performance of the TAN application when using various fusion methods.

We conducted the whole study in an office by using the collected data. No ship was teleoperated for real, but the teleoperation interfaces were restricted to accommodate the low throughput connection.

2.3 User Study

We evaluated our implementations with a user study of 16 participants, recruited mainly from Lund University and the shipyard Saab Kockums AB, in 20-minute long trial sessions with the task and scenarios described below. We recorded what the users saw in VR, as well as the TAN application GUI and its performance data. We informed the participants of the possibility of withdrawing at any time, and they agreed upon the use of screen recordings and other data for research purposes. Lund University ethics council did not require reviews of this kind of study since no personal data was studied. Four of the user study videos can be seen on YouTube[3]. The videos show both the teleoperation GUI and the TAN application GUI for two of the users. One of the users used $GUI^{without}$ (without augmented landmarks), and the other used GUI^{with} (with augmented landmarks).

After an introduction phase based on written instructions and a quick oral summary, the user used the GUI in VR to remotely supervise the ship. The main task was to point towards the same objects in both the virtual 3D environment and the 360° panoramic image, resulting in a bearing to a landmark. The teleoperation tool sent these bearings to the TAN application, which updated and increased the position's accuracy. Half of the subjects were randomly assigned using the GUI^{with}, and the other half were assigned the $GUI^{without}$ where they had to find the landmarks by themselves. Our main questions to evaluate in the study were:

- Do the bearings from the operators increase the position accuracy for the TAN application, despite the low quality of the 360° images?
- Do users experience they gain trust in the system's ability to navigate?
- Did users gain or lose performance when augmenting specific landmarks that the operators were to take bearing measurements from, instead of letting the operators freely pick landmarks that they thought would be good?

[3]https://youtu.be/HwnIPuX-Azg, https://youtu.be/zu40PEsk5cQ, https://youtu.be/PCkAQhyAC6Q, and https://youtu.be/HTm2GEZsxh0

We compared the mean position error for each participant's recorded data from the user study (objective results).

After the experiments, the participants evaluated the GUI subjectively by answering the following four questions on a scale of 1–10 (1 was best on the first, and ten was best on question two to four):

1. It was difficult to handle the tool.

2. I experienced that I had a good overview of the situation.

3. If the tool further evolves, I believe that a real ship can be teleoperated using this technique.

4. If I practice 100 hours, my ability to use the tool would enhance further.

3 Results

We have summarized the collected data from the user experiments in the objective and subjective results below, followed by some observations. We have interpreted the results in Section 4.

3.1 Objective Results

It is possible to estimate a ship's position by dead reckoning (DR) the position by using the compass and speed log. The problem with this method is that the error increases with time, as each measurement is based on the previous measurement, leading to a position error being accumulated over time. The TAN application uses a PF to compare the bottom depth and magnetic intensity with available maps to estimate the position more accurately. With this approach, the position error is not supposed to increase with time but, instead, holds its position relatively close to the correct position. We have Kalman filtered (KF) the mean of the PF's particle cloud. The KF provides a smoother and more accurate position estimation compared to only using the mean of the PF's cloud as a position estimation. By using bearings to landmarks, it is possible to reset the DR or PF's position estimation in the bearing direction by moving the particles or the DR estimation to the closest point in the bearing's direction, see Figure V.3 or any of the YouTube videos for an example.

In the following, we present graphs and statistical analysis of the position error performance. The mean values are summarized in Table V.2. As we based the user

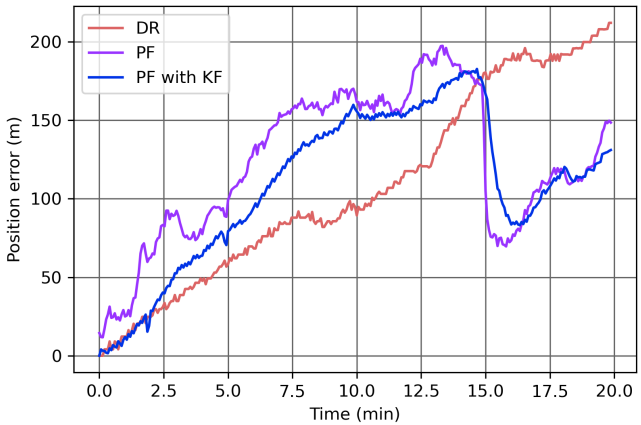

Figure V.9: Position accuracy when not receiving any bearings to landmarks at all. In this particular example, the PF performance is worse than DR the first 15 minutes. This can happen as the PF use the DR as basis for its calculation, spreads the particles randomly, and then corrects the particle positions by comparing the maps with sensor measurements. In this particular situation, the maps matches the measurements quite well for the first 15min, despite the position being 150m off. After 15min, the bottom depth do not match any more, which results in an adjustment of the particle cloud's mean position.

study on a recording from a field trial, the DR without any bearing updates is the same for all user tests.

Figure V.9 shows how the position error varies when not using any bearings to landmarks at all. As seen in the plot, the DR position error (red line) increased with time to around 200m after 20min. The purple line, showing the position error when using PF, peaks after 13min on about 200m. The accuracy is enhanced by Kalman filtering the PF (blue line), which peaks on about 175m. The mean error for DR was 111.6m, and the mean error for PF with KF was 109.1m. We can now use the value from PF with KF and see how the performance increases when the application receives bearings to landmarks.

Figure V.10 shows a graph constructed from the eight $GUI^{without}$ user trials. The graph presents the averaged position error over the 20-minute test. The DR position error increases with time (red line), but as the user takes bearings, the DR error is reset in the direction from the bearing (yellow line). As shown by the

Table V.2: Mean position error without bearings or with bearings from $GUI^{without}$ or GUI^{with}

Algorithm	**Without bearings**	**Bearings from $GUI^{without}$**	**Bearings from GUI^{with}**
DR	111.6m	71.8m	57.6m
PF	123.5m	51.4m	42.8m
PF with KF	109.1m	36.5m	34.9m

blue line, the KF corrected PF's mean error peaks at about 65m after 7min. The mean error of the bearing-updated DR was 71.8m (yellow line), and the bearing-updated PF with KF was 36.5m (blue line).

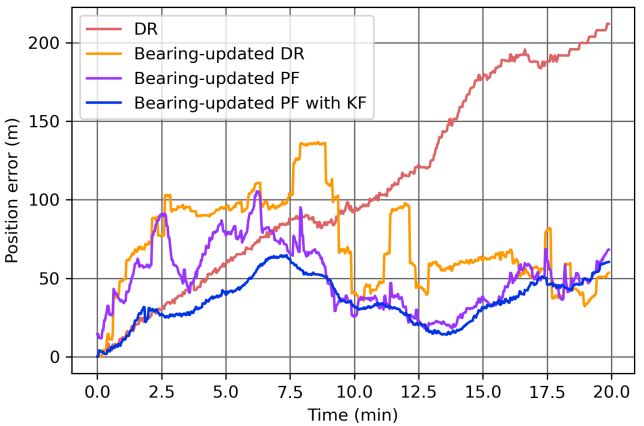

Figure V.10: Position accuracy averaged from eight user trials using $GUI^{without}$, compared to DR when not using any bearings at all (red line).

Figure V.11 shows a graph constructed from the eight GUI^{with} user trials. As shown by the blue line, the bearing-updated PF with KF mean error is relatively stable around 35-40m. The mean error of the bearing-updated DR was 57.6m (yellow line). The bearing-updated PF with KF was 34.9m (blue line), and peaked after about 17min on about 60m.

We found that the tests with both the $GUI^{without}$ and GUI^{with} significantly improved position accuracy by updating the TAN application with the bearings to-

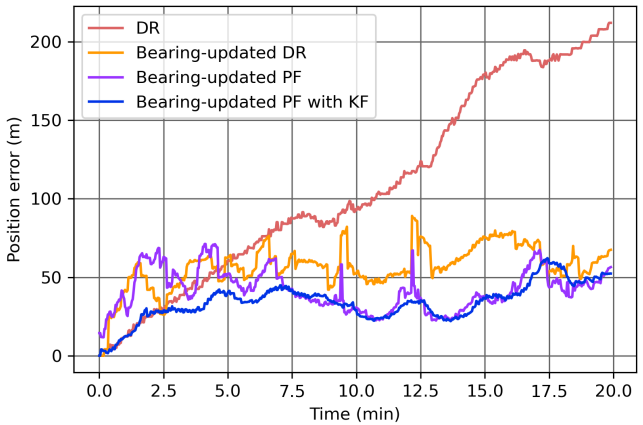

Figure V.11: Position accuracy averaged from eight user trials using GUI^{with}.

wards the landmarks. It was significantly better to use the bearing-updated PF with KF than just the bearing-updated DR, but also significantly better with bearing-updated DR compared to only DR (without bearings).

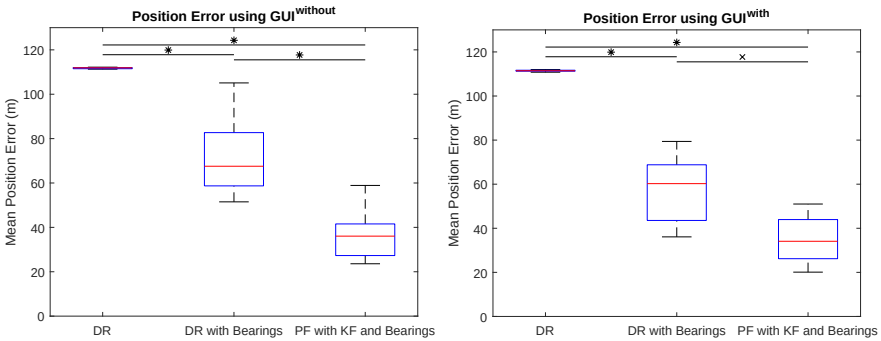

Figure V.12: The objective results summarizing the position accuracy when using the different methods. (x) and (*) denote comparisons with $p < 0.01$ and $p < 0.001$ respectively. Because we based the user study on a recording from a field trial, *DR* (to the left) is the same for all tests.

Figure V.12 summarizes the objective results, along with the p-values showing the significant difference, computed in a series of one-tailed t-tests. The mean val-

ues are presented in Table V.2. Even though it was quite a small user study, power tests (alfa=0.05, power>0.80) have shown that there were enough participants to support the significant results. However, there was no significant difference between the two user groups.

3.2 Subjective Results

Table V.3: Subjective Results Summary

Question	$GUI^{without}$	GUI^{with}
Difficult to Manage*	3.3	2.9
User Overview	6.3	6.9
Applicability for real-world usage	8.5	8.3
Gain from Training	8.4	8.9

*Lower score is better.

For the user evaluation's subjective results, the users using GUI^{with} gave better scores to all four questions except the question regarding the applicability for real-world usage. In general, though, the results were quite similar, and there have not been any significant differences. The scores, with a scale of 1–10 (1 was best on the first, and ten was best on question two to four), are presented in Table V.3. The users answered that the tool was not challenging to use (3.3 and 2.9) (lower score is better). They also had a good overview of the situation (6.3 and 6.9). Even more importantly, they believed a real-world ship would be possible to teleoperate in this way if the tool was further developed (8.5 and 8.3). They thought they would be even better handling the teleoperation tool after 100h of usage (8.4 and 8.9). Figure V.13 summarizes the subjective results.

We also asked the users to elaborate on good and bad aspects about the tool and how it felt using it.

Starting with the point that users wanted to be enhanced, most users (11 of 16) wanted either better resolution, higher frame-rate, or better lightning of the 360° image. Two persons lacked support for glasses, as the head-mounted display HTC-Vive is of the older type where glasses do not fit. One participant suggested adding support for taking a bearing during the turning of the ship, which we have not implemented yet. When the shore was close to the vessel, the 3D environment could cover the 360° image, which one person pointed out to aggravate the us-

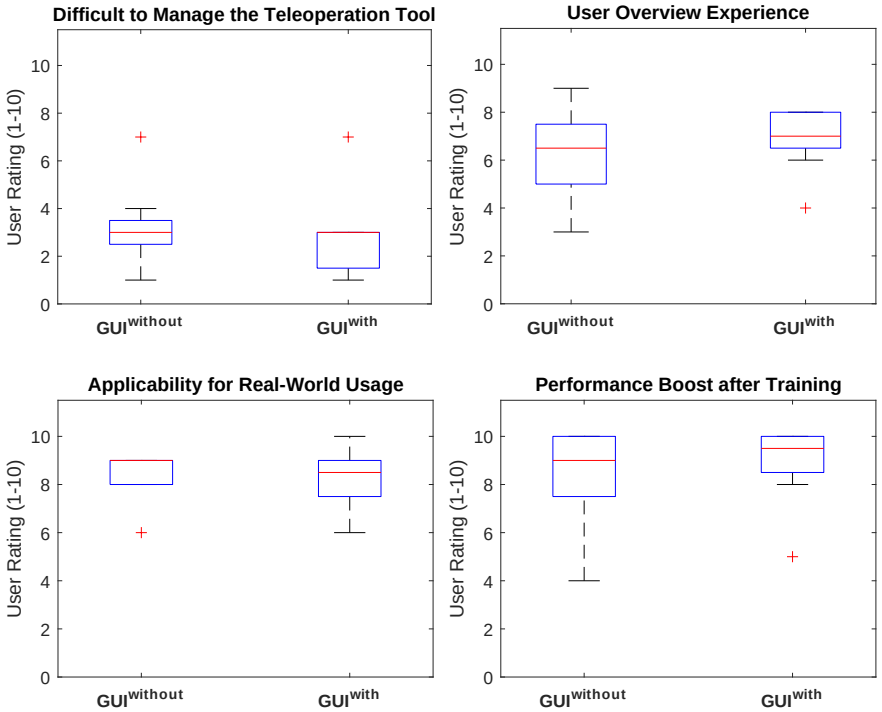

Figure V.13: Subjective results from the questionnaire. Users answered the following questions: (**a**) It was difficult to handle the tool. (Lower score is better.) (**b**) I experienced that I had a good overview of the situation. (User Overview Experience) (**c**) If the tool further evolves, I believe that a real ship can be teleoperated using this technique. (Applicability for Real-World Usage) (**d**) If I practice 100 hours, my ability to use the tool would enhance further. (Performance Boost after Training)

ability. There were also suggestions to enhance the 3D visualizations of buildings. Two persons found it a fun experience, while one person got bored after a while.

We asked the users about their VR experience, where the value 10 meant they were very experienced, and 1 meant they had no experience, resulting in the mean value of only 3.1. Still, 12 of the participants wrote that it was easy to use, easy to understand, or intuitive. Some had a problem understanding the tool during the first minutes but then said that they quickly learned. Three persons said they had either a good overview of the situation or that it was easy to orient, and another said that it was easy to find out if the estimated position did not match the 360° image.

One person reflected that he did not get any motion sickness, which surprised him, as he usually gets motion sickness from VR.

3.3 Observations

By observing the user's behavior during the study, it became clear that the users of $GUI^{without}$, in general, had more difficulties at the beginning of the study, as they needed to orient themselves and learn quickly what type of landmarks would be appropriate to pick. Some of them got stressed, especially initially, and some participants took very few bearings during the first five minutes. After this initial period, these users seemed to have learned the teleoperation tool and were very creative in finding new landmarks to improve the position accuracy.

The users of GUI^{with}, in general, figured out quite early what to do. Most of them acted quite skilled and took many bearings towards these fixed landmarks. We believe this task was not as challenging as with $GUI^{without}$, and some of the participants looked a bit bored after a while. Being bored indicate low cognitive load, leaving room for conducting other tasks simultaneously. For not having even higher positioning performance, we consider a large reason to be the difficulty of hitting the $GUI^{without}$'s landmark accurately in the vertical direction with the laser pointer. We discovered from the saved video files from the user study that the laser pointer has many times pointed at an object behind the intended object, resulting in lower performance. To get better accuracy from using the GUI^{with}, it should have been beneficial with more augmented landmarks, as the users could have handled many more.

4 Discussion

What we mainly wanted to see in this study was if the users could get good situational awareness and feel that they were positioned in the correct location by being able to easily compare the 360° image with the 3D environment. The questionnaire results, together with what the users wrote they experienced, have confirmed both these hypotheses. This is important, as it is difficult for a remote user to know if the position is accurate in a typical teleoperation system. Furthermore, the users have been given a good overview of the situation by using the 360° image. Relatively small buoys more than 500m away have been easily discovered.

We also wanted to confirm that the TAN application could gain in performance using bearings that the user took remotely. We did not know this before-

hand, as we knew that the images would have relatively low quality, given the communication link with poor throughput.

We also wanted to know if there were any considerable differences between the two GUI types, which the user study did not imply. Still, the different GUI versions have given us some insights, as there were different advantages and disadvantages of the versions.

To enhance the implementation further, we have learned that:

- The 360° image already has a low quality; hence it is helpful to increase the visibility as much as possible by, e.g., increasing the brightness.
- By using an augmented landmark to point towards, it is possible to get a more accurate position of the landmark, which is beneficial for the positioning system.
- Users are creative and can keep track of many objects. Do not limit the number of available augmented landmarks too much.
- The 360° image should not be covered by the 3D environment, even when the ship is very close to shore.

Some users wanted a higher resolution and frame-rate for the 360° image, which can be achieved when there is a better communication connection available with higher throughput. In this study, the throughput was very limited, though, as we wanted to see if it worked in the worst-case scenario.

The study provides knowledge about multiple aspects about how to create a teleoperation tool for an autonomous vessel, but the user-study has not intended to evaluate a complete system design. We believe more research is needed for this. We still do not know if VR is a good solution for multiple hours of operations, and we believe a final design for expert users should be designed in a different way, optimized for the intended usage and scenario.

5 Conclusion and Future Work

We have developed and tested a GUI for the teleoperation of an affordable Autonomous Surface Vehicle using a low throughput connection. Our findings show that users have had a good overview despite the low-quality images. The users have experienced the position as correctly estimated by easily matching the 3D environment with the 360° image. When it did not match, they quickly have reacted and

tried to solve the problem by updating the positioning system with new bearings. We can conclude that the positioning system has increased its accuracy by using these bearings, despite the low-quality link connection.

Together with the results from our previous work [146, 147], which focused on features to provide good situational awareness and safety, while maintaining a low cognitive load, we now believe we have all functions needed to combine all building blocks into a more comprehensive GUI with more complexity, tailored for trained expert users. Building upon this, we aim to conduct a new user study with expert users teleoperating the ship while having safety drivers on board to meet current regulations.

ACKNOWLEDGMENT

This work was partially supported by the Wallenberg AI, Autonomous Systems and Software Program (WASP) [1] funded by Knut and Alice Wallenberg Foundation. Saab Kockums AB [120] provided the ship used for the field trial.

Bibliography

Bibliography

[1] WASP. [Online]. Available: http://wasp-sweden.org/

[2] O. Levander, "Autonomous ships on the high seas," *IEEE Spectrum*, vol. 54, no. 2, pp. 26–31, 2017.

[3] (2018) IMO and the safety of navigation. Last accessed 22 October 2020. [Online]. Available: http://www.imo.org/en/OurWork/Safety/Navigation/Pages/Default.aspx

[4] T. Porathe, "Maritime autonomous surface ships (MASS) and the COLREGS: Do we need quantified rules or is "the ordinary practice of seamen" specific enough?" *the International Journal on Marine Navigation and Safety of Sea Transportation*, 2019.

[5] Craig Eason at Fathom.World. (2020) No rules on autonomous ships for another 10 years – at least. Last accessed 27 October 2020. [Online]. Available: https://fathom.world/no-rules-on-autonomous-ships-for-another-10-years-at-least/

[6] iXBlue. (2020) Marins series - military and strategic grades INS. Last accessed 12 November 2020. [Online]. Available: https://www.ixblue.com/products/marins-series

[7] (2020) Safety of Navigation Guide - SOLAS. Last accessed 23 November 2020. [Online]. Available: https://www.fcmarine.co.uk/wp-content/uploads/2017/10/SOLAS-EQUIPMENT-REQUIREMENTS.pdf

[8] Wikipedia. (2020) Gross tonnage. Last accessed 12 November 2020. [Online]. Available: https://en.wikipedia.org/wiki/Gross_tonnage

[9] Global Fishing Watch. What vessels are required to use AIS? What are global regulations and requirements for vessels to carry AIS? Last accessed 29 October 2020. [Online]. Available: https://globalfishingwatch.org/faqs/what-vessels-are-required-to-use-ais-what-are-global-regulations-and-requirements-for-vessels-to-carry-ais/

[10] Digisat. Maritime Internet Service. Last accessed 29 October 2020. [Online]. Available: https://www.digisat.org/maritime-satellite-internet

[11] (2020) Starlink: SpaceX wants to test sea-based Internet using an iconic vehicle. Last accessed 29 October 2020. [Online]. Available: https://www.inverse.com/innovation/starlink-spacex-test-sea-based-internet

[12] T. Porathe, J. Prison, and Y. Man, "Situation awareness in remote control centres for unmanned ships," in *Proceedings of Human Factors in Ship Design & Operation, 26-27 February 2014, London, UK*, 2014, p. 93.

[13] European Maritime Safety Agency. (2019) Annual overview of marine casualties and incidents 2019. Last accessed 26 October 2020. [Online]. Available: https://safety4sea.com/wp-content/uploads/2019/11/EMSA-Annual-Overview-of-Marine-Casualties-and-Incidents-2019-2019_11.pdf

[14] S. R. Chan, N. A. Hamid, and K. Mokhtar, "A theoretical review of human error in maritime accidents," *Advanced Science Letters*, vol. 22, no. 9, pp. 2109–2112, 2016.

[15] H. C. Burmeister, W. C. Bruhn, Ø. J. Rødseth, and T. Porathe, "Can unmanned ships improve navigational safety?" in *Proceedings of the Transport Research Arena, TRA 2014, 14-17 April 2014, Paris,*, 2014.

[16] (2018) Remote-controlled and autonomous ships in the maritime industry. Last accessed 9 September 2020. [Online]. Available: https://www.dnvgl.com/maritime/publications/remote-controlled-autonomous-ships-paper-download.html

[17] T. Fjelldal, "Autonomous systems design - An exploratory research study in the context of maritime shipping," Master's thesis, NTNU, 2018.

[18] H. C. Burmeister, W. Bruhn, Ø. J. Rødseth, and T. Porathe, "Autonomous unmanned merchant vessel and its contribution towards the e-navigation implementation: the MUNIN Perspective," *International Journal of e-Navigation and Maritime Economy*, vol. 1, pp. 1–13, 2014.

[19] Munin Research Project. (2016) Research in maritime autonomous systems - project results and technology potentials. Last accessed 17 October 2020.

[Online]. Available: http://www.unmanned-ship.org/munin/wp-content/uploads/2016/02/MUNIN-final-brochure.pdf

[20] Albert Embankment at International Maritime Organizatioin. (2018) UN body adopts climate change strategy for shipping. Last accessed 26 October 2020. [Online]. Available: https://www.imo.org/en/MediaCentre/PressBriefings/Pages/06GHGinitialstrategy.aspx

[21] O. Levander. (2018) Redefining Shipping - Towards Zero Waste. Last accessed 23 November 2020. [Online]. Available: https://www.alandia.com/sites/www.alandia.com/files/attachments/documents/levanderredefiningshipping24may2018.pdf

[22] Kongsberg Maritime. (2017) Autonomous ship project, key facts about YARA Birkeland. Last accessed 17 October 2020. [Online]. Available: https://www.km.kongsberg.com/ks/web/nokbg0240.nsf/AllWeb/4B8113B707A50A4FC125811D00407045?OpenDocument

[23] A. Łebkowski, "Design of an autonomous transport system for coastal areas," *TransNav: International Journal on Marine Navigation and Safety of Sea Transportation*, vol. 12, 2018.

[24] Varsha Saraogi, author at Ship Technology. (2019) How will autonomy shape the UK shipping industry? Last accessed 26 October 2020. [Online]. Available: https://www.ship-technology.com/features/how-will-autonomy-shape-the-uk-shipping-industry/

[25] O. Levander. (2018) Redefining Shipping. Last accessed 16 October 2018. [Online]. Available: http://bmsunited.com/Admin/Public/DWSDownload.aspx?File=%2FFiles%2FFiles%2FConference.Presentations%2F2-Redefining-shipping-2018-05-30.pdf

[26] DNV GL. (2015) The ReVolt - A new inspirational ship concept. Last accessed 19 October 2020. [Online]. Available: https://www.dnvgl.com/technology-innovation/revolt/index.html

[27] (2020) Oceanbird - the wind carries a shipping revolution. Last accessed 1 December 2020. [Online]. Available: https://www.walleniusmarine.com/our-services/ship-design-newbuilding/ship-design/wind-powered-vessels/

[28] U. Dhomé, N. Rolleberg, and J. Kuttenkeuler, "Energy efficient self-steering mechanism for an autonomous sailing vessel," in *OCEANS 2019-Marseille*. IEEE, 2019, pp. 1–6.

[29] (2020) Wind-powered cargo ship model sails in stockholm. Last accessed 1 December 2020. [Online]. Available: https://www.kth.se/en/aktuellt/nyheter/segelfartygens-chans-att-ta-revansch-1.1032322

[30] SWZ Maritime. (2020) Wind powered car carrier to set sail in late 2024. Last accessed 1 December 2020. [Online]. Available: https://www.swzmaritime.nl/news/2020/09/10/wind-powered-car-carrier-to-set-sail-in-late-2024/

[31] V. V. Thai and T. Latta, "Employment brand strategy for the shortage of seafarers," *International Journal of Shipping and Transport Logistics*, vol. 2, no. 4, pp. 411–428, 2010.

[32] SAE International. (2020) Society of automotive engineers. Last accessed 13 December 2020. [Online]. Available: https://www.sae.org/

[33] Wikipedia. (2018) Self-driving car. Last accessed 25 October 2018. [Online]. Available: https://en.wikipedia.org/wiki/Self-driving_car

[34] D. Newcomb. (2018) Why self-driving cars will require a 'god view' eye in the sky. Last accessed 2 November 2020. [Online]. Available: https://uk.pcmag.com/news-analysis/92963/why-self-driving-cars-will-require-a-god-view-eye-in-the-sky

[35] Einride. (2019) Einride showcases new teleoperation solution at mobile world congress. Last accessed 28 October 2020. [Online]. Available: https://www.einride.tech/news/einride-showcases-new-teleoperation-solution-at-mobile-world-congress

[36] Å, Alström at Volvo. (2019) Remote-controlled wheel loaders to be tested when Volvo CE receives Sweden's first 5g network for industry. Last accessed 28 October 2020. [Online]. Available: https://www.volvoce.com/global/en/news-and-events/press-releases/2019/remote-controlled-wheel-loaders-to-be-tested-when-volvo-ce-receives-sweden-first-5g-network-for-indu/

[37] Alex Davies at Wired. (2019) Nissan's Path to Self-Driving Cars? Humans in Call Centers. Last accessed 28 October 2020. [Online]. Available: https://www.wired.com/2017/01/nissans-self-driving-teleoperation/

[38] E. Jokioinen, J. Poikonen, R. Jalonen, and J. Saarni, "Remote and autonomous ships - the next steps," *AAWA Position Paper, Rolls Royce plc, London*, 2016.

[39] (2018) Being a responsible industry: An industry code of practice version 2. Last accessed 27 October 2020. [Online]. Available: https://www.maritimeuk.org/media-centre/publications/maritime-autonomous-surface-ships-uk-code-practice/

[40] DNV GL, "Class guideline-autonomous and remotely operated ships," DNVGL-CG-0264, September, Tech. Rep., 2018.

[41] (2017) Shipright - design and construction - additional design procedures - design code for unmanned marine systems. Last accessed 28 October 2020. [Online]. Available: https://www.cdinfo.lr.org/information/documents/ShipRight/Design%20and%20Construction/Additional%20Design%20Procedures/Design%20Code%20for%20Unmanned%20Marine%20Systems/Design%20Code%20for%20Unmanned%20Marine%20Systems,%20February%202017.pdf

[42] (2018) IMO takes first steps to address autonomous ships. Last accessed 28 October 2020. [Online]. Available: https://www.imo.org/en/MediaCentre/PressBriefings/Pages/08-MSC-99-MASS-scoping.aspx

[43] A. Felski and K. Zwolak, "The ocean-going autonomous ship—challenges and threats," *Journal of Marine Science and Engineering*, vol. 8, no. 1, p. 41, 2020.

[44] A. Hevner and S. Chatterjee, "Design science research in information systems," in *Design research in information systems*. Springer, 2010, pp. 9–22.

[45] K. Peffers, T. Tuunanen, M. A. Rothenberger, and S. Chatterjee, "A design science research methodology for information systems research," *Journal of management information systems*, vol. 24, no. 3, pp. 45–77, 2007.

[46] J. E. Manley, "Unmanned surface vehicles, 15 years of development," in *OCEANS 2008*. IEEE, 2008, pp. 1–4.

[47] M. Caccia, M. Bibuli, R. Bono, G. Bruzzone, G. Bruzzone, and E. Spirandelli, "Aluminum hull USV for coastal water and seafloor monitoring," in *OCEANS 2009-EUROPE*. IEEE, 2009, pp. 1–5.

[48] J. Alves, P. Oliveira, R. Oliveira, A. Pascoal, M. Rufino, L. Sebastiao, and C. Silvestre, "Vehicle and mission control of the DELFIM autonomous surface craft," in *14th Mediterranean Conference on Control and Automation 2006. MED'06.* IEEE, 2006, pp. 1–6.

[49] (2020) AMS ROBOAT. Last accessed 18 October 2020. [Online]. Available: http://www.ams-institute.org/roboat/

[50] L. Camilli, "Designing ocean drones for maritime security: the use of integrated sensing modalities to enhance situational awareness," *Proceedings of Marine Technology Society and IEEE Oceanic Engineering Society OCEANS*, 2015.

[51] Jonathan Batty at IBM. Sea trials begin for Mayflower Autonomous Ship's 'AI Captain'. Last accessed 2 November 2020. [Online]. Available: https://newsroom.ibm.com/2020-03-05-Sea-Trials-Begin-for-Mayflower-Autonomous-Ships-AI-Captain

[52] Mayflower Autonomous Ship. It's time for the Mayflower Autonomous Ship. Last accessed 2 November 2020. [Online]. Available: https://mas400.com/#countdown

[53] Venture Beat. AI, AI, Captain! How the Mayflower Autonomous Ship will cross the Atlantic. Last accessed 2 November 2020. [Online]. Available: https://venturebeat.com/2020/03/04/ai-ai-captain-how-the-mayflower-autonomous-ship-will-cross-the-atlantic/

[54] (2020) Kongsberg Maritime. Last accessed 9 November 2020. [Online]. Available: https://www.kongsberg.com/maritime/

[55] YARA. YARA Birkeland press kit. Last accessed 2 November 2020. [Online]. Available: https://www.yara.com/news-and-media/press-kits/yara-birkeland-press-kit/

[56] Paul Sawers at VentureBeat. (2020) The role of autonomous ships in a world wary of pandemics. Last accessed 27 October 2020. [Online].

Available: https://venturebeat.com/2020/08/17/the-role-of-autonomous-ships-in-a-world-wary-of-pandemics/

[57] Kongsberg Maritime. (2020) Automatic ferry enters regular service following world-first crossing with passengers onboard. Last accessed 3 November 2018. [Online]. Available: https://www.kongsberg.com/maritime/about-us/news-and-media/news-archive/2020/first-adaptive-transit-on-bastofosen-vi/

[58] ——. (2020) HORIZON 2020: The Autoship project has started. Last accessed 3 November 2020. [Online]. Available: https://www.kongsberg.com/maritime/about-us/news-and-media/news-archive/2020/autoship-programme/

[59] Kongsberg. (2018) Rolls-Royce and Finferries demonstrate world's first Fully Autonomous Ferry. Last accessed 10 October 2020. [Online]. Available: https://www.rolls-royce.com/media/press-releases/2018/03-12-2018-rr-and-finferries-demonstrate-worlds-first-fully-autonomous-ferry.aspx

[60] Geogarage blog. (2018) Rolls-Royce demonstrates fully autonomous passenger ferry in Finland. Last accessed 9 November 2020. [Online]. Available: http://blog.geogarage.com/2018/12/rolls-royce-demonstrates-fully.html

[61] (2020) Sea Hunter: inside the US Navy's autonomous submarine tracking vessel. Last accessed 19 October 2020. [Online]. Available: https://www.naval-technology.com/features/sea-hunter-inside-us-navys-autonomous-submarine-tracking-vessel/

[62] (2018) Autonomous Sea Rescue Tested – WARA Public Safety demonstration. Last accessed 3 November 2020. [Online]. Available: https://wasp-sweden.org/autonomous-sea-rescue-tested-wara-public-safety-demonstration/

[63] People's Daily. (2016) China develops high-speed intelligent unmanned sea vessel. Last accessed 19 October 2020. [Online]. Available: http://en.people.cn/n3/2016/1104/c98649-9137482.html

[64] Wikipedia. (2020) GNSS applications. Last accessed 12 December 2020. [Online]. Available: https://en.wikipedia.org/wiki/GNSS_applications

[65] T. E. Humphreys, B. M. Ledvina, M. L. Psiaki, B. W. O'Hanlon, and P. M. Kintner, "Assessing the spoofing threat: Development of a portable GPS civilian spoofer," in *Radionavigation Laboratory Conference Proceedings*, 2008.

[66] N. Merlinge, J. Brusey, N. Horri, K. Dahia, and H. Piet-Lahanier, "Enhanced cooperative navigation by data fusion from IMU, ambiguous terrain navigation, and coarse relative states," in *2017 IEEE 56th Annual Conference on Decision and Control (CDC)*. IEEE, 2017, pp. 375–380.

[67] S. Carreno, P. Wilson, P. Ridao, and Y. Petillot, "A survey on terrain based navigation for AUVs," in *OCEANS 2010*. IEEE, 2010, pp. 1–7.

[68] R. Karlsson and F. Gustafsson, "Bayesian surface and underwater navigation," *IEEE Transactions on Signal Processing*, vol. 54, no. 11, pp. 4204–4213, 2006.

[69] D. Peng, T. Zhou, J. Folkesson, and C. Xu, "Robust particle filter based on huber function for underwater terrain-aided navigation," *IET Radar, Sonar & Navigation*, vol. 13, no. 11, pp. 1867–1875, 2019.

[70] F. Gustafsson, F. Gunnarsson, N. Bergman, U. Forssell, J. Jansson, R. Karlsson, and P.-J. Nordlund, *Particle filters for positioning, navigation and tracking*. Linköping University Electronic Press, 2001.

[71] G. T. Donovan, "Position error correction for an autonomous underwater vehicle inertial navigation system (ins) using a particle filter," *IEEE Journal of Oceanic Engineering*, vol. 37, no. 3, pp. 431–445, 2012.

[72] T. Nakatani, T. Ura, T. Sakamaki, and J. Kojima, "Terrain based localization for pinpoint observation of deep seafloors," in *OCEANS 2009-EUROPE*. IEEE, 2009, pp. 1–6.

[73] N. Fairfield and D. Wettergreen, "Active localization on the ocean floor with multibeam sonar," in *OCEANS 2008*. IEEE, 2008, pp. 1–10.

[74] K. B. Anonsen and O. Hallingstad, "Terrain aided underwater navigation using point mass and particle filters," in *Position, location, and navigation symposium, 2006 IEEE/ION*. IEEE, 2006, pp. 1027–1035.

[75] F. C. Teixeira, J. Quintas, P. Maurya, and A. Pascoal, "Robust particle filter formulations with application to terrain-aided navigation," *International Journal of Adaptive Control and Signal Processing*, vol. 31, no. 4, pp. 608–651, 2017.

[76] M. Zhou, R. Bachmayer, and B. deYoung, "Working towards adaptive sensing for terrain-aided navigation," in *2019 International Conference on Robotics and Automation (ICRA)*. IEEE, 2019, pp. 3450–3456.

[77] I. Nygren, "Terrain navigation for underwater vehicles," Ph.D. dissertation, KTH, 2005.

[78] G. Salavasidis, A. Munafò, C. A. Harris, T. Prampart, R. Templeton, M. Smart, D. T. Roper, M. Pebody, S. D. McPhail, E. Rogers *et al.*, "Terrain-aided navigation for long-endurance and deep-rated autonomous underwater vehicles," *Journal of Field Robotics*, vol. 36, no. 2, pp. 447–474, 2019.

[79] S. Dektor and S. Rock, "Improving robustness of terrain-relative navigation for AUVs in regions with flat terrain," in *2012 IEEE/OES Autonomous Underwater Vehicles (AUV)*. IEEE, 2012, pp. 1–7.

[80] ——, "Robust adaptive terrain-relative navigation," in *Oceans - St. John's*. IEEE, 2014, pp. 1–10.

[81] E. Le Grand and S. Thrun, "3-axis magnetic field mapping and fusion for indoor localization," in *2012 IEEE International Conference on Multisensor Fusion and Integration for Intelligent Systems (MFI)*. IEEE, 2012, pp. 358–364.

[82] M. Frassl, M. Angermann, M. Lichtenstern, P. Robertson, B. J. Julian, and M. Doniec, "Magnetic maps of indoor environments for precise localization of legged and non-legged locomotion," in *2013 IEEE/RSJ International Conference on Intelligent Robots and Systems*. IEEE, 2013, pp. 913–920.

[83] B. Grelsson, A. Robinson, M. Felsberg, and F. S. Khan, "GPS-level accurate camera localization with HorizonNet," *Journal of Field Robotics*, vol. 37, no. 6, pp. 951–971, 2020.

[84] J. Olofsson, G. Hendeby, F. Gustafsson, D. Maas, and S. Maranò, "GNSS-Free Maritime Navigation using Radar and Digital Elevation Models," in

2020 IEEE 23rd International Conference on Information Fusion (FUSION). IEEE, 2020, pp. 1–8.

[85] C. Musso, A. Bresson, Y. Bidel, N. Zahzam, K. Dahia, J.-M. Allard, and B. Sacleux, "Absolute gravimeter for terrain-aided navigation," in *2017 20th International Conference on Information Fusion (Fusion)*. IEEE, 2017, pp. 1–7.

[86] R. N. Shepard and J. Metzler, "Mental rotation of three-dimensional objects," *Science*, vol. 171, no. 3972, pp. 701–703, 1971.

[87] T. Porathe, "3-D nautical charts and safe navigation," Ph.D. dissertation, Institutionen för Innovation, Design och Produktutveckling, Mälardalen University, 2006.

[88] ——, "User-centered map design," in *Usability Professionals' Association Conference*, 2007.

[89] ——, "Measuring effective map design for route guidance: an experiment comparing electronic map display principles," *Information Design Journal*, vol. 16, no. 3, pp. 190–201, 2008.

[90] S. Witt, "Technologies used for navigation," *Novel Interaction Techniques for Oceangoings, University of Passau*, 2017.

[91] J. I. Lipton, A. J. Fay, and D. Rus, "Baxter's homunculus: Virtual reality spaces for teleoperation in manufacturing," *IEEE Robotics and Automation Letters*, vol. 3, no. 1, pp. 179–186, 2018.

[92] M. Mostefa, L. K. El Boudadi, A. Loukil, K. Mohamed, and D. Amine, "Design of mobile robot teleoperation system based on virtual reality," in *Control, Engineering & Information Technology (CEIT), 2015 3rd International Conference on*. IEEE, 2015, pp. 1–6.

[93] S. Lu, M. Y. Zhang, T. Ersal, and X. J. Yang, "Effects of a delay compensation aid on teleoperation of unmanned ground vehicles," in *Companion of the 2018 ACM/IEEE International Conference on Human-Robot Interaction*. ACM, 2018, pp. 179–180.

[94] C. Lundberg, H. I. Christensen, and A. Hedstrom, "The use of robots in harsh and unstructured field applications," in *ROMAN 2005. IEEE International Workshop on Robot and Human Interactive Communication, 2005.* IEEE, 2005, pp. 143–150.

[95] Y. Zheng, M. J. Brudnak, P. Jayakumar, J. L. Stein, and T. Ersal, "Evaluation of a Predictor-Based Framework in High-Speed Teleoperated Military UGVs," *IEEE Transactions on Human-Machine Systems*, 2020.

[96] R. Luz, J. Corujeira, L. Grisoni, F. Giraud, J. L. Silva, and R. Ventura, "On the Use of Haptic Tablets for UGV Teleoperation in Unstructured Environments: System Design and Evaluation," *IEEE Access*, vol. 7, pp. 95 431–95 442, 2019.

[97] X. Shen, Z. J. Chong, S. Pendleton, G. M. J. Fu, B. Qin, E. Frazzoli, and M. H. Ang, "Teleoperation of on-road vehicles via immersive telepresence using off-the-shelf components," in *Intelligent Autonomous Systems 13*. Springer, 2016, pp. 1419–1433.

[98] A. Hosseini and M. Lienkamp, "Enhancing telepresence during the teleoperation of road vehicles using HMD-based mixed reality," in *Intelligent Vehicles Symposium (IV), 2016 IEEE*. IEEE, 2016, pp. 1366–1373.

[99] S. Neumeier, N. Gay, C. Dannheim, and C. Facchi, "On the way to autonomous vehicles teleoperated driving," in *AmE 2018-Automotive meets Electronics; 9th GMM-Symposium*. VDE, 2018, pp. 1–6.

[100] H. Hedayati, M. Walker, and D. Szafir, "Improving collocated robot teleoperation with augmented reality," in *Proceedings of the 2018 ACM/IEEE International Conference on Human-Robot Interaction*. ACM, 2018, pp. 78–86.

[101] F. Perez-Grau, R. Ragel, F. Caballero, A. Viguria, and A. Ollero, "Semi-autonomous teleoperation of UAVs in search and rescue scenarios," in *Unmanned Aircraft Systems (ICUAS), 2017 International Conference on*. IEEE, 2017, pp. 1066–1074.

[102] L. Nava-Balanzar, J. Sanchez-Gaytán, F. Fonseca-Navarro, T. Salgado-Jimenez, A. Gómez-Espinosa, and A. Ramirez-Martinez, "Towards teleoperation and automatic control features of an unmanned surface vessel -

ROV system: Preliminary results," in *International Conference on Informatics in Control, Automation and Robotics*, 2017.

[103] S. Neumeier, P. Wintersberger, A.-K. Frison, A. Becher, C. Facchi, and A. Riener, "Teleoperation: The holy grail to solve problems of automated driving? Sure, but latency matters," in *Proceedings of the 11th International Conference on Automotive User Interfaces and Interactive Vehicular Applications*, 2019, pp. 186–197.

[104] S. Lu, M. Y. Zhang, T. Ersal, and X. J. Yang, "Workload management in teleoperation of unmanned ground vehicles: Effects of a delay compensation aid on human operators' workload and teleoperation performance," *International Journal of Human–Computer Interaction*, vol. 35, no. 19, pp. 1820–1830, 2019.

[105] A. Hosseini, F. Richthammer, and M. Lienkamp, "Predictive haptic feedback for safe lateral control of teleoperated road vehicles in urban areas," in *2016 IEEE 83rd Vehicular Technology Conference (VTC Spring)*. IEEE, 2016, pp. 1–7.

[106] F. Chucholowski, M. Sauer, and M. Lienkamp, "Evaluation of display methods for teleoperation of road vehicles," *Journal of Unmanned System Technology*, vol. 3, no. 3, pp. 80–85, 2016.

[107] Shippers' journal. (2017) World's First Remotely-Controlled Commercial Vessel Put to the Test in Copenhagen. Last accessed 9 November 2020. [Online]. Available: http://www.shippersjournal.com/news/article.html?no=23154

[108] T. Williams, N. Tran, J. Rands, and N. T. Dantam, "Augmented, mixed, and virtual reality enabling of robot deixis," in *the International Conference on Virtual, Augmented and Mixed Reality*, 2018.

[109] C. Benton and J. Koonce, "Augmented reality: A new tool to increase safety in maritime navigation," 2014.

[110] J.-C. Morgère, J.-P. Diguet, and J. Laurent, "Electronic navigational chart generator for a marine mobile augmented reality system," in *Oceans-St. John's, 2014*. IEEE, 2014, pp. 1–9.

[111] M. K. Mollandsøy and P. H. Pedersen, "Augmented reality og head mounted display-navigatørens verktøy i en teknologisk fremtid," B.S. thesis, Sjøkrigsskolen, 2017.

[112] O. Hugues, J.-M. Cieutat, and P. Guitton, "An experimental augmented reality platform for assisted maritime navigation," in *Proceedings of the 1st Augmented Human International Conference*. ACM, 2010, p. 12.

[113] O. Jaeyong, S. Park, and O.-S. Kwon, "Advanced navigation aids system based on augmented reality," *International Journal of e-Navigation and Maritime Economy*, vol. 5, pp. 21–31, 2016.

[114] M. Lager, E. A. Topp, and J. Malec, "Long-Term Accuracy in Sea Navigation without using GNSS Systems," in *30th Annual Workshop of the Swedish Artificial Intelligence Society SAIS 2017, May 15–16, 2017, Karlskrona, Sweden*, no. 137. Linköping University Electronic Press, 2017, pp. 10–19.

[115] ——, "Underwater terrain navigation using standard sea charts and magnetic field maps," in *IEEE International Conference on Multisensor Fusion and Integration for Intelligent Systems (MFI 2017)*. IEEE, 2017, DOI: 10.1109/MFI.2017.8170410.

[116] A. Krizhevsky, I. Sutskever, and G. E. Hinton, "Imagenet classification with deep convolutional neural networks," *Communications of the ACM*, vol. 60, no. 6, pp. 84–90, 2017.

[117] X. Wang, J. Jiao, J. Yin, W. Zhao, X. Han, and B. Sun, "Underwater sonar image classification using adaptive weights convolutional neural network," *Applied Acoustics*, vol. 146, pp. 145–154, 2019.

[118] D. C. Ciresan, U. Meier, J. Masci, L. M. Gambardella, and J. Schmidhuber, "Flexible, high performance convolutional neural networks for image classification," in *Twenty-second international joint conference on artificial intelligence*, 2011.

[119] Unity 3D. [Online]. Available: https://unity.com/

[120] Saab Kockums AB. [Online]. Available: https://www.saab.com/products/naval

[121] Saab. (2020) Saab digital air traffic solutions. Last accessed 5 November 2020. [Online]. Available: https://www.saab.com/sites/saab-digital-air-traffic-solutions

[122] R. Karlsson, F. Gustafsson, and T. Karlsson, "Particle filtering and cramer-rao lower bound for underwater navigation," in *Acoustics, Speech, and Signal Processing, 2003. Proceedings.(ICASSP'03). 2003 IEEE International Conference on*, vol. 6. IEEE, 2003, pp. VI–65.

[123] K. B. Ánonsen and O. Hallingstad, "Sigma point Kalman filter for underwater terrain-based navigation," *IFAC Proceedings Volumes*, vol. 40, no. 17, pp. 106–110, 2007.

[124] P.-J. Nordlund, "Sequential monte carlo filters and integrated navigation," Ph.D. dissertation, Thesis no. 945, Linköping University., Linköping, Sweden, 2002.

[125] D. K. Meduna, S. M. Rock, and R. McEwen, "Low-cost terrain relative navigation for long-range AUVs," in *OCEANS 2008*. IEEE, 2008, pp. 1–7.

[126] J. Melo and A. Matos, "Survey on advances on terrain based navigation for autonomous underwater vehicles," *Ocean Engineering*, vol. 139, pp. 250–264, 2017.

[127] M. Angermann and P. Robertson, "Inertial-based joint mapping and positioning for pedestrian navigation," in *Proc. ION GNSS*, 2009.

[128] F. Dellaert, D. Fox, W. Burgard, and S. Thrun, "Monte carlo localization for mobile robots," in *Robotics and Automation, 1999. Proceedings. 1999 IEEE International Conference on*, vol. 2. IEEE, 1999, pp. 1322–1328.

[129] L. A. Klein, *Sensor and data fusion: a tool for information assessment and decision making*. SPIE press Bellingham, 2004, vol. 324.

[130] M. Lager, E. A. Topp, and J. Malec, "Remote supervision of an unmanned surface vessel-a comparison of interfaces," in *2019 14th ACM/IEEE International Conference on Human-Robot Interaction (HRI)*. IEEE, 2019, pp. 546–547, DOI: 10.1109/hri.2019.8673100.

[131] ——, "Underwater terrain navigation during realistic scenarios," in *Multisensor Fusion and Integration for Intelligent Systems*. Springer, 2017, pp. 186–209, DOI: 10.1007/978-3-319-90509-9_11.

[132] F. Gustafsson, "Particle filter theory and practice with positioning applications," *IEEE Aerospace and Electronic Systems Magazine*, vol. 25, no. 7, pp. 53–82, 2010.

[133] M. Schiaretti, L. Chen, and R. R. Negenborn, "Survey on autonomous surface vessels: Part I - A new detailed definition of autonomy levels," in *International Conference on Computational Logistics*. Springer, 2017, pp. 219–233.

[134] L. Camilli, "Designing ocean drones for maritime security: The use of integrated sensing modalities to enhance situational awareness." in *Proceedings of Marine Technology Society and IEEE Oceanic Engineering Society OCEANS 2015 Environmental Intelligence*. IEEE, 2015.

[135] P. Norgren, M. Ludvigsen, T. Ingebretsen, and V. E. Hovstein, "Tracking and remote monitoring of an autonomous underwater vehicle using an unmanned surface vehicle in the Trondheim fjord," in *OCEANS'15 MTS/IEEE Washington*. IEEE, 2015, pp. 1–6.

[136] (2019) Wikipedia - piraya specification. Last accessed 29 October 2020. [Online]. Available: https://en.wikipedia.org/wiki/Unmanned_surface_vehicle_Piraya

[137] P. Flanagan, P. Cavanagh, and O. E. Favreau, "Independent orientation-selective mechanisms for the cardinal directions of colour space," *Vision research*, vol. 30, no. 5, pp. 769–778, 1990.

[138] K. Chintamani, A. Cao, R. D. Ellis, C.-A. Tan, and A. K. Pandya, "An analysis of teleoperator performance in conditions of display-control misalignments with and without movement cues," *Journal of Cognitive Engineering and Decision Making*, vol. 5, no. 2, pp. 139–155, 2011.

[139] C. C. Sheffer and F. C. Vaughan, "Application of cognitive modeling to tactical scene generation," *Johns Hopkins APL technical digest*, vol. 20, no. 3, p. 253, 1999.

[140] R. Murphy, "Disaster Robotics. Intelligent robotics and autonomous agents series," *The MIT Press*, 2014.

[141] P. M. d'Orey, A. Hosseini, J. Azevedo, F. Diermeyer, M. Ferreira, and M. Lienkamp, "Hail-a-drone: Enabling teleoperated taxi fleets," in *Intelligent Vehicles Symposium (IV), 2016 IEEE*. IEEE, 2016, pp. 774–781.

[142] D. Maltese, O. Deyla, G. Vernet, C. Preux, G. Hilt, and P.-O. Nougues, "New generation of naval IRST: Example of EOMS NG," in *Infrared Technology and Applications XXXVI*, vol. 7660. International Society for Optics and Photonics, 2010, p. 766004.

[143] Kongsberg. (2018) Technology for the Ferries of the Future. Last accessed 10 October 2020. [Online]. Available: https://www.kongsberg.com/maritime/about-us/news-and-media/news-archive/2018/technology-for-the-ferries-of-the-future/

[144] (2018) Remote-controlled and autonomous ships in the maritime industry. Last accessed 9 September 2020. [Online]. Available: https://www.dnvgl.com/maritime/publications/remote-controlled-autonomous-ships-paper-download.html

[145] M. Lager, E. A. Topp, and J. Malec, "Robust terrain-aided navigation through sensor fusion," in *2020 IEEE 23rd International Conference on Information Fusion (FUSION)*. IEEE, 2020, pp. 1–8, DOI: 10.23919/fusion45008.2020.9190578.

[146] ——, "Remote operation of unmanned surface vessel through virtual reality-a low cognitive load approach," in *Proceedings of the 1st International Workshop on Virtual, Augmented, and Mixed Reality for HRI (VAM-HRI)*, 2018, DOI: 10.6084/m9.figshare.13537019.

[147] M. Lager and E. A. Topp, "Remote supervision of an autonomous surface vehicle using virtual reality," *IFAC-PapersOnLine*, vol. 52, no. 8, pp. 387–392, 2019, DOI: 10.1016/j.ifacol.2019.08.104.

List of Acronyms

List of Acronyms

Abbreviations

AI Artificial Intelligence

AIS Automatic Identification System

AR Augmented Reality

ASC Autonomous Surface Craft

ASV Autonomous Surface Vessel

CNN Convolutional Neural Network

CO_2 Carbon Dioxide

COLREG Convention on the International Regulations for Preventing Collisions at Sea

DARPA Defense Advanced Research Projects Agency

DGPS Differential Global Navigation System

DNV GL Det Norske Veritas Germanischer Lloyd

DR Dead Reckoning

DSRM Design Science Research Methodology

ECDIS Electronic Chart Display and Information System

ECV Ego-Centric View

FPV First Person View

GHG Greenhouse Gas

GMDSS Global Maritime Distress and Safety System

GNSS Global Navigation Satellite System

GPS Global Navigation System

GPU Graphics Processing Unit

GT Gross Tonnage

GUI Graphical User Interface

HMD Head Mounted Display

IMO International Maritime Organization

IMU Inertial Measuring Unit

INS Inertial Navigation System

IR Infra-Red

Lidar Light Detection and Ranging

MASS Maritime Autonomous Surface Ship

ML Machine Learning

NM Nautical Mile

NO_x A generic term for the mono-nitrogen oxides: Nitric oxide and Nitrogen dioxide

NPU Neural Processing Unit

PDF Probability Density Function

PF Particle Filter

RQ Research Question

SA Situational Awareness

SAE Society of Automative Engineers

SAR Search and Rescue

SARUMS Safety and Regulations for European Unmanned Maritime Systems

SCC Shore Control Center

SOLAS Safety of Life at Sea

STCW International Convention on Standards of Training Certification and Watch-keeping for Seafarers

TAN Terrain-Aided Navigation

TeV Tethered View

UGV Unmanned Ground Vehicle

USV Unmanned Surface Vessel

USV Unmanned Surface Vehicle

VE Virtual Environment

VHF Very High Frequency

VR Virtual Reality

WAM-V Wave Adaptive Modular Vessel

WASP Wallenberg, AI Autonomous Systems and Software Program

Appendix

Appendix: Conference Posters

Poster I: Digital Cognitive Companion for Marine Vessels

Presented during poster session on WASP Winter conference in Stockholm 2017.

Poster II: Underwater Terrain Navigation Using Standard Sea Charts and Magnetic Field Maps

Presented during poster session on MFI in Daegu 2017.

Poster III: Remote Operation of Unmanned Surface Vessel through Virtual Reality - a low cognitive load approach

Presented during poster session on WAM HRI Workshop in Chicago 2018.

Poster IV: Smart Technologies for Unmanned Ships

Presented during poster session on WASP Winter conference in Linköping 2020.

DIGITAL COGNITIVE COMPANION FOR MARINE VESSELS

Mårten Lager, Department of Computer Science at LTH

SAAB

LUNDS UNIVERSITET

Description

A naval ship that can process the OODA loop quicker than its opponent gains an advantage. The speed of the OODA loop is therefore of significant importance for measuring the performance of a naval ship.

You improve your OODA loop by:

- Having better sensors
- Using your sensor data in a better way
- Collaborating with other platforms (low cost gives more platforms)

You worsen your opponent's OODA loop by:

- Having a low signature (you should hide, be small, be silent, and have stealth capability)

This research will show where and how human operators can be replaced or complemented by efficient algorithms, in order to remove bottle-necks in the operator work-flow. Sensor data will be used in a better way, the platforms will become smaller, and the cost will be reduced.

Background & Motivation

A typical architecture of a naval ship, where each sensor operator is responsible for which data that should be forwarded to the fusion system CMS.

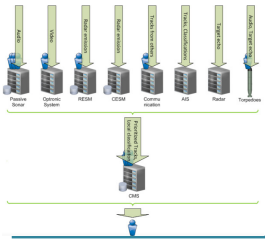

The current trend is that naval ships are being equipped with an increasing number of increasingly complex sensor systems. Along with this evolution, the need for more operators to supervise the new sensor systems arises. The operators are often becoming the OODA loop's bottle-neck, because the operators need to process so much data.

Research Goal & Questions

The proposed architecture, where the operators work with the fusioned and processed information, and gain from previous experiences saved in the knowledge base.

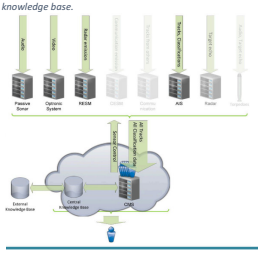

The main goal of this project is to develop a solution where operators can efficiently interact with the system on a more abstracted level, where new fusion algorithms replace some of the work that operators perform in present solutions.

Methods & Preliminary Results

Swedish submarine control room on-board HMS Södermanland.

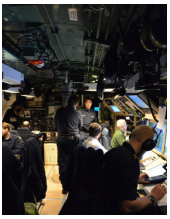

I will use the following research methods:

1. Literature survey to learn about state-of-the-art sensor fusion algorithms
2. Field-study, to get a better understanding of work-flow and bottlenecks on a naval vessel
3. Implementation of new algorithms
4. Feedback from end-users

Roadmap & Milestones

The ultimate goal is to develop a complete architecture where all relevant information is fusioned, and where the operators and machines help each other interpreting the surrounding area. The following sub-projects will lead in the direction of that goal:

- **Positioning the naval vessel without GPS**, combining IMU-data, bottom depth and magnetic measurements
- **Classifying surrounding ships** using computer vision interpretation
- **Fusing abstracted information on a higher level**, such as pre-classification information from different sensors. The operators should then assist the system by confirming/rejecting classification suggestions

The Swedish Visby class corvette.

The submarine A26.

WASP WALLENBERG AUTONOMOUS SYSTEMS AND SOFTWARE PROGRAM

Underwater Terrain Navigation Using Standard Sea Charts and Magnetic Field Maps

Mårten Lager, Elin Anna Topp, Jacek Malec

SAAB TECHNOLOGIES

LUND UNIVERSITY

Can we localize a ship by just comparing the measured depth with a normal sea chart? - Yes, it works fine!

Background and Motivation

- Ships today rely on GPS
- GPS disadvantages:
  - dependent on external systems
  - Can be jammed
  - Can be spoofed
- Some ships and vehicles can not receive GPS transmission.

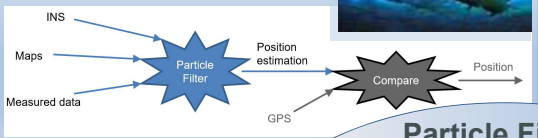

Interpretation of Maps

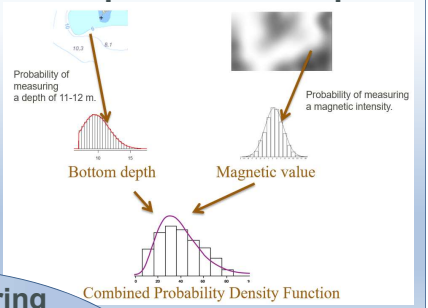

Particle Filtering

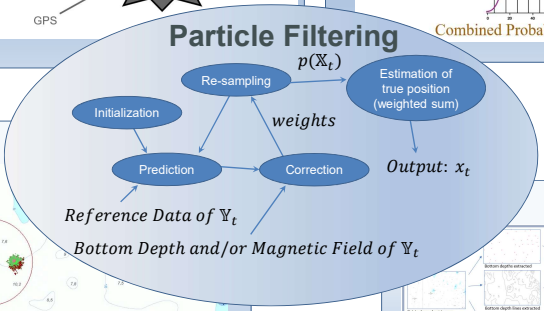

Simulation

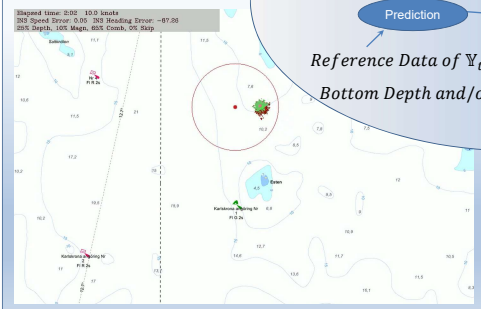

Workflow

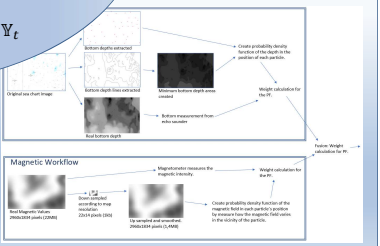

Data Fusion in Correction Step

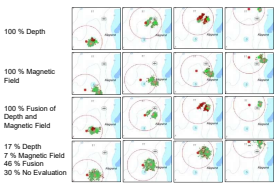

Various evaluation methods have been tested alone and in combination with others.

The simulation shows that a well balanced mix of different evaluation methods gives a robust and accurate solution.

Results and Conclusion

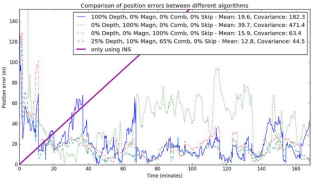

- Good performance when comparing bottom depth with sea chart.
- Accuracy and robustness are increased when fusing bottom depth and magnetic field measurements.
- We only have simulation results. Actual sea tests are planned in the future.

{marten.lager,elin_anna.topp,jacek.malec}@cs.lth.se
Department of Computer Science
LTH, Lund University
Sweden

WASP WALLENBERG AUTONOMOUS SYSTEMS AND SOFTWARE PROGRAM

Remote Operation of Unmanned Surface Vessel through Virtual Reality - a low cognitive load approach

Mårten Lager, Elin Anna Topp, Jacek Malec

SAAB

LUND UNIVERSITY

How can we design a GUI, so that we safely can control a USV remotely? What about cognitive load?

Background and Motivation

Why Unmanned Surface Vessel (USV)?
- Cost-effective
- Work-environment
- Safety
- Work in hazardous environments

Why remote-operation:
- Humans can handle complex dynamic environments

Why VR?
- Can provide a realistic environment comparable to what the operator is used to
- Can augment information and guide the operator

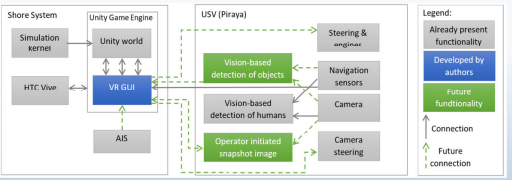

Operational Views

Features to reduce the cognitive load

Virtual groundings and seamarks

AIS information

Detected objects from real world

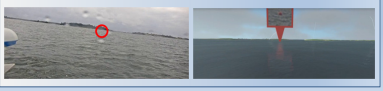

Overlaid seachart and compass

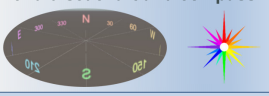

Results

- Naval operators found the cognitive load to be reduced, due to the operator was fed with valuable information.

Future

- Add features for control.
- Add other features
- Start doing live sea trials.
- Evaluate GUI by unexperienced and experienced operators.

{marten.lager,elin_anna.topp,jacek.malec}@cs.lth.se
Department of Computer Science
LTH, Lund University
Sweden

WASP WALLENBERG AUTONOMOUS SYSTEMS AND SOFTWARE PROGRAM

Smart Technologies for unmanned ships

Mårten Lager, Lund University
Computer Science Department

LUND UNIVERSITY

SAAB

Research Area

In this project, methods are presented to enhance the capability of two building blocks that are important for autonomous ships; a positioning system, and a system for remote supervision.

GPS-free navigation by fusion of bottom depth and magnetic field with CNN support

Overall description
Uses Bayesian calculations to compare the **bottom depth** and **magnetic field** measurements with known sea charts and magnetic field maps, in order to estimate the position. To optimize how the sensor data shall be fusioned, **CNN** adjusts the weights, after analyzing the map around the estimated position.

Our main contribution
State-of-the-art techniques for this method normally use low accuracy navigation sensors and high-resolution maps, which can hardly be used in real life. We rely on available normal **sea charts** and **low-resolution magnetic field maps** instead.

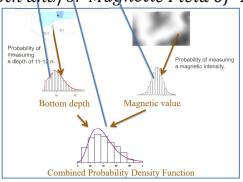

Results
- Good performance when comparing bottom depth with sea chart.
- Accuracy and robustness are increased when fusing bottom depth and magnetic field measurements.

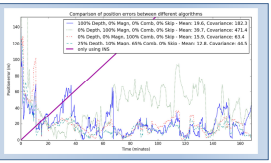

Remote supervision in VR

What has been done
Three GUI types have been created for **remote supervision** of an Unmanned Surface Vessel via a **low bandwidth** connection. Two in **3D** (presented in **VR** and on a **laptop**) and one **traditional 2D GUI**. The GUIs have been compared in a **user study**.

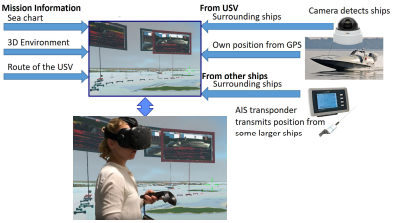

Why remote-supervision?
- Humans can handle complex dynamic environments

Why VR?
- Can provide a realistic environment comparable to what the operator is used to on a real ship
- Can augment information and guide the operator
- Do not need to transfer all videos, as most objects are already known in the Virtual World.

User Study Results
The users of the two 3D GUIs were **better at reacting to dangerous situations** than Traditional GUI users, and they could **keep track of the surroundings more accurately**. The users experienced the two 3D GUIs to be more **Easy to Use**, and believed the 3D GUIs, and especially the VR version to be the **Best Expert Tool** after several hours of training.

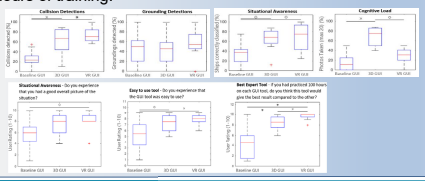

marten.lager@cs.lth.se
Department of Computer Science
LTH, Lund University
Sweden

Webpage:

WASP WALLENBERG AI, AUTONOMOUS SYSTEMS AND SOFTWARE PROGRAM